The Concorde 264 supersonic airliner. Flying more than twice as fast as the speed of sound, as discussed in the present chapter, the Concorde is a milestone in commercial aviation. However, this great technical achievement is accompanied by high expense for the traveller. *(Courtesy of Don Riepe/Peter Arnold, Inc.)*

Chapter 9
Compressible Flow

Motivation. All eight of our previous chapters have been concerned with "low-speed" or "incompressible" flow, i.e., where the fluid velocity is much less than its speed of sound. In fact, we did not even develop an expression for the speed of sound of a fluid. That is done in this chapter.

When a fluid moves at speeds comparable to its speed of sound, density changes become significant and the flow is termed *compressible*. Such flows are difficult to obtain in liquids, since high pressures of order 1000 atm are needed to generate sonic velocities. In gases, however, a pressure ratio of only 2:1 will likely cause sonic flow. Thus compressible gas flow is quite common, and this subject is often called *gas dynamics*.

Probably the two most important and distinctive effects of compressibility on flow are (1) *choking*, wherein the duct flow rate is sharply limited by the sonic condition, and (2) *shock waves*, which are nearly discontinuous property changes in a supersonic flow. The purpose of this chapter is to explain such striking phenomena and to familiarize the reader with engineering calculations of compressible flow.

Speaking of calculations, the present chapter is made to order for the Engineering Equation Solver (EES) in App. E. Compressible-flow analysis is filled with scores of complicated algebraic equations, most of which are very difficult to manipulate or invert. Consequently, for nearly a century, compressible-flow textbooks have relied upon extensive tables of Mach number relations (see App. B) for numerical work. With EES, however, any set of equations in this chapter can be typed out and solved for any variable—see part (*b*) of Example 9.13 for an especially intricate example. With such a tool, App. B serves only as a backup and indeed may soon vanish from textbooks.

9.1 Introduction

We took a brief look in Chap. 4 [Eqs. (4.13) to (4.17)] to see when we might safely neglect the compressibility inherent in every real fluid. We found that the proper criterion for a nearly incompressible flow was a small Mach number

$$\text{Ma} = \frac{V}{a} \ll 1$$

where V is the flow velocity and a is the speed of sound of the fluid. Under small-Mach-number conditions, changes in fluid density are everywhere small in the flow field. The energy equation becomes uncoupled, and temperature effects can be either ignored or

put aside for later study. The equation of state degenerates into the simple statement that density is nearly constant. This means that an incompressible flow requires only a momentum and continuity analysis, as we showed with many examples in Chaps. 7 and 8.

This chapter treats compressible flows, which have Mach numbers greater than about 0.3 and thus exhibit nonnegligible density changes. If the density change is significant, it follows from the equation of state that the temperature and pressure changes are also substantial. Large temperature changes imply that the energy equation can no longer be neglected. Therefore the work is doubled from two basic equations to four

1. Continuity equation
2. Momentum equation
3. Energy equation
4. Equation of state

to be solved simultaneously for four unknowns: pressure, density, temperature, and flow velocity (p, ρ, T, V). Thus the general theory of compressible flow is quite complicated, and we try here to make further simplifications, especially by assuming a reversible adiabatic or *isentropic* flow.

The Mach Number

The Mach number is the dominant parameter in compressible-flow analysis, with different effects depending upon its magnitude. Aerodynamicists especially make a distinction between the various ranges of Mach number, and the following rough classifications are commonly used:

Ma $<$ 0.3:	*incompressible flow*, where density effects are negligible.
0.3 $<$ Ma $<$ 0.8:	*subsonic flow*, where density effects are important but no shock waves appear.
0.8 $<$ Ma $<$ 1.2:	*transonic flow*, where shock waves first appear, dividing subsonic and supersonic regions of the flow. Powered flight in the transonic region is difficult because of the mixed character of the flow field.
1.2 $<$ Ma $<$ 3.0:	*supersonic flow*, where shock waves are present but there are no subsonic regions.
3.0 $<$ Ma:	*hypersonic flow* [13], where shock waves and other flow changes are especially strong.

The numerical values listed above are only rough guides. These five categories of flow are appropriate to external high-speed aerodynamics. For internal (duct) flows, the most important question is simply whether the flow is subsonic (Ma $<$ 1) or supersonic (Ma $>$ 1), because the effect of area changes reverses, as we show in Sec. 9.4. Since supersonic-flow effects may go against intuition, you should study these differences carefully.

The Specific-Heat Ratio

In addition to geometry and Mach number, compressible-flow calculations also depend upon a second dimensionless parameter, the *specific-heat ratio* of the gas:

$$k = \frac{c_p}{c_v} \tag{9.1}$$

Earlier, in Chaps. 1 and 4, we used the same symbol k to denote the thermal conductivity of a fluid. We apologize for the duplication; thermal conductivity does not appear in these later chapters of the text.

Recall from Fig. 1.3 that k for the common gases decreases slowly with temperature and lies between 1.0 and 1.7. Variations in k have only a slight effect upon compressible-flow computations, and air, $k \approx 1.40$, is the dominant fluid of interest. Therefore, although we assign some problems involving, e.g., steam and CO_2 and helium, the compressible-flow tables in App. B are based solely upon the single value $k = 1.40$ for air.

This text contains only a single chapter on compressible flow, but, as usual, whole books have been written on the subject. References 1 to 6, 26, 29, and 33 are introductory, fairly elementary treatments, while Refs. 7 to 14, 27 to 28, 31 to 32, and 35 are advanced. From time to time we shall defer some specialized topic to these texts.

We note in passing that there are at least two flow patterns which depend strongly upon very small density differences, acoustics, and natural convection. Acoustics [9, 14] is the study of sound-wave propagation, which is accompanied by extremely small changes in density, pressure, and temperature. Natural convection is the gentle circulating pattern set up by buoyancy forces in a fluid stratified by uneven heating or uneven concentration of dissolved materials. Here we are concerned only with steady compressible flow where the fluid velocity is of magnitude comparable to that of the speed of sound.

The Perfect Gas

In principle, compressible-flow calculations can be made for any fluid equation of state, and we shall assign problems involving the steam tables [15], the gas tables [16], and liquids [Eq. (1.19)]. But in fact most elementary treatments are confined to the perfect gas with constant specific heats

$$p = \rho RT \qquad R = c_p - c_v = \text{const} \qquad k = \frac{c_p}{c_v} = \text{const} \qquad (9.2)$$

For all real gases, c_p, c_v, and k vary with temperature but only moderately; for example, c_p of air increases 30 percent as temperature increases from 0 to 5000°F. Since we rarely deal with such large temperature changes, it is quite reasonable to assume constant specific heats.

Recall from Sec. 1.6 that the gas constant is related to a universal constant Λ divided by the gas molecular weight

$$R_{\text{gas}} = \frac{\Lambda}{M_{\text{gas}}} \qquad (9.3)$$

where $\qquad \Lambda = 49{,}720 \text{ ft}^2/(\text{s}^2 \cdot °\text{R}) = 8314 \text{ m}^2/(\text{s}^2 \cdot \text{K})$

For air, $M = 28.97$, and we shall adopt the following property values for air throughout this chapter:

$$R = 1717 \text{ ft}^2/(\text{s}^2 \cdot °\text{R}) = 287 \text{ m}^2/(\text{s}^2 \cdot \text{K}) \qquad k = 1.400$$

$$c_v = \frac{R}{k-1} = 4293 \text{ ft}^2/(\text{s}^2 \cdot °\text{R}) = 718 \text{ m}^2/(\text{s}^2 \cdot \text{K}) \qquad (9.4)$$

$$c_p = \frac{kR}{k-1} = 6010 \text{ ft}^2/(\text{s}^2 \cdot °\text{R}) = 1005 \text{ m}^2/(\text{s}^2 \cdot \text{K})$$

Experimental values of k for eight common gases were shown in Fig. 1.3. From this figure and the molecular weight, the other properties can be computed, as in Eqs. (9.4).

The changes in the internal energy $\hat{u}$ and enthalpy h of a perfect gas are computed for constant specific heats as

$$\hat{u}_2 - \hat{u}_1 = c_v(T_2 - T_1) \qquad h_2 - h_1 = c_p(T_2 - T_1) \tag{9.5}$$

For variable specific heats one must integrate $\hat{u} = \int c_v \, dT$ and $h = \int c_p \, dT$ or use the gas tables [16]. Most modern thermodynamics texts now contain software for evaluating properties of nonideal gases [17].

Isentropic Process

The isentropic approximation is common in compressible-flow theory. We compute the entropy change from the first and second laws of thermodynamics for a pure substance [17 or 18]

$$T \, ds = dh - \frac{dp}{\rho} \tag{9.6}$$

Introducing $dh = c_p \, dT$ for a perfect gas and solving for ds, we substitute $\rho T = p/R$ from the perfect-gas law and obtain

$$\int_1^2 ds = \int_1^2 c_p \frac{dT}{T} - R \int_1^2 \frac{dp}{p} \tag{9.7}$$

If c_p is variable, the gas tables will be needed, but for constant c_p we obtain the analytic results

$$s_2 - s_1 = c_p \ln \frac{T_2}{T_1} - R \ln \frac{p_2}{p_1} = c_v \ln \frac{T_2}{T_1} - R \ln \frac{\rho_2}{\rho_1} \tag{9.8}$$

Equations (9.8) are used to compute the entropy change across a shock wave (Sec. 9.5), which is an irreversible process.

For isentropic flow, we set $s_2 = s_1$ and obtain the interesting power-law relations for an isentropic perfect gas

$$\frac{p_2}{p_1} = \left(\frac{T_2}{T_1}\right)^{k/(k-1)} = \left(\frac{\rho_2}{\rho_1}\right)^k \tag{9.9}$$

These relations are used in Sec. 9.3.

EXAMPLE 9.1

Argon flows through a tube such that its initial condition is $p_1 = 1.7$ MPa and $\rho_1 = 18$ kg/m^3 and its final condition is $p_2 = 248$ kPa and $T_2 = 400$ K. Estimate (a) the initial temperature, (b) the final density, (c) the change in enthalpy, and (d) the change in entropy of the gas.

Solution

From Table A.4 for argon, $R = 208$ m^2/(s$^2 \cdot$ K) and $k = 1.67$. Therefore estimate its specific heat at constant pressure from Eq. (9.4):

$$c_p = \frac{kR}{k-1} = \frac{1.67(208)}{1.67 - 1} \approx 519 \ \text{m}^2/(\text{s}^2 \cdot \text{K})$$

The initial temperature and final density are estimated from the ideal gas law, Eq. (9.2):

$$T_1 = \frac{p_1}{\rho_1 R} = \frac{1.7 \ \text{E6 N/m}^2}{(18 \ \text{kg/m}^3)[208 \ \text{m}^2/(\text{s}^2 \cdot \text{K})]} = 454 \ \text{K} \qquad \textit{Ans. (a)}$$

$$\rho_2 = \frac{p_2}{T_2 R} = \frac{248 \ \text{E3 N/m}^2}{(400 \ \text{K})[208 \ \text{m}^2/(\text{s}^2 \cdot \text{K})]} = 2.98 \ \text{kg/m}^3 \qquad \textit{Ans. (b)}$$

From Eq. (9.5) the enthalpy change is

$$h_2 - h_1 = c_p(T_2 - T_1) = 519(400 - 454) \approx -28{,}000 \ \text{J/kg (or m}^2/\text{s}^2) \qquad \textit{Ans. (c)}$$

The argon temperature and enthalpy decrease as we move down the tube. Actually, there may not be any external cooling; i.e., the fluid enthalpy may be converted by friction to increased kinetic energy (Sec. 9.7).

Finally, the entropy change is computed from Eq. (9.8):

$$s_2 - s_1 = c_p \ln \frac{T_2}{T_1} - R \ln \frac{p_2}{p_1}$$

$$= 519 \ln \frac{400}{454} - 208 \ln \frac{0.248 \ \text{E6}}{1.7 \ \text{E6}}$$

$$= -66 + 400 \approx 334 \ \text{m}^2/(\text{s}^2 \cdot \text{K}) \qquad \textit{Ans. (d)}$$

The fluid entropy has increased. If there is no heat transfer, this indicates an irreversible process. Note that entropy has the same units as the gas constant and specific heat.

This problem is not just arbitrary numbers. It correctly simulates the behavior of argon moving subsonically through a tube with large frictional effects (Sec. 9.7).

9.2 The Speed of Sound

The so-called speed of sound is the rate of propagation of a pressure pulse of infinitesimal strength through a still fluid. It is a thermodynamic property of a fluid. Let us analyze it by first considering a pulse of finite strength, as in Fig. 9.1. In Fig. 9.1a the pulse, or pressure wave, moves at speed C toward the still fluid (p, ρ, T, $V = 0$) at the left, leaving behind at the right a fluid of increased properties ($p + \Delta p$, $\rho + \Delta \rho$, $T + \Delta T$) and a fluid velocity ΔV toward the left following the wave but much slower. We can determine these effects by making a control-volume analysis across the wave. To avoid the unsteady terms which would be necessary in Fig. 9.1a, we adopt instead the control volume of Fig. 9.1b, which moves at wave speed C to the left. The wave appears fixed from this viewpoint, and the fluid appears to have velocity C on the left and $C - \Delta V$ on the right. The thermodynamic properties p, ρ, and T are not affected by this change of viewpoint.

The flow in Fig. 9.1b is steady and one-dimensional across the wave. The continuity equation is thus, from Eq. (3.24),

$$\rho A C = (\rho + \Delta \rho)(A)(C - \Delta V)$$

or $$\Delta V = C \frac{\Delta \rho}{\rho + \Delta \rho} \qquad (9.10)$$
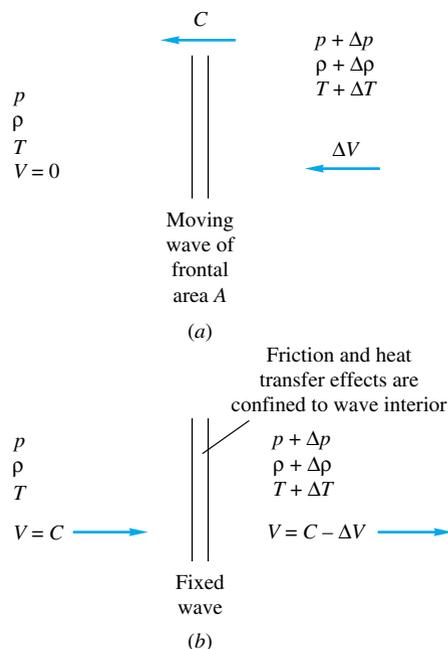
Fig. 9.1 Control-volume analysis of a finite-strength pressure wave: (*a*) control volume fixed to still fluid at left; (*b*) control volume moving left at wave speed *C*.

This proves our contention that the induced fluid velocity on the right is much smaller than the wave speed *C*. In the limit of infinitesimal wave strength (sound wave) this speed is itself infinitesimal.

Notice that there are no velocity gradients on either side of the wave. Therefore, even if fluid viscosity is large, frictional effects are confined to the interior of the wave. Advanced texts [for example, 14] show that the thickness of pressure waves in gases is of order 10^{-6} ft at atmospheric pressure. Thus we can safely neglect friction and apply the one-dimensional momentum equation (3.40) across the wave

$$\sum F_{\text{right}} = \dot{m}(V_{\text{out}} - V_{\text{in}})$$

or
$$pA - (p + \Delta p)A = (\rho A C)(C - \Delta V - C) \tag{9.11}$$

Again the area cancels, and we can solve for the pressure change

$$\Delta p = \rho C \, \Delta V \tag{9.12}$$

If the wave strength is very small, the pressure change is small.

Finally combine Eqs. (9.10) and (9.12) to give an expression for the wave speed

$$C^2 = \frac{\Delta p}{\Delta \rho}\left(1 + \frac{\Delta \rho}{\rho}\right) \tag{9.13}$$

The larger the strength $\Delta \rho / \rho$ of the wave, the faster the wave speed; i.e., powerful explosion waves move much more quickly than sound waves. In the limit of infinitesimal strength $\Delta \rho \rightarrow 0$, we have what is defined to be the speed of sound *a* of a fluid:

$$a^2 = \frac{\partial p}{\partial \rho} \tag{9.14}$$

Table 9.1 Sound Speed of Various Materials at 60°F (15.5°C) and 1 atm

Material	a, ft/s	a, m/s
Gases:		
H_2	4,246	1,294
He	3,281	1,000
Air	1,117	340
Ar	1,040	317
CO_2	873	266
CH_4	607	185
$^{238}UF_6$	297	91
Liquids:		
Glycerin	6,100	1,860
Water	4,890	1,490
Mercury	4,760	1,450
Ethyl alcohol	3,940	1,200
Solids:*		
Aluminum	16,900	5,150
Steel	16,600	5,060
Hickory	13,200	4,020
Ice	10,500	3,200

*Plane waves. Solids also have a *shear-wave speed*.

But the evaluation of the derivative requires knowledge of the thermodynamic process undergone by the fluid as the wave passes. Sir Isaac Newton in 1686 made a famous error by deriving a formula for sound speed which was equivalent to assuming an isothermal process, the result being 20 percent low for air, for example. He rationalized the discrepancy as being due to the "crassitude" (dust particles, etc.) in the air; the error is certainly understandable when we reflect that it was made 180 years before the proper basis was laid for the second law of thermodynamics.

We now see that the correct process must be *adiabatic* because there are no temperature gradients except inside the wave itself. For vanishing-strength sound waves we therefore have an infinitesimal adiabatic or isentropic process. The correct expression for the sound speed is

$$a = \left(\left. \frac{\partial p}{\partial \rho} \right|_s \right)^{1/2} = \left(k \left. \frac{\partial p}{\partial \rho} \right|_T \right)^{1/2} \tag{9.15}$$

for any fluid, gas or liquid. Even a solid has a sound speed.

For a perfect gas, From Eq. (9.2) or (9.9), we deduce that the speed of sound is

$$a = \left(\frac{kp}{\rho} \right)^{1/2} = (kRT)^{1/2} \tag{9.16}$$

The speed of sound increases as the square root of the absolute temperature. For air, with $k = 1.4$ and $R = 1717$, an easily memorized dimensional formula is

$$a \text{ (ft/s)} \approx 49[T \text{ (°R)}]^{1/2}$$
$$a \text{ (m/s)} \approx 20[T \text{ (K)}]^{1/2} \tag{9.17}$$

At sea-level standard temperature, $60°F = 520°R$, $a = 1117$ ft/s. This decreases in the upper atmosphere, which is cooler; at 50,000-ft standard altitude, $T = -69.7°F = 389.9°R$ and $a = 49(389.9)^{1/2} = 968$ ft/s, or 13 percent less.

Some representative values of sound speed in various materials are given in Table 9.1. For liquids and solids it is common to define the *bulk modulus K* of the material

$$K = -\mathcal{V} \left. \frac{\partial p}{\partial \mathcal{V}} \right|_s = \rho \left. \frac{\partial p}{\partial \rho} \right|_s \tag{9.18}$$

For example, at standard conditions, the bulk modulus of carbon tetrachloride is 163,000 lbf/in² absolute, and its density is 3.09 slugs/ft³. Its speed of sound is therefore $[163,000(144)/3.09]^{1/2} = 2756$ ft/s, or 840 m/s. Steel has a bulk modulus of about 29×10^6 lbf/in² absolute and water about 320×10^3 lbf/in² absolute, or 90 times less.

For solids, it is sometimes assumed that the bulk modulus is approximately equivalent to Young's modulus of elasticity E, but in fact their ratio depends upon Poisson's ratio σ

$$\frac{E}{K} = 3(1 - 2\sigma) \tag{9.19}$$

The two are equal for $\sigma = \frac{1}{3}$, which is approximately the case for many common metals such as steel and aluminum.

EXAMPLE 9.2

Estimate the speed of sound of carbon monoxide at 200-kPa pressure and 300°C in m/s.

Solution

From Table A.4, for CO, the molecular weight is 28.01 and $k \approx 1.40$. Thus from Eq. (9.3) $R_{CO} = 8314/28.01 = 297$ m^2/(s$^2 \cdot$ K), and the given temperature is 300°C + 273 = 573 K. Thus from Eq. (9.16) we estimate

$$a_{CO} = (kRT)^{1/2} = [1.40(297)(573)]^{1/2} = 488 \text{ m/s} \qquad\qquad Ans.$$

9.3 Adiabatic and Isentropic Steady Flow

As mentioned in Sec. 9.1, the isentropic approximation greatly simplifies a compressible-flow calculation. So does the assumption of adiabatic flow, even if nonisentropic.

Consider high-speed flow of a gas past an insulated wall, as in Fig. 9.2. There is no shaft work delivered to any part of the fluid. Therefore every streamtube in the flow satisfies the steady-flow energy equation in the form of Eq. (3.66)

$$h_1 + \tfrac{1}{2}V_1^2 + gz_1 = h_2 + \tfrac{1}{2}V_2^2 + gz_2 - q + w_v \qquad\qquad (9.20)$$

where point 1 is upstream of point 2. You may wish to review the details of Eq. (3.66) and its development. We saw in Example 3.16 that potential-energy changes of a gas are extremely small compared with kinetic-energy and enthalpy terms. We shall neglect the terms gz_1 and gz_2 in all gas-dynamic analyses.

Inside the thermal and velocity boundary layers in Fig. 9.2 the heat-transfer and viscous-work terms q and w_v are not zero. But outside the boundary layer q and w_v are zero by definition, so that the outer flow satisfies the simple relation

$$h_1 + \tfrac{1}{2}V_1^2 = h_2 + \tfrac{1}{2}V_2^2 = \text{const} \qquad\qquad (9.21)$$

The constant in Eq. (9.21) is equal to the maximum enthalpy which the fluid would achieve if brought to rest adiabatically. We call this value h_0, the *stagnation enthalpy* of the flow. Thus we rewrite Eq. (9.21) in the form

$$h + \tfrac{1}{2}V^2 = h_0 = \text{const} \qquad\qquad (9.22)$$
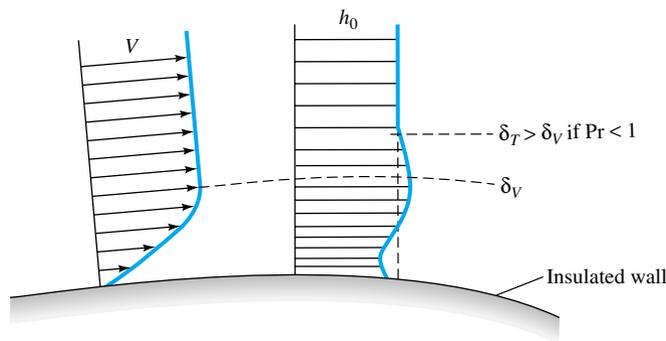
Fig. 9.2 Velocity and stagnation-enthalpy distributions near an insulated wall in a typical high-speed gas flow.

This should hold for steady adiabatic flow of any compressible fluid outside the boundary layer. The wall in Fig. 9.2 could be either the surface of an immersed body or the wall of a duct. We have shown the details of Fig. 9.2; typically the thermal-layer thickness δ_T is greater than the velocity-layer thickness δ_V because most gases have a dimensionless Prandtl number Pr less than unity (see, e.g., Ref. 19, sec. 4-3.2). Note that the stagnation enthalpy varies inside the thermal boundary layer, but its average value is the same as that at the outer layer due to the insulated wall.

For nonperfect gases we may have to use the steam tables [15] or the gas tables [16] to implement Eq. (9.22). But for a perfect gas $h = c_p T$, and Eq. (9.22) becomes

$$c_p T + \tfrac{1}{2} V^2 = c_p T_0 \tag{9.23}$$

This establishes the stagnation temperature T_0 of an adiabatic perfect-gas flow, i.e., the temperature it achieves when decelerated to rest adiabatically.

An alternate interpretation of Eq. (9.22) occurs when the enthalpy and temperature drop to (absolute) zero, so that the velocity achieves a maximum value

$$V_{\max} = (2h_0)^{1/2} = (2c_p T_0)^{1/2} \tag{9.24}$$

No higher flow velocity can occur unless additional energy is added to the fluid through shaft work or heat transfer (Sec. 9.8).

Mach-Number Relations

The dimensionless form of Eq. (9.23) brings in the Mach number Ma as a parameter, by using Eq. (9.16) for the speed of sound of a perfect gas. Divide through by $c_p T$ to obtain

$$1 + \frac{V^2}{2c_p T} = \frac{T_0}{T} \tag{9.25}$$

But, from the perfect-gas law, $c_p T = [kR/(k - 1)]T = a^2/(k - 1)$, so that Eq. (9.25) becomes

$$1 + \frac{(k - 1)V^2}{2a^2} = \frac{T_0}{T}$$

or
$$\frac{T_0}{T} = 1 + \frac{k - 1}{2} \text{Ma}^2 \qquad \text{Ma} = \frac{V}{a} \tag{9.26}$$

This relation is plotted in Fig. 9.3 versus the Mach number for $k = 1.4$. At Ma $= 5$ the temperature has dropped to $\tfrac{1}{6} T_0$.

Since $a \propto T^{1/2}$, the ratio a_0/a is the square root of (9.26)

$$\frac{a_0}{a} = \left(\frac{T_0}{T} \right)^{1/2} = \left[1 + \frac{1}{2} (k - 1)\text{Ma}^2 \right]^{1/2} \tag{9.27}$$

Equation (9.27) is also plotted in Fig. 9.3. At Ma $= 5$ the speed of sound has dropped to 41 percent of the stagnation value.

Isentropic Pressure and Density Relations

Note that Eqs. (9.26) and (9.27) require only adiabatic flow and hold even in the presence of irreversibilities such as friction losses or shock waves.
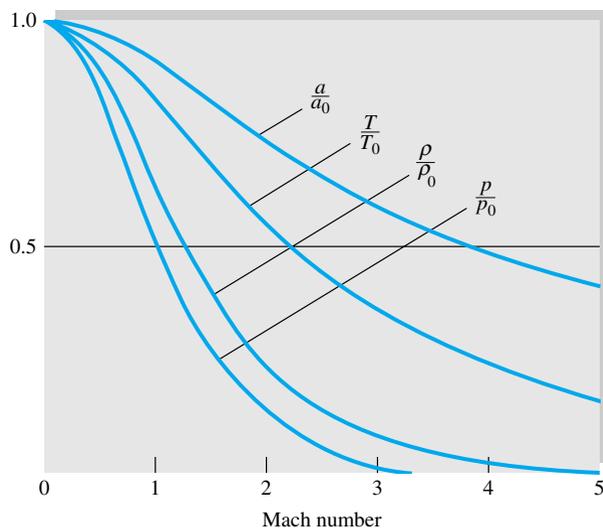
Fig. 9.3 Adiabatic $(T/T_0$ and $a/a_0)$ and isentropic $(p/p_0$ and $\rho/\rho_0)$ properties versus Mach number for $k = 1.4$.

If the flow is also *isentropic*, then for a perfect gas the pressure and density ratios can be computed from Eq. (9.9) as a power of the temperature ratio

$$\frac{p_0}{p} = \left(\frac{T_0}{T}\right)^{k/(k-1)} = \left[1 + \frac{1}{2}(k-1)\,\mathrm{Ma}^2\right]^{k/(k-1)} \tag{9.28a}$$

$$\frac{\rho_0}{\rho} = \left(\frac{T_0}{T}\right)^{1/(k-1)} = \left[1 + \frac{1}{2}(k-1)\,\mathrm{Ma}^2\right]^{1/(k-1)} \tag{9.28b}$$

These relations are also plotted in Fig. 9.3; at Ma = 5 the density is 1.13 percent of its stagnation value, and the pressure is only 0.19 percent of stagnation pressure.

The quantities p_0 and ρ_0 are the isentropic stagnation pressure and density, respectively, i.e., the pressure and density which the flow would achieve if brought isentropically to rest. In an adiabatic nonisentropic flow p_0 and ρ_0 retain their local meaning, but they vary throughout the flow as the entropy changes due to friction or shock waves. The quantities h_0, T_0, and a_0 are constant in an adiabatic nonisentropic flow (see Sec. 9.7 for further details).

Relationship to Bernoulli's Equation

The isentropic assumptions (9.28) are effective, but are they realistic? Yes. To see why, differentiate Eq. (9.22)

Adiabatic: $$dh + V\,dV = 0 \tag{9.29}$$

Meanwhile, from Eq. (9.6), if $ds = 0$ (isentropic process),

$$dh = \frac{dp}{\rho} \tag{9.30}$$

Combining (9.29) and (9.30), we find that an isentropic streamtube flow must be

$$\frac{dp}{\rho} + V\,dV = 0 \tag{9.31}$$

But this is exactly the Bernoulli relation, Eq. (3.75), for steady frictionless flow with negligible gravity terms. Thus we see that the isentropic-flow assumption is equivalent to use of the Bernoulli or streamline form of the frictionless momentum equation.

Critical Values at the Sonic Point

The stagnation values (a_0, T_0, p_0, ρ_0) are useful reference conditions in a compressible flow, but of comparable usefulness are the conditions where the flow is sonic, Ma = 1.0. These sonic, or *critical*, properties are denoted by asterisks: p^*, ρ^*, a^*, and T^*. They are certain ratios of the stagnation properties as given by Eqs. (9.26) to (9.28) when Ma = 1.0; for $k = 1.4$

$$\frac{p^*}{p_0} = \left(\frac{2}{k+1}\right)^{k/(k-1)} = 0.5283 \qquad \frac{\rho^*}{\rho_0} = \left(\frac{2}{k+1}\right)^{1/(k-1)} = 0.6339$$

$$\frac{T^*}{T_0} = \frac{2}{k+1} = 0.8333 \qquad \frac{a^*}{a_0} = \left(\frac{2}{k+1}\right)^{1/2} = 0.9129$$

$$(9.32)$$

In all isentropic flow, all critical properties are constant; in adiabatic nonisentropic flow, a^* and T^* are constant, but p^* and ρ^* may vary.

The critical velocity V^* equals the sonic sound speed a^* by definition and is often used as a reference velocity in isentropic or adiabatic flow

$$V^* = a^* = (kRT^*)^{1/2} = \left(\frac{2k}{k+1} RT_0\right)^{1/2} \qquad (9.33)$$

The usefulness of these critical values will become clearer as we study compressible duct flow with friction or heat transfer later in this chapter.

Some Useful Numbers for Air

Since the great bulk of our practical calculations are for air, $k = 1.4$, the stagnation-property ratios p/p_0, etc., from Eqs. (9.26) to (9.28), are tabulated for this value in Table B.1. The increments in Mach number are rather coarse in this table because the values are only meant as a guide; these equations are now a trivial matter to manipulate on a hand calculator. Thirty years ago every text had extensive compressible-flow tables with Mach-number spacings of about 0.01, so that accurate values could be interpolated.

For $k = 1.4$, the following numerical versions of the isentropic and adiabatic flow formulas are obtained:

$$\frac{T_0}{T} = 1 + 0.2\ \text{Ma}^2 \qquad \frac{\rho_0}{\rho} = (1 + 0.2\ \text{Ma}^2)^{2.5}$$

$$\frac{p_0}{p} = (1 + 0.2\ \text{Ma}^2)^{3.5}$$

$$(9.34)$$

Or, if we are given the properties, it is equally easy to solve for the Mach number (again with $k = 1.4$)

$$\text{Ma}^2 = 5\left(\frac{T_0}{T} - 1\right) = 5\left[\left(\frac{\rho_0}{\rho}\right)^{2/5} - 1\right] = 5\left[\left(\frac{p_0}{p}\right)^{2/7} - 1\right] \qquad (9.35)$$

Note that these isentropic-flow formulas serve as the equivalent of the frictionless adiabatic momentum and energy equations. They relate velocity to physical properties for a perfect gas, but they are *not* the "solution" to a gas-dynamics problem. The complete

solution is not obtained until the continuity equation has also been satisfied, for either one-dimensional (Sec. 9.4) or multidimensional (Sec. 9.9) flow.

One final note: These isentropic-ratio–versus–Mach-number formulas are seductive, tempting one to solve all problems by jumping right into the tables. Actually, many problems involving (dimensional) velocity and temperature can be solved more easily from the original raw dimensional energy equation (9.23) plus the perfect-gas law (9.2), as the next example will illustrate.

EXAMPLE 9.3

Air flows adiabatically through a duct. At point 1 the velocity is 240 m/s, with $T_1 = 320$ K and $p_1 = 170$ kPa. Compute (a) T_0, (b) p_{01}, (c) ρ_0, (d) Ma, (e) V_{max}, and (f) V^*. At point 2 further downstream $V_2 = 290$ m/s and $p_2 = 135$ kPa. (g) What is the stagnation pressure p_{02}?

Solution

For air take $k = 1.4$, $c_p = 1005$ m²/(s² · K), and $R = 287$ m²/(s² · K). With V_1 and T_1 known, we can compute T_{01} from Eq. (9.23) without using the Mach number:

$$T_{01} = T_1 + \frac{V_1^2}{2c_p} = 320 + \frac{(240 \text{ m/s})^2}{2[1005 \text{ m}^2/(\text{s}^2 \cdot \text{K})]} = 320 + 29 = 349 \text{ K} \qquad \textit{Ans. (a)}$$

Then compute Ma_1 from the known temperature ratio, using Eq. (9.35):

$$Ma_1^2 = 5\left(\frac{349}{320} - 1\right) = 0.453 \qquad Ma_1 = 0.67 \qquad \textit{Ans. (d)}$$

Alternately compute $a_1 = \sqrt{kRT_1} = 359$ m/s, whence $Ma_1 = V_1/a_1 = 240/359 = 0.67$. The stagnation pressure at section 1 follows from Eq. (9.34):

$$p_{01} = p_1(1 + 0.2 \, Ma_1^2)^{3.5} = (170 \text{ kPa})[1 + 0.2(0.67)^2]^{3.5} = 230 \text{ kPa} \qquad \textit{Ans. (b)}$$

We need the density from the perfect-gas law before we can compute the stagnation density:

$$\rho_1 = \frac{p_1}{RT_1} = \frac{170,000}{(287)(320)} = 1.85 \text{ kg/m}^3$$

whence $$\rho_{01} = \rho_1(1 + 0.2 \, Ma_1^2)^{2.5} = (1.85)[1 + 0.2(0.67)^2]^{2.5} = 2.29 \text{ kg/m}^3 \qquad \textit{Ans. (c)}$$

Alternately, we could have gone directly to $\rho_0 = p_0/(RT_0) = (230\,\text{E3})/[(287)(349)] = 2.29$ kg/m³. Meanwhile, the maximum velocity follows from Eq. (9.24):

$$V_{max} = (2c_p T_0)^{1/2} = [2(1005)(349)]^{1/2} = 838 \text{ m/s} \qquad \textit{Ans. (e)}$$

and the sonic velocity from Eq. (9.33) is

$$V^* = \left(\frac{2k}{k+1} RT_0\right)^{1/2} = \left[\frac{2(1.4)}{1.4 + 1} (287)(349)\right]^{1/2} = 342 \text{ m/s} \qquad \textit{Ans. (f)}$$

At point 2, the temperature is not given, but since we know the flow is adiabatic, the stagnation temperature is constant: $T_{02} = T_{01} = 349$ K. Thus, from Eq. (9.23),

$$T_2 = T_{02} - \frac{V_2^2}{2c_p} = 349 - \frac{(290)^2}{2(1005)} = 307 \text{ K}$$

Then, although the flow itself is not isentropic, the local stagnation pressure is computed by the *local* isentropic condition

$$p_{02} = p_2\left(\frac{T_{02}}{T_2}\right)^{k/(k-1)} = (135)\left(\frac{349}{307}\right)^{3.5} = 211 \text{ kPa} \qquad \text{Ans. (g)}$$

This is 8 percent less than the upstream stagnation pressure p_{01}. Notice that, in this last part, we took advantage of the given information (T_{02}, p_2, V_2) to obtain p_{02} in an efficient manner. You may verify by comparison that approaching this part through the (unknown) Mach number Ma_2 is more laborious.

9.4 Isentropic Flow with Area Changes

By combining the isentropic- and/or adiabatic-flow relations with the equation of continuity we can study practical compressible-flow problems. This section treats the one-dimensional flow approximation.

Figure 9.4 illustrates the one-dimensional flow assumption. A real flow, Fig. 9.4a, has no slip at the walls and a velocity profile $V(x, y)$ which varies across the duct section (compare with Fig. 7.8). If, however, the area change is small and the wall radius of curvature large

$$\frac{dh}{dx} \ll 1 \qquad h(x) \ll R(x) \qquad (9.36)$$

then the flow is approximately one-dimensional, as in Fig. 9.4b, with $V \approx V(x)$ reacting to area change $A(x)$. Compressible-flow nozzles and diffusers do not always satisfy conditions (9.36), but we use the one-dimensional theory anyway because of its simplicity.

For steady one-dimensional flow the equation of continuity is, from Eq. (3.24),

$$\rho(x)V(x)A(x) = \dot{m} = \text{const} \qquad (9.37)$$

Before applying this to duct theory, we can learn a lot from the differential form of Eq. (9.37)

$$\frac{d\rho}{\rho} + \frac{dV}{V} + \frac{dA}{A} = 0 \qquad (9.38)$$

The differential forms of the frictionless momentum equation (9.31) and the sound-speed relation (9.15) are recalled here for convenience:
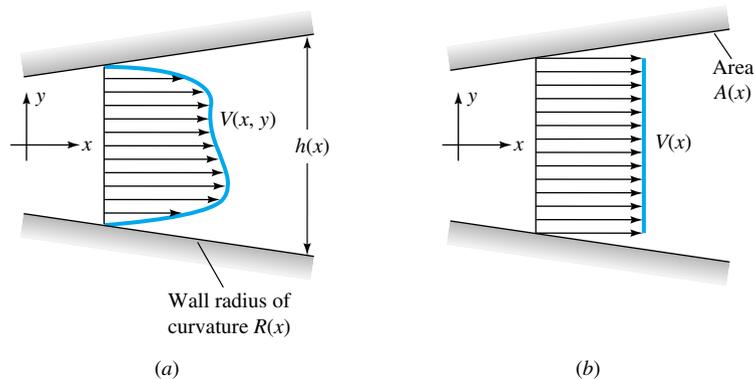
Fig. 9.4 Compressible flow through a duct: (a) real-fluid velocity profile; (b) one-dimensional approximation.

Duct geometry	Subsonic Ma < 1	Supersonic Ma > 1
$dA > 0$	$dV < 0$ $dp > 0$ Subsonic diffuser	$dV > 0$ $dp < 0$ Supersonic nozzle
$dA < 0$	$dV > 0$ $dp < 0$ Subsonic nozzle	$dV < 0$ $dp > 0$ Supersonic diffuser
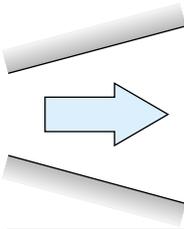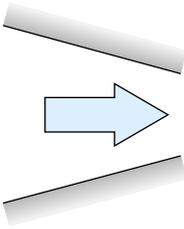
Fig. 9.5 Effect of Mach number on property changes with area change in duct flow.

Momentum
$$\frac{dp}{\rho} + V\,dV = 0$$

Sound speed:
$$dp = a^2\,d\rho$$

(9.39)

Now eliminate dp and $d\rho$ between Eqs. (9.38) and (9.39) to obtain the following relation between velocity change and area change in isentropic duct flow:

$$\frac{dV}{V} = \frac{dA}{A}\frac{1}{\mathrm{Ma}^2 - 1} = -\frac{dp}{\rho V^2}$$

(9.40)

Inspection of this equation, without actually solving it, reveals a fascinating aspect of compressible flow: Property changes are of opposite sign for subsonic and supersonic flow because of the term $\mathrm{Ma}^2 - 1$. There are four combinations of area change and Mach number, summarized in Fig. 9.5.

From earlier chapters we are used to subsonic behavior (Ma < 1): When area increases, velocity decreases and pressure increases, which is denoted a subsonic diffuser. But in supersonic flow (Ma > 1), the velocity actually increases when the area increases, a supersonic nozzle. The same opposing behavior occurs for an area decrease, which speeds up a subsonic flow and slows down a supersonic flow.

What about the sonic point Ma = 1? Since infinite acceleration is physically impossible, Eq. (9.40) indicates that dV can be finite only when $dA = 0$, that is, a minimum area (throat) or a maximum area (bulge). In Fig. 9.6 we patch together a throat section and a bulge section, using the rules from Fig. 9.5. The throat or converging-diverging section can smoothly accelerate a subsonic flow through sonic to supersonic flow, as in Fig. 9.6a. This is the only way a supersonic flow can be created by expanding the gas from a stagnant reservoir. The bulge section fails; the bulge Mach number moves away from a sonic condition rather than toward it.

Although supersonic flow downstream of a nozzle requires a sonic throat, the op-

Fig. 9.6 From Eq. (9.40), in flow through a throat (*a*) the fluid can accelerate smoothly through sonic and supersonic flow. In flow through the bulge (*b*) the flow at the bulge cannot be sonic on physical grounds.
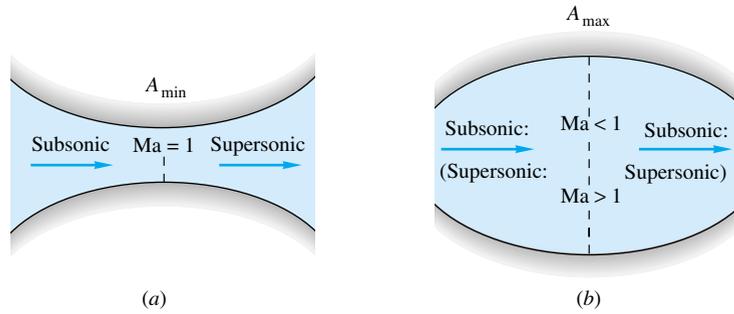
posite is not true: A compressible gas can pass through a throat section without becoming sonic.

Perfect-Gas Relations

We can use the perfect-gas and isentropic-flow relations to convert the continuity relation (9.37) into an algebraic expression involving only area and Mach number, as follows. Equate the mass flow at any section to the mass flow under sonic conditions (which may not actually occur in the duct)

$$\rho VA = \rho^* V^* A^*$$

or

$$\frac{A}{A^*} = \frac{\rho^*}{\rho} \frac{V^*}{V} \tag{9.41}$$

Both the terms on the right are functions only of Mach number for isentropic flow. From Eqs. (9.28) and (9.32)

$$\frac{\rho^*}{\rho} = \frac{\rho^*}{\rho_0} \frac{\rho_0}{\rho} = \left\{ \frac{2}{k + 1} \left[1 + \frac{1}{2} (k - 1) \, \text{Ma}^2 \right] \right\}^{1/(k-1)} \tag{9.42}$$

From Eqs. (9.26) and (9.32) we obtain

$$\frac{V^*}{V} = \frac{(kRT^*)^{1/2}}{V} = \frac{(kRT)^{1/2}}{V} \left(\frac{T^*}{T_0} \right)^{1/2} \left(\frac{T_0}{T} \right)^{1/2}$$

$$= \frac{1}{\text{Ma}} \left\{ \frac{2}{k + 1} \left[1 + \frac{1}{2} (k - 1) \, \text{Ma}^2 \right] \right\}^{1/2} \tag{9.43}$$

Combining Eqs. (9.41) to (9.43), we get the desired result

$$\frac{A}{A^*} = \frac{1}{\text{Ma}} \left[\frac{1 + \frac{1}{2}(k - 1) \, \text{Ma}^2}{\frac{1}{2}(k + 1)} \right]^{(1/2)(k+1)/(k-1)} \tag{9.44}$$

For $k = 1.4$, Eq. (9.44) takes the numerical form

$$\frac{A}{A^*} = \frac{1}{\text{Ma}} \frac{(1 + 0.2 \, \text{Ma}^2)^3}{1.728} \tag{9.45}$$

which is plotted in Fig. 9.7. Equations (9.45) and (9.34) enable us to solve any one-dimensional isentropic-airflow problem given, say, the shape of the duct $A(x)$ and the stagnation conditions and assuming that there are no shock waves in the duct.
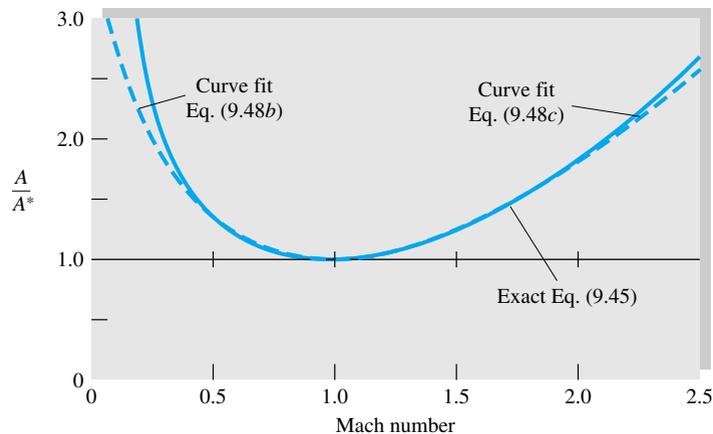
Fig. 9.7 Area ratio versus Mach number for isentropic flow of a perfect gas with $k = 1.4$.

Figure 9.7 shows that the minimum area which can occur in a given isentropic duct flow is the sonic, or critical, throat area. All other duct sections must have A greater than A^*. In many flows a critical sonic throat is not actually present, and the flow in the duct is either entirely subsonic or, more rarely, entirely supersonic.

Choking

From Eq. (9.41) the inverse ratio A^*/A equals $\rho V/(\rho^* V^*)$, the mass flow per unit area at any section compared with the critical mass flow per unit area. From Fig. 9.7 this inverse ratio rises from zero at $\mathrm{Ma} = 0$ to unity at $\mathrm{Ma} = 1$ and back down to zero at large Ma. Thus, for given stagnation conditions, the maximum possible mass flow passes through a duct when its throat is at the critical or sonic condition. The duct is then said to be *choked* and can carry no additional mass flow unless the throat is widened. If the throat is constricted further, the mass flow through the duct must decrease.

From Eqs. (9.32) and (9.33) the maximum mass flow is

$$\dot{m}_{max} = \rho^* A^* V^* = \rho_0 \left(\frac{2}{k+1} \right)^{1/(k-1)} A^* \left(\frac{2k}{k+1} RT_0 \right)^{1/2}$$

$$= k^{1/2} \left(\frac{2}{k+1} \right)^{(1/2)(k+1)/(k-1)} A^* \rho_0 (RT_0)^{1/2} \qquad (9.46a)$$

For $k = 1.4$ this reduces to

$$\dot{m}_{max} = 0.6847 A^* \rho_0 (RT_0)^{1/2} = \frac{0.6847 p_0 A^*}{(RT_0)^{1/2}} \qquad (9.46b)$$

For isentropic flow through a duct, the maximum mass flow possible is proportional to the throat area and stagnation pressure and inversely proportional to the square root of the stagnation temperature. These are somewhat abstract facts, so let us illustrate with some examples.

The Local Mass-Flow Function

Equation (9.46) gives the *maximum* mass flow, which occurs at the choking condition (sonic exit). It can be modified to predict the actual (nonmaximum) mass flow at any

section where local area A and pressure p are known.[1] The algebra is convoluted, so here we give only the final result, expressed in dimensionless form:

$$\text{Mass-flow function} = \frac{\dot{m}}{A}\frac{\sqrt{RT_0}}{p_0} = \sqrt{\frac{2k}{k-1}\left(\frac{p}{p_0}\right)^{2/k}\left[1-\left(\frac{p}{p_0}\right)^{(k-1)/k}\right]} \quad (9.47)$$

We stress that p and A in this relation are the *local* values at position x. As p/p_0 falls, this function rises rapidly and then levels out at the maximum of Eq. (9.46). A few values may be tabulated here for $k = 1.4$:

p/p_0	1.0	0.98	0.95	0.9	0.8	0.7	0.6	≤ 0.5283
Function	0.0	0.1978	0.3076	0.4226	0.5607	0.6383	0.6769	**0.6847**

Equation (9.47) is handy if stagnation conditions are known and the flow is not choked.

The only cumbersome algebra in these problems is the inversion of Eq. (9.45) to compute the Mach number when A/A^* is known. If available, EES is ideal for this situation and will yield Ma in a flash. In the absence of EES, the following curve-fitted formulas are suggested; given A/A^*, they estimate the Mach number within ± 2 percent for $k = 1.4$ if you stay within the ranges listed for each formula:

$$\text{Ma} \approx \begin{cases} \dfrac{1 + 0.27(A/A^*)^{-2}}{1.728A/A^*} & 1.34 < \dfrac{A}{A^*} < \infty & (9.48a) \\[2ex] 1 - 0.88\left(\ln\dfrac{A}{A^*}\right)^{0.45} & 1.0 < \dfrac{A}{A^*} < 1.34 & (9.48b) \\[2ex] 1 + 1.2\left(\dfrac{A}{A^*} - 1\right)^{1/2} & 1.0 < \dfrac{A}{A^*} < 2.9 & (9.48c) \\[2ex] \left[216\dfrac{A}{A^*} - 254\left(\dfrac{A}{A^*}\right)^{2/3}\right]^{1/5} & 2.9 < \dfrac{A}{A^*} < \infty & (9.48d) \end{cases}$$

with braces labeled: subsonic flow for (9.48a) and (9.48b); supersonic flow for (9.48c) and (9.48d).

Formulas (9.48a) and (9.48d) are asymptotically correct as $A/A^* \to \infty$, while (9.48b) and (9.48c) are just curve fits. However, formulas (9.48b) and (9.48c) are seen in Fig. 9.7 to be accurate within their recommended ranges.

Note that two solutions are possible for a given A/A^*, one subsonic and one supersonic. The proper solution cannot be selected without further information, e.g., known pressure or temperature at the given duct section.

EXAMPLE 9.4

Air flows isentropically through a duct. At section 1 the area is 0.05 m² and $V_1 = 180$ m/s, $p_1 = 500$ kPa, and $T_1 = 470$ K. Compute (a) T_0, (b) Ma_1, (c) p_0, and (d) both A^* and $\dot{m}$. If at section 2 the area is 0.036 m², compute Ma_2 and p_2 if the flow is (e) subsonic or (f) supersonic. Assume $k = 1.4$.

Solution

Part (a) A general sketch of the problem is shown in Fig. E9.4. With V_1 and T_1 known, the energy equation (9.23) gives

---

[1] The author is indebted to Georges Aigret, of Chimay, Belgium, for suggesting this useful function.
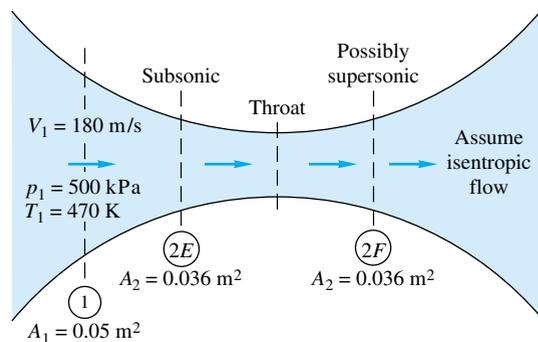
E9.4

$$T_0 = T_1 + \frac{V_1^2}{2c_p} = 470 + \frac{(180)^2}{2(1005)} = 486 \text{ K} \qquad \text{Ans. (a)}$$

Part (b)

The local sound speed $a_1 = \sqrt{kRT_1} = [(1.4)(287)(470)]^{1/2} = 435$ m/s. Hence

$$\text{Ma}_1 = \frac{V_1}{a_1} = \frac{180}{435} = 0.414 \qquad \text{Ans. (b)}$$

Part (c)

With Ma_1 known, the stagnation pressure follows from Eq. (9.34):

$$p_0 = p_1(1 + 0.2\,\text{Ma}_1^2)^{3.5} = (500 \text{ kPa})[1 + 0.2(0.414)^2]^{3.5} = 563 \text{ kPa} \qquad \text{Ans. (c)}$$

Part (d)

Similarly, from Eq. (9.45), the critical sonic-throat area is

$$\frac{A_1}{A^*} = \frac{(1 + 0.2\,\text{Ma}_1^2)^3}{1.728\,\text{Ma}_1} = \frac{[1 + 0.2(0.414)^2]^3}{1.728(0.414)} = 1.547$$

or

$$A^* = \frac{A_1}{1.547} = \frac{0.05 \text{ m}^2}{1.547} = 0.0323 \text{ m}^2 \qquad \text{Ans. (d)}$$

This throat must *actually be present* in the duct if the flow is to become supersonic.

We now know A^*. So to compute the mass flow we can use Eq. (9.46), which remains valid, based on the numerical value of A^*, whether or not a throat actually exists:

$$\dot{m} = 0.6847 \frac{p_0 A^*}{\sqrt{RT_0}} = 0.6847 \frac{(563{,}000)(0.0323)}{\sqrt{(287)(486)}} = 33.4 \text{ kg/s} \qquad \text{Ans. (d)}$$

Or we could fare equally well with our new "local mass flow" formula, Eq. (9.47), using, say, the pressure and area at section 1. Given $p_1/p_0 = 500/563 = 0.889$, Eq. (9.47) yields

$$\dot{m} \frac{\sqrt{287(486)}}{563{,}000(0.05)} = \sqrt{\frac{2(1.4)}{0.4}} (0.889)^{2/1.4}[1 - (0.889)^{0.4/1.4}] = 0.447 \qquad \dot{m} = 33.4 \frac{\text{kg}}{\text{s}} \quad \text{Ans. (d)}$$

Part (e)

EES

Assume *subsonic* flow corresponds to section 2E in Fig. E9.4. The duct contracts to an area ratio $A_2/A^* = 0.036/0.0323 = 1.115$, which we find on the left side of Fig. 9.7 or the subsonic part of Table B.1. Neither the figure nor the table is that accurate. There are two accurate options. First, Eq. (9.48b) gives the estimate $\text{Ma}_2 \approx 1 - 0.88 \ln (1.115)^{0.45} \approx 0.676$ (error less than 0.5 percent). Second, EES (App. E) will give an arbitrarily accurate solution with only three statements (in SI units):

```
A2 = 0.036
Astar = 0.0323
A2/Astar = (1+0.2*Ma2^2)^3/1.2^3/Ma2
```

Specify that you want a *subsonic* solution (e.g., limit $Ma_2 < 1$), and EES reports

$$Ma_2 = \mathbf{0.6758} \qquad\qquad Ans.\ (e)$$

[Ask for a supersonic solution and you receive $Ma_2 = 1.4001$, which is the answer to part (*f*).] The pressure is given by the isentropic relation

$$p_2 = \frac{p_0}{[1 + 0.2(0.676)^2]^{3.5}} = \frac{563 \text{ kPa}}{1.358} \approx 415 \text{ kPa} \qquad Ans.\ (e)$$

Part (*e*) does *not* require a throat, sonic or otherwise; the flow could simply be contracting subsonically from A_1 to A_2.

Part (f) This time assume *supersonic* flow, corresponding to section 2F in Fig. E9.4. Again the area ratio is $A_2/A^* = 0.036/0.0323 = 1.115$, and we look on the *right* side of Fig. 9.7 or the supersonic part of Table B.1—the latter can be read quite accurately as $Ma_2 \approx 1.40$. Again there are two other accurate options. First, Eq. (9.48*c*) gives the curve-fit estimate $Ma_2 \approx 1 + 1.2(1.115 - 1)1^{1/2} \approx 1.407$, only 0.5 percent high. Second, EES will give a very accurate solution with the same three statements from part (*e*). Specify that you want a *supersonic* solution (e.g., limit $Ma_2 > 1$), and EES reports

$$Ma_2 = \mathbf{1.4001} \qquad\qquad Ans.\ (f)$$

Again the pressure is given by the isentropic relation at the new Mach number:

$$p_2 = \frac{p_0}{[1 + 0.2(1.4001)^2]^{3.5}} = \frac{563 \text{ kPa}}{3.183} = 177 \text{ kPa} \qquad Ans.\ (f)$$

Note that the supersonic-flow pressure level is much less than p_2 in part (*e*), and a sonic throat *must* have occurred between sections 1 and 2F.

EXAMPLE 9.5

It is desired to expand air from $p_0 = 200$ kPa and $T_0 = 500$ K through a throat to an exit Mach number of 2.5. If the desired mass flow is 3 kg/s, compute (*a*) the throat area and the exit (*b*) pressure, (*c*) temperature, (*d*) velocity, and (*e*) area, assuming isentropic flow, with $k = 1.4$.

Solution

The throat area follows from Eq. (9.47), because the throat flow must be sonic to produce a supersonic exit:

$$A^* = \frac{\dot{m}(RT_0)^{1/2}}{0.6847 p_0} = \frac{3.0[287(500)]^{1/2}}{0.6847(200{,}000)} = 0.00830 \text{ m}^2 = \frac{1}{4}\,\pi D^{*2}$$

or

$$D_{\text{throat}} = 10.3 \text{ cm} \qquad\qquad Ans.\ (a)$$

With the exit Mach number known, the isentropic-flow relations give the pressure and temperature:

$$p_e = \frac{p_0}{[1 + 0.2(2.5)^2]^{3.5}} = \frac{200{,}000}{17.08} = 11{,}700 \text{ Pa} \qquad Ans.\ (b)$$

$$T_e = \frac{T_0}{1 + 0.2(2.5)^2} = \frac{500}{2.25} = 222 \text{ K} \qquad\qquad Ans.\ (c)$$

The exit velocity follows from the known Mach number and temperature

$$V_e = \text{Ma}_e \ (kRT_e)^{1/2} = 2.5[1.4(287)(222)]^{1/2} = 2.5(299 \text{ m/s}) = 747 \text{ m/s} \qquad Ans. \ (d)$$

The exit area follows from the known throat area and exit Mach number and Eq. (9.45):

$$\frac{A_e}{A^*} = \frac{[1 + 0.2(2.5)^2]^3}{1.728(2.5)} = 2.64$$

or

$$A_e = 2.64A^* = 2.64(0.0083 \text{ m}^2) = 0.0219 \text{ m}^2 = \tfrac{1}{4}\pi D_e^2$$

or

$$D_e = 16.7 \text{ cm} \qquad\qquad Ans. \ (e)$$

One point might be noted: The computation of the throat area A^* did not depend in any way on the numerical value of the exit Mach number. The exit was supersonic; therefore the throat is sonic and choked, and no further information is needed.

9.5 The Normal-Shock Wave

A common irreversibility occurring in supersonic internal or external flows is the normal-shock wave sketched in Fig. 9.8. Except at near-vacuum pressures such shock waves are very thin (a few micrometers thick) and approximate a discontinuous change in flow properties. We select a control volume just before and after the wave, as in Fig. 9.8.

The analysis is identical to that of Fig. 9.1; i.e., a shock wave is a fixed strong pressure wave. To compute all property changes rather than just the wave speed, we use all our basic one-dimensional steady-flow relations, letting section 1 be upstream and section 2 be downstream:

$$\rho_1 V_1 = \rho_2 V_2 = G = \text{const} \tag{9.49a}$$

$$p_1 - p_2 = \rho_2 V_2^2 - \rho_1 V_1^2 \tag{9.49b}$$

Energy:
$$h_1 + \tfrac{1}{2}V_1^2 = h_2 + \tfrac{1}{2}V_2^2 = h_0 = \text{const} \tag{9.49c}$$

Perfect gas:
$$\frac{p_1}{\rho_1 T_1} = \frac{p_2}{\rho_2 T_2} \tag{9.49d}$$

Constant c_p:
$$h = c_p T \qquad k = \text{const} \tag{9.49e}$$

Note that we have canceled out the areas $A_1 \approx A_2$, which is justified even in a variable duct section because of the thinness of the wave. The first successful analyses of these normal-shock relations are credited to W. J. M. Rankine (1870) and A. Hugoniot (1887), hence the modern term *Rankine-Hugoniot relations*. If we assume that the upstream conditions (p_1, V_1, ρ_1, h_1, T_1) are known, Eqs. (9.49) are five algebraic relations in the five unknowns (p_2, V_2, ρ_2, h_2, T_2). Because of the velocity-squared term, two solutions are found, and the correct one is determined from the second law of thermodynamics, which requires that $s_2 > s_1$.

The velocities V_1 and V_2 can be eliminated from Eqs. (9.49a) to (9.49c) to obtain the Rankine-Hugoniot relation

$$h_2 - h_1 = \frac{1}{2} \ (p_2 - p_1)\left(\frac{1}{\rho_2} + \frac{1}{\rho_1}\right) \tag{9.50}$$
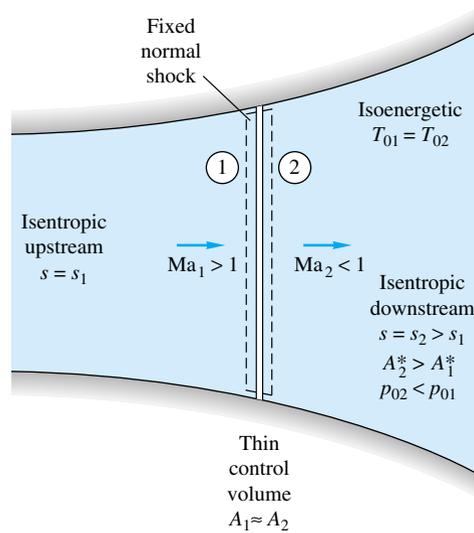
Fig. 9.8 Flow through a fixed normal-shock wave.

This contains only thermodynamic properties and is independent of the equation of state. Introducing the perfect-gas law $h = c_p T = kp/[(k-1)\rho]$, we can rewrite this as

$$\frac{\rho_2}{\rho_1} = \frac{1 + \beta p_2/p_1}{\beta + p_2/p_1} \qquad \beta = \frac{k+1}{k-1} \tag{9.51}$$

We can compare this with the isentropic-flow relation for a very weak pressure wave in a perfect gas

$$\frac{\rho_2}{\rho_1} = \left(\frac{p_2}{p_1}\right)^{1/k} \tag{9.52}$$

Also, the actual change in entropy across the shock can be computed from the perfect-gas relation

$$\frac{s_2 - s_1}{c_v} = \ln\left[\frac{p_2}{p_1}\left(\frac{\rho_1}{\rho_2}\right)^k\right] \tag{9.53}$$

Assuming a given wave strength p_2/p_1, we can compute the density ratio and the entropy change and list them as follows for $k = 1.4$:

$\dfrac{p_2}{p_1}$	ρ_2/ρ_1		$\dfrac{s_2 - s_1}{c_v}$
	Eq. (9.51)	**Isentropic**	
0.5	0.6154	0.6095	−0.0134
0.9	0.9275	0.9275	−0.00005
1.0	1.0	1.0	0.0
1.1	1.00704	1.00705	0.00004
1.5	1.3333	1.3359	0.0027
2.0	1.6250	1.6407	0.0134

We see that the entropy change is negative if the pressure decreases across the shock, which violates the second law. Thus a rarefaction shock is impossible in a perfect gas.[2] We see also that weak-shock waves ($p_2/p_1 \leq 2.0$) are very nearly isentropic.

Mach-Number Relations

For a perfect gas all the property ratios across the normal shock are unique functions of k and the upstream Mach number Ma_1. For example, if we eliminate ρ_2 and V_2 from Eqs. (9.49a) to (9.49c) and introduce $h = kp/[(k - 1)\rho]$, we obtain

$$\frac{p_2}{p_1} = \frac{1}{k + 1}\left[\frac{2\rho_1 V_1^2}{p_1} - (k - 1)\right] \tag{9.54}$$

But for a perfect gas $\rho_1 V_1^2/p_1 = kV_1^2/(kRT_1) = k\,Ma_1^2$, so that Eq. (9.54) is equivalent to

$$\frac{p_2}{p_1} = \frac{1}{k + 1}[2k\,Ma_1^2 - (k - 1)] \tag{9.55}$$

From this equation we see that, for any k, $p_2 > p_1$ only if $Ma_1 > 1.0$. Thus for flow through a normal-shock wave, the upstream Mach number must be supersonic to satisfy the second law of thermodynamics.

What about the downstream Mach number? From the perfect-gas identity $\rho V^2 = kp\,Ma^2$, we can rewrite Eq. (9.49b) as

$$\frac{p_2}{p_1} = \frac{1 + k\,Ma_1^2}{1 + k\,Ma_2^2} \tag{9.56}$$

which relates the pressure ratio to both Mach numbers. By equating Eqs. (9.55) and (9.56) we can solve for

$$Ma_2^2 = \frac{(k - 1)\,Ma_1^2 + 2}{2k\,Ma_1^2 - (k - 1)} \tag{9.57}$$

Since Ma_1 must be supersonic, this equation predicts for all $k > 1$ that Ma_2 must be subsonic. Thus a normal-shock wave decelerates a flow almost discontinuously from supersonic to subsonic conditions.

Further manipulation of the basic relations (9.49) for a perfect gas gives additional equations relating the change in properties across a normal-shock wave in a perfect gas

$$\frac{\rho_2}{\rho_1} = \frac{(k + 1)\,Ma_1^2}{(k - 1)\,Ma_1^2 + 2} = \frac{V_1}{V_2}$$

$$\frac{T_2}{T_1} = [2 + (k - 1)\,Ma_1^2]\frac{2k\,Ma_1^2 - (k - 1)}{(k + 1)^2\,Ma_1^2} \tag{9.58}$$

$$T_{02} = T_{01}$$

$$\frac{p_{02}}{p_{01}} = \frac{\rho_{02}}{\rho_{01}} = \left[\frac{(k + 1)\,Ma_1^2}{2 + (k - 1)\,Ma_1^2}\right]^{k/(k-1)}\left[\frac{k + 1}{2k\,Ma_1^2 - (k - 1)}\right]^{1/(k-1)}$$

Of additional interest is the fact that the critical, or sonic, throat area A^* in a duct increases across a normal shock

---

[2] This is true also for most real gases; see Ref. 14, sec. 7.3.

$$\frac{A_2^*}{A_1^*} = \frac{Ma_2}{Ma_1}\left[\frac{2+(k-1)\,Ma_1^2}{2+(k-1)\,Ma_2^2}\right]^{(1/2)(k+1)/(k-1)} \tag{9.59}$$

All these relations are given in Table B.2 and plotted versus upstream Mach number Ma_1 in Fig. 9.9 for $k = 1.4$. We see that pressure increases greatly while temperature and density increase moderately. The effective throat area A^* increases slowly at first and then rapidly. The failure of students to account for this change in A^* is a common source of error in shock calculations.

The stagnation temperature remains the same, but the stagnation pressure and density decrease in the same ratio; i.e., the flow across the shock is adiabatic but non-isentropic. Other basic principles governing the behavior of shock waves can be summarized as follows:

1. The upstream flow is supersonic, and the downstream flow is subsonic.
2. For perfect gases (and also for real fluids except under bizarre thermodynamic conditions) rarefaction shocks are impossible, and only a compression shock can exist.
3. The entropy increases across a shock with consequent decreases in stagnation pressure and stagnation density and an increase in the effective sonic-throat area.
4. Weak shock waves are very nearly isentropic.

Normal-shock waves form in ducts under transient conditions, e.g., shock tubes, and in steady flow for certain ranges of the downstream pressure. Figure 9.10*a* shows a normal shock in a supersonic nozzle. Flow is from left to right. The oblique wave pattern to the left is formed by roughness elements on the nozzle walls and indicates that the upstream flow is supersonic. Note the absence of these Mach waves (see Sec. 9.10) in the subsonic flow downstream.
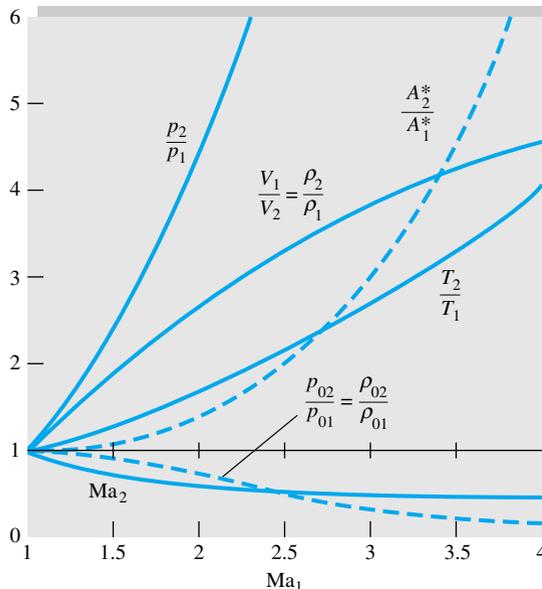
Fig. 9.9 Change in flow properties across a normal-shock wave for $k = 1.4$.

(a)
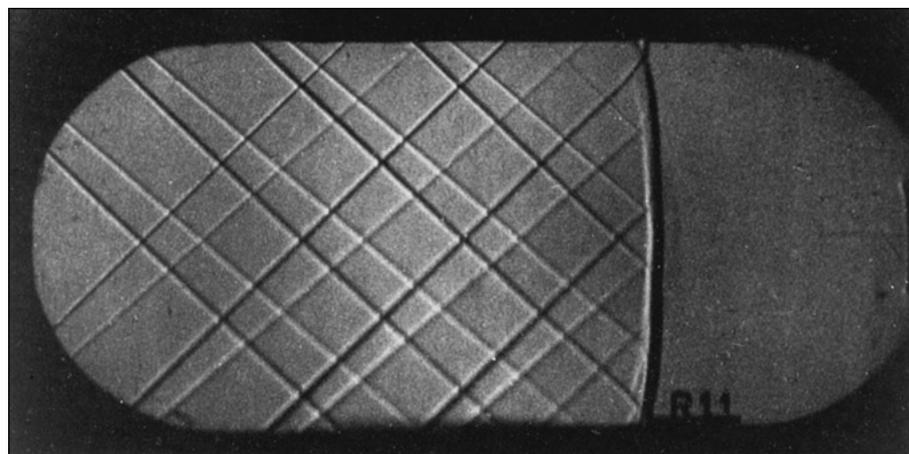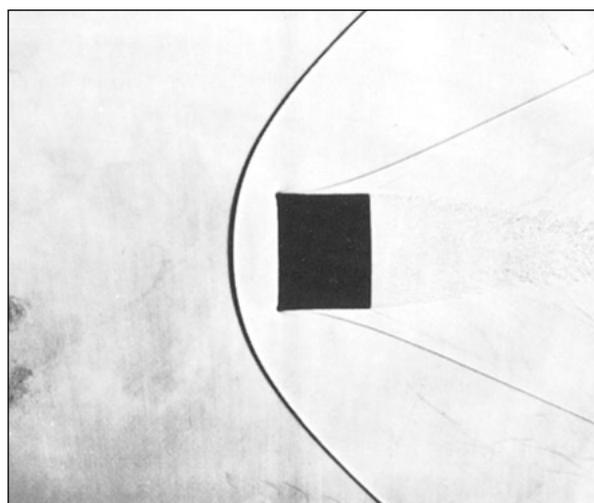
Fig. 9.10 Normal shocks form in both internal and external flows: (a) Normal shock in a duct; note the Mach-wave pattern to the left (upstream), indicating supersonic flow. *(Courtesy of U.S. Air Force Arnold Engineering Development Center.)* (b) Supersonic flow past a blunt body creates a normal shock at the nose; the apparent shock thickness and body-corner curvature are optical distortions. *(Courtesy of U.S. Army Ballistic Research Laboratory, Aberdeen Proving Ground.)*

(b)

Normal-shock waves occur not only in supersonic duct flows but also in a variety of supersonic external flows. An example is the supersonic flow past a blunt body shown in Fig. 9.10b. The bow shock is curved, with a portion in front of the body which is essentially normal to the oncoming flow. This normal portion of the bow shock satisfies the property-change conditions just as outlined in this section. The flow inside the shock near the body nose is thus subsonic and at relatively high temperature $T_2 > T_1$, and convective heat transfer is especially high in this region.

Each nonnormal portion of the bow shock in Fig. 9.10b satisfies the oblique-shock relations to be outlined in Sec. 9.9. Note also the oblique recompression shock on the sides of the body. What has happened is that the subsonic nose flow has accelerated around the corners back to supersonic flow at low pressure, which must then pass through the second shock to match the higher downstream pressure conditions.

Note the fine-grained turbulent wake structure in the rear of the body in Fig. 9.10b. The turbulent boundary layer along the sides of the body is also clearly visible.

The analysis of a complex multidimensional supersonic flow such as in Fig. 9.10 is beyond the scope of this book. For further information see, e.g., Ref. 14, chap. 9, or Ref. 8, chap. 16.

Moving Normal Shocks

The preceding analysis of the fixed shock applies equally well to the moving shock if we reverse the transformation used in Fig. 9.1. To make the upstream conditions simulate a still fluid, we move the shock of Fig. 9.8 to the left at speed V_1; that is, we fix our coordinates to a control volume moving with the shock. The downstream flow then appears to move to the left at a slower speed $V_1 - V_2$ following the shock. The thermodynamic properties are not changed by this transformation, so that all our Eqs. (9.50) to (9.59) are still valid.
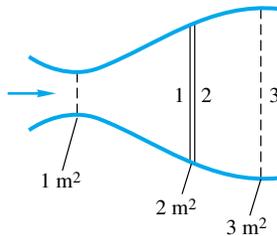
EXAMPLE 9.6

Air flows from a reservoir where $p = 300$ kPa and $T = 500$ K through a throat to section 1 in Fig. E9.6, where there is a normal-shock wave. Compute (a) p_1, (b) p_2, (c) p_{02}, (d) A_2^*, (e) p_{03}, (f) A_3^*, (g) p_3, (h) T_{03}, and (i) T_3.

Solution

E9.6

The reservoir conditions are the stagnation properties, which, for assumed one-dimensional adiabatic frictionless flow, hold through the throat up to section 1

$$p_{01} = 300 \text{ kPa} \qquad T_{01} = 500 \text{ K}$$

A shock wave cannot exist unless Ma_1 is supersonic; therefore the flow must have accelerated through a throat which is sonic

$$A_t = A_1^* = 1 \text{ m}^2$$

We can now find the Mach number Ma_1 from the known isentropic area ratio

$$\frac{A_1}{A_1^*} = \frac{2 \text{ m}^2}{1 \text{ m}^2} = 2.0$$

From Eq. (9.48c)

$$Ma_1 \approx 1 + 1.2(2.0 - 1)^{1/2} = 2.20$$

Further iteration with Eq. (9.45) would give $Ma_1 = 2.1972$, showing that Eq. (9.48c) gives satisfactory accuracy. The pressure p_1 follows from the isentropic relation (9.28) (or Table B.1)

$$\frac{p_{01}}{p_1} = [1 + 0.2(2.20)^2]^{3.5} = 10.7$$

or $$p_1 = \frac{300 \text{ kPa}}{10.7} = 28.06 \text{ kPa} \qquad\qquad Ans. (a)$$

The pressure p_2 is now obtained from Ma_1 and the normal-shock relation (9.55) or Table B.2

$$\frac{p_2}{p_1} = \frac{1}{2.4}[2.8(2.20)^2 - 0.4] = 5.48$$

or $$p_2 = 5.48(28.06) = 154 \text{ kPa}$$ Ans. (b)

In similar manner, for $Ma_1 = 2.20$, $p_{02}/p_{01} = 0.628$ from Eq. (9.58) and $A_2^*/A_1^* = 1.592$ from Eq. (9.59), or we can read Table B.2 for these values. Thus

$$p_{02} = 0.628(300 \text{ kPa}) = 188 \text{ kPa}$$ Ans. (c)

$$A_2^* = 1.592(1 \text{ m}^2) = 1.592 \text{ m}^2$$ Ans. (d)

The flow from section 2 to 3 is isentropic (but at higher entropy than the flow upstream of the shock). Thus

$$p_{03} = p_{02} = 188 \text{ kPa}$$ Ans. (e)

$$A_3^* = A_2^* = 1.592 \text{ m}^2$$ Ans. (f)

Knowing A_3^*, we can now compute p_3 by finding Ma_3 and without bothering to find Ma_2 (which happens to equal 0.547). The area ratio at section 3 is

$$\frac{A_3}{A_3^*} = \frac{3 \text{ m}^2}{1.592 \text{ m}^2} = 1.884$$

Then, since Ma_3 is known to be subsonic because it is downstream of a normal shock, we use Eq. (9.48a) to estimate

$$Ma_3 \approx \frac{1 + 0.27/(1.884)^2}{1.728(1.884)} = 0.330$$

The pressure p_3 then follows from the isentropic relation (9.28) or Table B.1

$$\frac{p_{03}}{p_3} = [1 + 0.2(0.330)^2]^{3.5} = 1.078$$

or $$p_3 = \frac{188 \text{ kPa}}{1.078} = 174 \text{ kPa}$$ Ans. (g)

Meanwhile, the flow is adiabatic throughout the duct; thus

$$T_{01} = T_{02} = T_{03} = 500 \text{ K}$$ Ans. (h)

Therefore, finally, from the adiabatic relation (9.26)

$$\frac{T_{03}}{T_3} = 1 + 0.2(0.330)^2 = 1.022$$

or $$T_3 = \frac{500 \text{ K}}{1.022} = 489 \text{ K}$$ Ans. (i)

Notice that this type of duct-flow problem, with or without a shock wave, requires straightforward application of algebraic perfect-gas relations coupled with a little thought given to which formula is appropriate for the particular situation.

EXAMPLE 9.7

An explosion in air, $k = 1.4$, creates a spherical shock wave propagating radially into still air at standard conditions. At the instant shown in Fig. E9.7, the pressure just inside the shock is 200 lbf/in² absolute. Estimate (a) the shock speed C and (b) the air velocity V just inside the shock.

E9.7

C

$p = 14.7$ 1bf/in² abs
$T = 520°$ R

200 1bf/in² abs

V

POW!
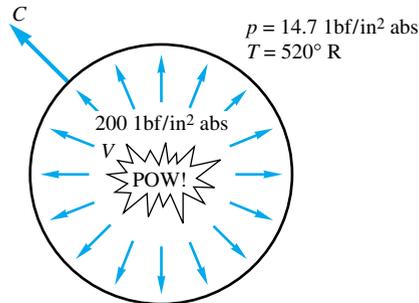
Solution

Part (a) In spite of the spherical geometry the flow across the shock moves normal to the spherical wavefront; hence the normal-shock relations (9.50) to (9.59) apply. Fixing our control volume to the moving shock, we find that the proper conditions to use in Fig. 9.8 are

$$C = V_1 \qquad p_1 = 14.7 \text{ lbf/in}^2 \text{ absolute} \qquad T_1 = 520°\text{R}$$

$$V = V_1 - V_2 \qquad p_2 = 200 \text{ lbf/in}^2 \text{ absolute}$$

The speed of sound outside the shock is $a_1 \approx 49 T_1^{1/2} = 1117$ ft/s. We can find Ma_1 from the known pressure ratio across the shock

$$\frac{p_2}{p_1} = \frac{200 \text{ lbf/in}^2 \text{ absolute}}{14.7 \text{ lbf/in}^2 \text{ absolute}} = 13.61$$

From Eq. (9.55) or Table B.2

$$13.61 = \frac{1}{2.4}(2.8 \text{ Ma}_1^2 - 0.4) \qquad \text{or} \qquad \text{Ma}_1 = 3.436$$

Then, by definition of the Mach number,

$$C = V_1 = \text{Ma}_1 \, a_1 = 3.436(1117 \text{ ft/s}) = 3840 \text{ ft/s} \qquad \qquad Ans. \ (a)$$

Part (b) To find V_2, we need the temperature or sound speed inside the shock. Since Ma_1 is known, from Eq. (9.58) or Table B.2 for $Ma_1 = 3.436$ we compute $T_2/T_1 = 3.228$. Then

$$T_2 = 3.228 T_1 = 3.228(520°\text{R}) = 1679°\text{R}$$

At such a high temperature we should account for non-perfect-gas effects or at least use the gas tables [16], but we won't. Here just estimate from the perfect-gas energy equation (9.23) that

$$V_2^2 = 2c_p(T_1 - T_2) + V_1^2 = 2(6010)(520 - 1679) + (3840)^2 = 815,000$$

or $$V_2 \approx 903 \text{ ft/s}$$

Notice that we did this without bothering to compute Ma_2, which equals 0.454, or $a_2 \approx 49 T_2^{1/2} = 2000$ ft/s.

Finally, the air velocity behind the shock is

$$V = V_1 - V_2 = 3840 - 903 \approx 2940 \text{ ft/s} \qquad \textit{Ans. (b)}$$

Thus a powerful explosion creates a brief but intense blast wind as it passes.[3]

9.6 Operation of Converging and Diverging Nozzles

By combining the isentropic-flow and normal-shock relations plus the concept of sonic throat choking, we can outline the characteristics of converging and diverging nozzles.

Converging Nozzle

First consider the converging nozzle sketched in Fig. 9.11a. There is an upstream reservoir at stagnation pressure p_0. The flow is induced by lowering the downstream outside, or *back*, pressure p_b below p_0, resulting in the sequence of states a to e shown in Fig. 9.11b and c.

For a moderate drop in p_b to states a and b, the throat pressure is higher than the critical value p^* which would make the throat sonic. The flow in the nozzle is subsonic throughout, and the jet exit pressure p_e equals the back pressure p_b. The mass flow is predicted by subsonic isentropic theory and is less than the critical value $\dot{m}_{max}$, as shown in Fig. 9.11c.

For condition c, the back pressure exactly equals the critical pressure p^* of the throat. The throat becomes sonic, the jet exit flow is sonic, $p_e = p_b$, and the mass flow equals its maximum value from Eq. (9.46). The flow upstream of the throat is subsonic everywhere and predicted by isentropic theory based on the local area ratio $A(x)/A^*$ and Table B.1.

Finally, if p_b is lowered further to conditions d or e below p^*, the nozzle cannot respond further because it is choked at its maximum throat mass flow. The throat remains sonic with $p_e = p^*$, and the nozzle-pressure distribution is the same as in state c, as sketched in Fig. 9.11b. The exit jet expands supersonically so that the jet pressure can be reduced from p^* down to p_b. The jet structure is complex and multidimensional and is not shown here. Being supersonic, the jet cannot send any signal upstream to influence the choked flow conditions in the nozzle.

If the stagnation plenum chamber is large or supplemented by a compressor, and if the discharge chamber is larger or supplemented by a vacuum pump, the converging-nozzle flow will be steady or nearly so. Otherwise the nozzle will be blowing down, with p_0 decreasing and p_b increasing, and the flow states will be changing from, say, state e backward to state a. Blowdown calculations are usually made by a quasi-steady analysis based on isentropic steady-flow theory for the instantaneous pressures $p_0(t)$ and $p_b(t)$.

EXAMPLE 9.8

A converging nozzle has a throat area of 6 cm^2 and stagnation air conditions of 120 kPa and 400 K. Compute the exit pressure and mass flow if the back pressure is (a) 90 kPa and (b) 45 kPa. Assume $k = 1.4$.

---

[3] This is the principle of the *shock-tube wind tunnel*, in which a controlled explosion creates a brief flow at very high Mach number, with data taken by fast-response instruments. See, e.g., Ref. 5, sec. 4.5.
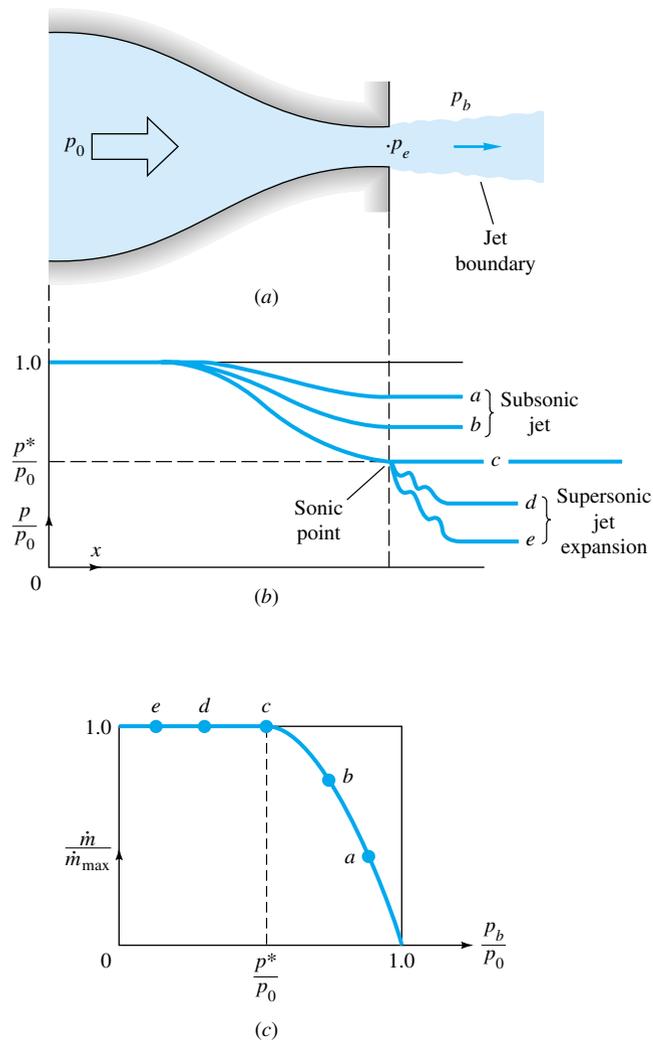
Fig. 9.11 Operation of a converging nozzle: (a) nozzle geometry showing characteristic pressures; (b) pressure distribution caused by various back pressures; (c) mass flow versus back pressure.

Solution

From Eq. (9.32) for $k = 1.4$ the critical (sonic) throat pressure is

$$\frac{p^*}{p_0} = 0.5283 \qquad \text{or} \qquad p^* = (0.5283)(120 \text{ kPa}) = 63.4 \text{ kPa}$$

If the back pressure is less than this amount, the nozzle flow is choked.

Part (a) For $p_b = 90$ kPa $> p^*$, the flow is subsonic, not choked. The exit pressure is $p_e = p_b$. The throat Mach number is found from the isentropic relation (9.35) or Table B.1:

$$\text{Ma}_e^2 = 5\left[\left(\frac{p_0}{p_e}\right)^{2/7} - 1\right] = 5\left[\left(\frac{120}{90}\right)^{2/7} - 1\right] = 0.4283 \qquad \text{Ma}_e = 0.654$$

To find the mass flow, we could proceed with a serial attack on Ma_e, T_e, a_e, V_e, and ρ_e, hence

to compute $\rho_e A_e V_e$. However, since the local pressure is known, this part is ideally suited for the dimensionless mass-flow function in Eq. (9.47). With $p_e/p_0 = 90/120 = 0.75$, compute

$$\frac{\dot{m}\sqrt{RT_0}}{Ap_0} = \sqrt{\frac{2(1.4)}{0.4}(0.75)^{2/1.4}[1 - (0.75)^{0.4/1.4}]} = 0.6052$$

hence
$$\dot{m} = 0.6052\frac{(0.0006)(120,000)}{\sqrt{287(400)}} = 0.129 \text{ kg/s} \qquad \qquad \text{Ans. (a)}$$

for
$$p_e = p_b = 90 \text{ kPa} \qquad \qquad \text{Ans. (a)}$$

Part (b) For $p_b = 45$ kPa $< p^*$, the flow is choked, similar to condition d in Fig. 9.11b. The exit pressure is sonic:

$$p_e = p^* = 63.4 \text{ kPa} \qquad \qquad \text{Ans. (b)}$$

The (choked) mass flow is a maximum from Eq. (9.46b):

$$\dot{m} = \dot{m}_{\max} = \frac{0.6847 p_0 A_e}{(RT_0)^{1/2}} = \frac{0.6847(120,000)(0.0006)}{[287(400)]^{1/2}} = 0.145 \text{ kg/s} \qquad \text{Ans. (b)}$$

Any back pressure less than 63.4 kPa would cause this same choked mass flow. Note that the 50 percent increase in exit Mach number, from 0.654 to 1.0, has increased the mass flow only 12 percent, from 0.128 to 0.145 kg/s.

Converging-Diverging Nozzle

Now consider the converging-diverging nozzle sketched in Fig. 9.12a. If the back pressure p_b is low enough, there will be supersonic flow in the diverging portion and a variety of shock-wave conditions may occur, which are sketched in Fig. 9.12b. Let the back pressure be gradually decreased.

For curves A and B in Fig. 9.12b the back pressure is not low enough to induce sonic flow in the throat, and the flow in the nozzle is subsonic throughout. The pressure distribution is computed from subsonic isentropic area-change relations, e.g., Table B.1. The exit pressure $p_e = p_b$, and the jet is subsonic.

For curve C the area ratio A_e/A_t exactly equals the critical ratio A_e/A^* for a subsonic Ma_e in Table B.1. The throat becomes sonic, and the mass flux reaches a maximum in Fig. 9.12c. The remainder of the nozzle flow is subsonic, including the exit jet, and $p_e = p_b$.

Now jump for a moment to curve H. Here p_b is such that p_b/p_0 exactly corresponds to the critical-area ratio A_e/A^* for a *supersonic* Ma_e in Table B.1. The diverging flow is entirely supersonic, including the jet flow, and $p_e = p_b$. This is called the *design pressure ratio* of the nozzle and is the back pressure suitable for operating a supersonic wind tunnel or an efficient rocket exhaust.

Now back up and suppose that p_b lies between curves C and H, which is impossible according to purely isentropic-flow calculations. Then back pressures D to F occur in Fig. 9.12b. The throat remains choked at the sonic value, and we can match $p_e = p_b$ by placing a normal shock at just the right place in the diverging section to cause a *subsonic-diffuser* flow back to the back-pressure condition. The mass flow remains at maximum in Fig. 9.12c. At back pressure F the required normal shock stands in the duct exit. At back pressure G no single normal shock can do the job, and so the flow compresses outside the exit in a complex series of oblique shocks until it matches p_b.
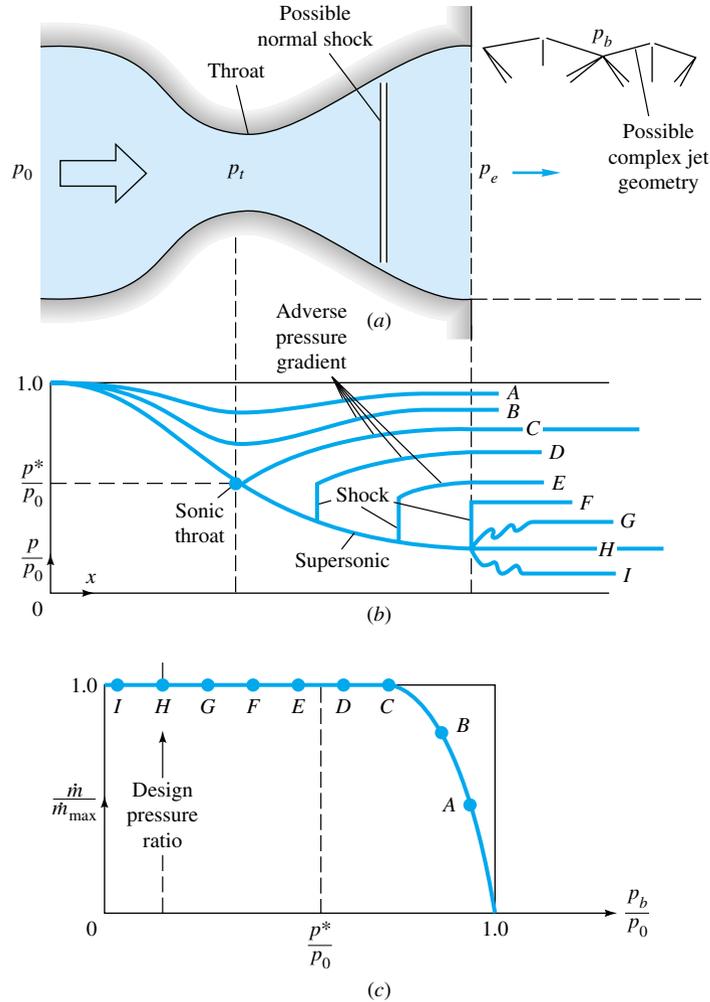
Fig. 9.12 Operation of a converging-diverging nozzle: (*a*) nozzle geometry with possible flow configurations; (*b*) pressure distribution caused by various back pressures; (*c*) mass flow versus back pressure.

Finally, at back pressure *I*, p_b is lower than the design pressure *H*, but the nozzle is choked and cannot respond. The exit flow expands in a complex series of supersonic wave motions until it matches the low back pressure. See, e.g., Ref. 9, sec. 5.4, for further details of these off-design jet-flow configurations.

Note that for p_b less than back pressure *C*, there is supersonic flow in the nozzle and the throat can receive no signal from the exit behavior. The flow remains choked, and the throat has no idea what the exit conditions are.

Note also that the normal shock-patching idea is idealized. Downstream of the shock the nozzle flow has an adverse pressure gradient, usually leading to wall boundary-layer separation. Blockage by the greatly thickened separated layer interacts strongly with the core flow (recall Fig. 6.27) and usually induces a series of weak two-dimensional compression shocks rather than a single one-dimensional normal shock (see, e.g., Ref. 14, pp. 292 and 293, for further details).

EXAMPLE 9.9

A converging-diverging nozzle (Fig. 9.12a) has a throat area of 0.002 m^2 and an exit area of 0.008 m^2. Air stagnation conditions are $p_0 = 1000$ kPa and $T_0 = 500$ K. Compute the exit pressure and mass flow for (a) design condition and the exit pressure and mass flow if (b) $p_b \approx$ 300 kPa and (c) $p_b \approx 900$ kPa. Assume $k = 1.4$.

Solution

Part (a) The design condition corresponds to supersonic isentropic flow at the given area ratio $A_e/A_t = 0.008/0.002 = 4.0$. We can find the design Mach number either by iteration of the area-ratio formula (9.45), using EES, or by the curve fit (9.48d)

$$\text{Ma}_{e,\text{design}} \approx [216(4.0) - 254(4.0)^{2/3}]^{1/5} \approx 2.95 \qquad (\text{exact} = 2.9402)$$

The accuracy of the curve fit is seen to be satisfactory. The design pressure ratio follows from Eq. (9.34)

$$\frac{p_0}{p_e} = [1 + 0.2(2.95)^2]^{3.5} = 34.1$$

or
$$p_{e,\text{design}} = \frac{1000 \text{ kPa}}{34.1} = 29.3 \text{ kPa} \qquad\qquad \textit{Ans. (a)}$$

Since the throat is clearly sonic at design conditions, Eq. (9.46b) applies

$$\dot{m}_{\text{design}} = \dot{m}_{\text{max}} = \frac{0.6847 p_0 A_t}{(RT_0)^{1/2}} = \frac{0.6847(10^6 \text{ Pa})(0.002 \text{ m}^2)}{[287(500)]^{1/2}} \qquad \textit{Ans. (a)}$$

$$= 3.61 \text{ kg/s}$$

Part (b) For $p_b = 300$ kPa we are definitely far below the subsonic isentropic condition C in Fig. 9.12b, but we may even be below condition F with a normal shock in the exit, i.e., in condition G, where oblique shocks occur outside the exit plane. If it is condition G, then $p_e = p_{e,\text{design}} = 29.3$ kPa because no shock has yet occurred. To find out, compute condition F by assuming an exit normal shock with $\text{Ma}_1 = 2.95$, that is, the design Mach number just upstream of the shock. From Eq. (9.55)

$$\frac{p_2}{p_1} = \frac{1}{2.4}[2.8(2.95)^2 - 0.4] = 9.99$$

or
$$p_2 = 9.99 p_1 = 9.99 p_{e,\text{design}} = 293 \text{ kPa}$$

Since this is less than the given $p_b = 300$ kPa, there is a normal shock just upstream of the exit plane (condition E). The exit flow is subsonic and equals the back pressure

$$p_e = p_b = 300 \text{ kPa} \qquad\qquad \textit{Ans. (b)}$$

Also
$$\dot{m} = \dot{m}_{\text{max}} = 3.61 \text{ kg/s} \qquad\qquad \textit{Ans. (b)}$$

The throat is still sonic and choked at its maximum mass flow.

Part (c) Finally, for $p_b = 900$ kPa, which is up near condition C, we compute Ma_e and p_e for condition C as a comparison. Again $A_e/A_t = 4.0$ for this condition, with a subsonic Ma_e estimated from the curve-fitted Eq. (9.48a):

$$\text{Ma}_e(C) \approx \frac{1 + 0.27/(4.0)^2}{1.728(4.0)} = 0.147 \qquad (\text{exact} = 0.14655)$$

Then the isentropic exit-pressure ratio for this condition is

$$\frac{p_0}{p_e} = [1 + 0.2(0.147)^2]^{3.5} = 1.0152$$

or

$$p_e = \frac{1000}{1.0152} = 985 \text{ kPa}$$

The given back pressure of 900 kPa is less than this value, corresponding roughly to condition D in Fig. 9.12b. Thus for this case there is a normal shock just downstream of the throat, and the throat is choked

$$p_e = p_b = 900 \text{ kPa} \qquad \dot{m} = \dot{m}_{\text{max}} = 3.61 \text{ kg/s} \qquad \qquad Ans. \ (c)$$

For this large exit-area ratio, the exit pressure would have to be larger than 985 kPa to cause a subsonic flow in the throat and a mass flow less than maximum.

9.7 Compressible Duct Flow with Friction[4]

Section 9.4 showed the effect of area change on a compressible flow while neglecting friction and heat transfer. We could now add friction and heat transfer to the area change and consider coupled effects, which is done in advanced texts [for example, 8, chap. 8]. Instead, as an elementary introduction, this section treats only the effect of friction, neglecting area change and heat transfer. The basic assumptions are

1. Steady one-dimensional adiabatic flow
2. Perfect gas with constant specific heats
3. Constant-area straight duct
4. Negligible shaft-work and potential-energy changes
5. Wall shear stress correlated by a Darcy friction factor

In effect, we are studying a Moody-type pipe-friction problem but with large changes in kinetic energy, enthalpy, and pressure in the flow.

Consider the elemental duct control volume of area A and length dx in Fig. 9.13. The area is constant, but other flow properties (p, ρ, T, h, V) may vary with x. Appli-

[4] This section may be omitted without loss of continuity.
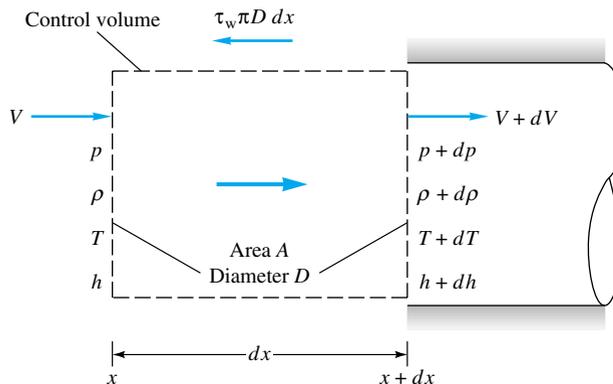
Fig. 9.13 Elemental control volume for flow in a constant-area duct with friction.

cation of the three conservation laws to this control volume gives three differential equations

Continuity:
$$\rho V = \frac{\dot{m}}{A} = G = \text{const}$$

or
$$\frac{d\rho}{\rho} + \frac{dV}{V} = 0 \qquad (9.60a)$$

x momentum: $pA - (p + dp)A - \tau_w \pi D \, dx = \dot{m}(V + dV - V)$

or
$$dp + \frac{4\tau_w dx}{D} + \rho V \, dV = 0 \qquad (9.60b)$$

Energy:
$$h + \tfrac{1}{2}V^2 = h_0 = c_p T_0 = c_p T + \tfrac{1}{2}V^2$$

or
$$c_p \, dT + V \, dV = 0 \qquad (9.60c)$$

Since these three equations have five unknowns—p, ρ, T, V, and τ_w—we need two additional relations. One is the perfect-gas law

$$p = \rho RT \qquad \text{or} \qquad \frac{dp}{p} = \frac{d\rho}{\rho} + \frac{dT}{T} \qquad (9.61)$$

To eliminate τ_w as an unknown, it is assumed that wall shear is correlated by a local Darcy friction factor f

$$\tau_w = \tfrac{1}{8} f \rho V^2 = \tfrac{1}{8} fkp \, \text{Ma}^2 \qquad (9.62)$$

where the last form follows from the perfect-gas speed-of-sound expression $a^2 = kp/\rho$. In practice, f can be related to the local Reynolds number and wall roughness from, say, the Moody chart, Fig. 6.13.

Equations (9.60) and (9.61) are first-order differential equations and can be integrated, by using friction-factor data, from any inlet section 1, where p_1, T_1, V_1, etc., are known, to determine $p(x)$, $T(x)$, etc., along the duct. It is practically impossible to eliminate all but one variable to give, say, a single differential equation for $p(x)$, but all equations can be written in terms of the Mach number $\text{Ma}(x)$ and the friction factor, by using the definition of Mach number

$$V^2 = \text{Ma}^2 \, kRT$$

or
$$\frac{2 \, dV}{V} = \frac{2 \, d\,\text{Ma}}{\text{Ma}} + \frac{dT}{T} \qquad (9.63)$$

Adiabatic Flow

By eliminating variables between Eqs. (9.60) to (9.63), we obtain the working relations

$$\frac{dp}{p} = -k \, \text{Ma}^2 \, \frac{1 + (k - 1) \, \text{Ma}^2}{2(1 - \text{Ma}^2)} f \frac{dx}{D} \qquad (9.64a)$$

$$\frac{d\rho}{\rho} = -\frac{k \, \text{Ma}^2}{2(1 - \text{Ma}^2)} f \frac{dx}{D} = -\frac{dV}{V} \qquad (9.64b)$$

$$\frac{dp_0}{p_0} = \frac{d\rho_0}{\rho_0} = -\frac{1}{2} k \, \mathrm{Ma}^2 f \frac{dx}{D} \qquad (9.64c)$$

$$\frac{dT}{T} = -\frac{k(k-1) \, \mathrm{Ma}^4}{2(1 - \mathrm{Ma}^2)} f \frac{dx}{D} \qquad (9.64d)$$

$$\frac{d \, \mathrm{Ma}^2}{\mathrm{Ma}^2} = k \, \mathrm{Ma}^2 \frac{1 + \frac{1}{2}(k-1) \, \mathrm{Ma}^2}{1 - \mathrm{Ma}^2} f \frac{dx}{D} \qquad (9.64e)$$

All these except dp_0/p_0 have the factor $1 - \mathrm{Ma}^2$ in the denominator, so that, like the area-change formulas in Fig. 9.5, subsonic and supersonic flow have opposite effects:

Property	Subsonic	Supersonic
p	Decreases	Increases
ρ	Decreases	Increases
V	Increases	Decreases
p_0, ρ_0	Decreases	Decreases
T	Decreases	Increases
Ma	Increases	Decreases
Entropy	Increases	Increases

We have added to the list above that entropy must increase along the duct for either subsonic or supersonic flow as a consequence of the second law for adiabatic flow. For the same reason, stagnation pressure and density must both decrease.

The key parameter above is the Mach number. Whether the inlet flow is subsonic or supersonic, the duct Mach number always tends downstream toward $\mathrm{Ma} = 1$ because this is the path along which the entropy increases. If the pressure and density are computed from Eqs. (9.64a) and (9.64b) and the entropy from Eq. (9.53), the result can be plotted in Fig. 9.14 versus Mach number for $k = 1.4$. The maximum entropy occurs at $\mathrm{Ma} = 1$, so that the second law requires that the duct-flow properties continually approach the sonic point. Since p_0 and ρ_0 continually decrease along the duct due to the frictional (nonisentropic) losses, they are not useful as reference properties. Instead, the sonic properties p^*, ρ^*, T^*, p_0^*, and ρ_0^* are the appropriate constant reference quantities in adiabatic duct flow. The theory then computes the ratios p/p^*, T/T^*, etc., as a function of local Mach number and the integrated friction effect.

To derive working formulas, we first attack Eq. (9.64e), which relates the Mach number to friction. Separate the variables and integrate:

$$\int_0^{L^*} f \frac{dx}{D} = \int_{\mathrm{Ma}^2}^{1.0} \frac{1 - \mathrm{Ma}^2}{k \, \mathrm{Ma}^4 [1 + \frac{1}{2}(k-1) \, \mathrm{Ma}^2]} \, d \, \mathrm{Ma}^2 \qquad (9.65)$$

The upper limit is the sonic point, whether or not it is actually reached in the duct flow. The lower limit is arbitrarily placed at the position $x = 0$, where the Mach number is Ma. The result of the integration is

$$\frac{\bar{f} L^*}{D} = \frac{1 - \mathrm{Ma}^2}{k \, \mathrm{Ma}^2} + \frac{k+1}{2k} \ln \frac{(k+1) \, \mathrm{Ma}^2}{2 + (k-1) \, \mathrm{Ma}^2} \qquad (9.66)$$

where $\bar{f}$ is the average friction factor between 0 and L^*. In practice, an average f is always assumed, and no attempt is made to account for the slight changes in Reynolds
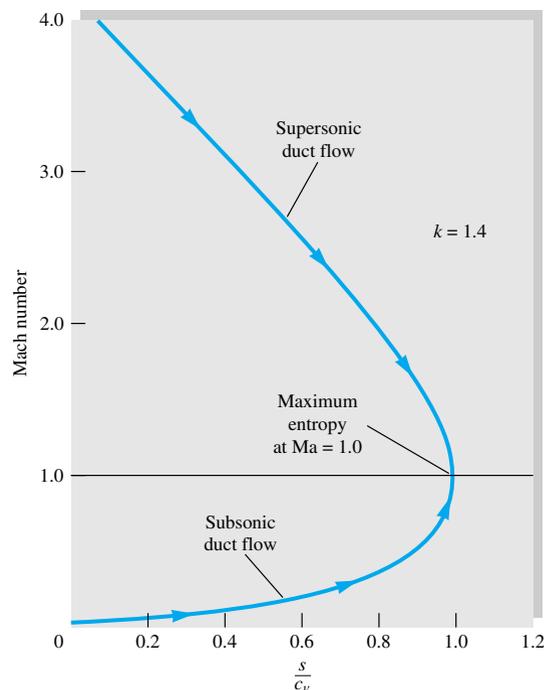
Fig. 9.14 Adiabatic frictional flow in a constant-area duct always approaches Ma = 1 to satisfy the second law of thermodynamics. The computed curve is independent of the value of the friction factor.

number along the duct. For noncircular ducts, D is replaced by the hydraulic diameter $D_h = (4 \times \text{area})/\text{perimeter}$ as in Eq. (6.74).

Equation (9.66) is tabulated versus Mach number in Table B.3. The length L^* is the length of duct required to develop a duct flow from Mach number Ma to the sonic point. Many problems involve short ducts which never become sonic, for which the solution uses the differences in the tabulated "maximum," or sonic, length. For example, the length ΔL required to develop from Ma_1 to Ma_2 is given by

$$\bar{f}\, \frac{\Delta L}{D} = \left(\frac{\bar{f}L^*}{D}\right)_1 - \left(\frac{\bar{f}L^*}{D}\right)_2 \tag{9.67}$$

This avoids the need for separate tabulations for short ducts.

It is recommended that the friction factor $\bar{f}$ be estimated from the Moody chart (Fig. 6.13) for the average Reynolds number and wall-roughness ratio of the duct. Available data [20] on duct friction for compressible flow show good agreement with the Moody chart for subsonic flow, but the measured data in supersonic duct flow are up to 50 percent less than the equivalent Moody friction factor.

EXAMPLE 9.10

Air flows subsonically in an adiabatic 2-cm-diameter duct. The average friction factor is 0.024. What length of duct is necessary to accelerate the flow from $Ma_1 = 0.1$ to $Ma_2 = 0.5$? What additional length will accelerate it to $Ma_3 = 1.0$? Assume $k = 1.4$.

Solution

Equation (9.67) applies, with values of $\bar{f}L^*/D$ computed from Eq. (9.66) or read from Table B.3:

$$\bar{f}\,\frac{\Delta L}{D} = \frac{0.024\,\Delta L}{0.02\text{ m}} = \left(\frac{\bar{f}L^*}{D}\right)_{\text{Ma}=0.1} - \left(\frac{\bar{f}L^*}{D}\right)_{\text{Ma}=0.5}$$

$$= 66.9216 - 1.0691 = 65.8525$$

Thus

$$\Delta L = \frac{65.8525(0.02\text{ m})}{0.024} = 55\text{ m} \qquad \textit{Ans. (a)}$$

The additional length $\Delta L'$ to go from Ma = 0.5 to Ma = 1.0 is taken directly from Table B.2

$$f\,\frac{\Delta L'}{D} = \left(\frac{fL^*}{D}\right)_{\text{Ma}=0.5} = 1.0691$$

or

$$\Delta L' = L^*_{\text{Ma}=0.5} = \frac{1.0691(0.02\text{ m})}{0.024} = 0.9\text{ m} \qquad \textit{Ans. (b)}$$

This is typical of these calculations: It takes 55 m to accelerate up to Ma = 0.5 and then only 0.9 m more to get all the way up to the sonic point.

Formulas for other flow properties along the duct can be derived from Eqs. (9.64). Equation (9.64e) can be used to eliminate $f\,dx/D$ from each of the other relations, giving, for example, dp/p as a function only of Ma and $d\,\text{Ma}^2/\text{Ma}^2$. For convenience in tabulating the results, each expression is then integrated all the way from (p, Ma) to the sonic point $(p^*, 1.0)$. The integrated results are

$$\frac{p}{p^*} = \frac{1}{\text{Ma}}\left[\frac{k+1}{2+(k-1)\,\text{Ma}^2}\right]^{1/2} \qquad (9.68a)$$

$$\frac{\rho}{\rho^*} = \frac{V^*}{V} = \frac{1}{\text{Ma}}\left[\frac{2+(k-1)\,\text{Ma}^2}{k+1}\right]^{1/2} \qquad (9.68b)$$

$$\frac{T}{T^*} = \frac{a^2}{a^{*2}} = \frac{k+1}{2+(k-1)\,\text{Ma}^2} \qquad (9.68c)$$

$$\frac{p_0}{p_0^*} = \frac{\rho_0}{\rho_0^*} = \frac{1}{\text{Ma}}\left[\frac{2+(k-1)\,\text{Ma}^2}{k+1}\right]^{(1/2)(k+1)/(k-1)} \qquad (9.68d)$$

All these ratios are also tabulated in Table B.3. For finding changes between points Ma_1 and Ma_2 which are not sonic, products of these ratios are used. For example,

$$\frac{p_2}{p_1} = \frac{p_2}{p^*}\frac{p^*}{p_1} \qquad (9.69)$$

since p^* is a constant reference value for the flow.

EXAMPLE 9.11

For the duct flow of Example 9.10 assume that, at $\text{Ma}_1 = 0.1$, we have $p_1 = 600$ kPa and $T_1 = 450$ K. At section 2 farther downstream, $\text{Ma}_2 = 0.5$. Compute (a) p_2, (b) T_2, (c) V_2, and (d) p_{02}.

Solution

As preliminary information we can compute V_1 and p_{01} from the given data:

$$V_1 = \text{Ma}_1 \, a_1 = 0.1[(1.4)(287)(450)]^{1/2} = 0.1(425 \text{ m/s}) = 42.5 \text{ m/s}$$

$$p_{01} = p_1(1 + 0.2 \text{ Ma}_1^2)^{3.5} = (600 \text{ kPa})[1 + 0.2(0.1)^2]^{3.5} = 604 \text{ kPa}$$

Now enter Table B.3 or Eqs. (9.68) to find the following property ratios:

Section	Ma	p/p^*	T/T^*	V/V^*	p_0/p_0^*
1	0.1	10.9435	1.1976	0.1094	5.8218
2	0.5	2.1381	1.1429	0.5345	1.3399

Use these ratios to compute all properties downstream:

$$p_2 = p_1 \frac{p_2/p^*}{p_1/p^*} = (600 \text{ kPa}) \frac{2.1381}{10.9435} = 117 \text{ kPa} \qquad \textit{Ans. (a)}$$

$$T_2 = T_1 \frac{T_2/T^*}{T_1/T^*} = (450 \text{ K}) \frac{1.1429}{1.1976} = 429 \text{ K} \qquad \textit{Ans. (b)}$$

$$V_2 = V_1 \frac{V_2/V^*}{V_1/V^*} = (42.5 \text{ m/s}) \frac{0.5345}{0.1094} = 208 \frac{\text{m}}{\text{s}} \qquad \textit{Ans. (c)}$$

$$p_{02} = p_{01} \frac{p_{02}/p_0^*}{p_{01}/p_0^*} = (604 \text{ kPa}) \frac{1.3399}{5.8218} = 139 \text{ kPa} \qquad \textit{Ans. (d)}$$

Note the 77 percent reduction in stagnation pressure due to friction. The formulas are seductive, so check your work by other means. For example, check $p_{02} = p_2(1 + 0.2 \text{ Ma}_2^2)^{3.5}$.

Choking due to Friction

The theory here predicts that for adiabatic frictional flow in a constant-area duct, no matter what the inlet Mach number Ma_1 is, the flow downstream tends toward the sonic point. There is a certain duct length $L^*(\text{Ma}_1)$ for which the exit Mach number will be exactly unity. The duct is then choked.

But what if the actual length L is greater than the predicted "maximum" length L^*? Then the flow conditions must change, and there are two classifications.

Subsonic inlet. If $L > L^*(\text{Ma}_1)$, the flow slows down until an inlet Mach number Ma_2 is reached such that $L = L^*(\text{Ma}_2)$. The exit flow is sonic, and the mass flow has been reduced by *frictional choking*. Further increases in duct length will continue to decrease the inlet Ma and mass flow.

Supersonic inlet. From Table B.3 we see that friction has a very large effect on supersonic duct flow. Even an infinite inlet Mach number will be reduced to sonic conditions in only 41 diameters for $\bar{f} = 0.02$. Some typical numerical values are shown in Fig. 9.15, assuming an inlet Ma = 3.0 and $\bar{f} = 0.02$. For this condition $L^* = 26$ diameters. If L is increased beyond $26D$, the flow will not choke but a normal shock will form at just the right place for the subsequent subsonic frictional flow to become sonic exactly at the exit. Figure 9.15 shows two examples, for $L/D = 40$ and 53. As the length increases, the required normal shock moves upstream until, for Fig. 9.15, the shock is at the inlet for $L/D = 63$. Further increase in L causes the shock to move upstream of
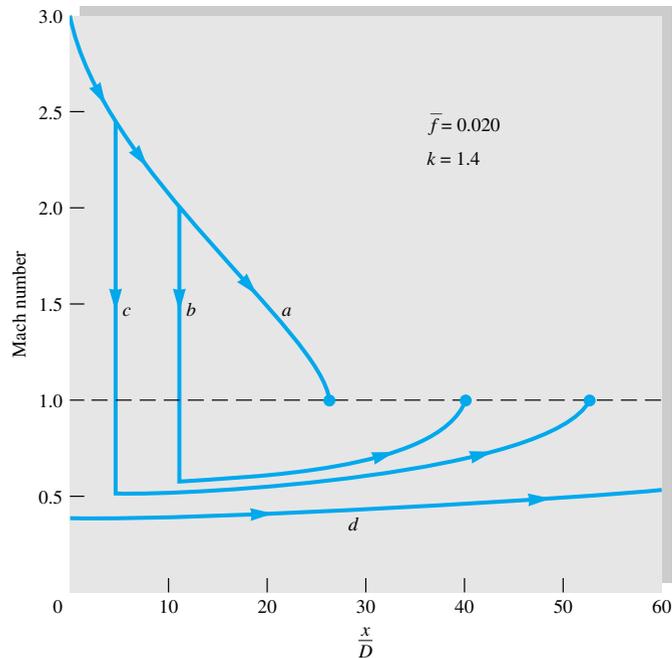
Fig. 9.15 Behavior of duct flow with a nominal supersonic inlet condition Ma = 3.0: (a) $L/D \leq 26$, flow is supersonic throughout duct; (b) $L/D = 40 > L^*/D$, normal shock at Ma = 2.0 with subsonic flow then accelerating to sonic exit point; (c) $L/D = 53$, shock must now occur at Ma = 2.5; (d) $L/D > 63$, flow must be entirely subsonic and choked at exit.

the inlet into the supersonic nozzle feeding the duct. Yet the mass flow is still the same as for the very short duct, because presumably the feed nozzle still has a sonic throat. Eventually, a very long duct will cause the feed-nozzle throat to become choked, thus reducing the duct mass flow. Thus supersonic friction changes the flow pattern if $L > L^*$ but does not choke the flow until L is much larger than L^*.

EXAMPLE 9.12

Air enters a 3-cm-diameter duct at $p_0 = 200$ kPa, $T_0 = 500$ K, and $V_1 = 100$ m/s. The friction factor is 0.02. Compute (a) the maximum duct length for these conditions, (b) the mass flow if the duct length is 15 m, and (c) the reduced mass flow if $L = 30$ m.

Solution

Part (a) First compute

$$T_1 = T_0 - \frac{\frac{1}{2}V_1^2}{c_p} = 500 - \frac{\frac{1}{2}(100 \text{ m/s})^2}{1005 \text{ m}^2/(\text{s}^2 \cdot \text{K})} = 500 - 5 = 495 \text{ K}$$

$$a_1 = (kRT_1)^{1/2} \approx 20(495)^{1/2} = 445 \text{ m/s}$$

Thus

$$\text{Ma}_1 = \frac{V_1}{a_1} = \frac{100}{445} = 0.225$$

For this Ma_1, from Eq. (9.66) or interpolation in Table B.3,

$$\frac{\bar{f}L^*}{D} = 11.0$$

The maximum duct length possible for these inlet conditions is

$$L^* = \frac{(\bar{f}L^*/D)D}{\bar{f}} = \frac{11.0(0.03 \text{ m})}{0.02} = 16.5 \text{ m}$$ *Ans. (a)*

Part (b) The given $L = 15$ m is less than L^*, and so the duct is not choked and the mass flow follows from inlet conditions

$$\rho_{01} = \frac{p_{01}}{RT_0} = \frac{200{,}000 \text{ Pa}}{287(500 \text{ K})} = 1.394 \text{ kg/m}^3$$

$$\rho_1 = \frac{\rho_{01}}{[1 + 0.2(0.225)^2]^{2.5}} = \frac{1.394}{1.0255} = 1.359 \text{ kg/m}^3$$

whence $$\dot{m} = \rho_1 AV_1 = (1.359 \text{ kg/m}^3)\left[\frac{\pi}{4}(0.03 \text{ m})^2\right](100 \text{ m/s})$$

$$= 0.0961 \text{ kg/s}$$ *Ans. (b)*

Part (c) Since $L = 30$ m is greater than L^*, the duct must choke back until $L = L^*$, corresponding to a lower inlet Ma_1:

$$L^* = L = 30 \text{ m}$$

$$\frac{\bar{f}L^*}{D} = \frac{0.02(30 \text{ m})}{0.03 \text{ m}} = 20.0$$

It is difficult to interpolate for $fL/D = 20$ in Table B.3 and impossible to invert Eq. (9.66) for the Mach number without laborious iteration. But it is a breeze for EES to solve Eq. (9.66) for the Mach number, using the following three statements:

```
k = 1.4
fLD = 20
fLD = (1 − Ma^2)/k/Ma^2 + (k + 1)/2/k*LN((k + 1)*Ma^2/(2 + (k − 1)*Ma^2))
```

Simply specify Ma < 1 in the Variable Information menu and EES cheerfully reports

$$\text{Ma}_{\text{choked}} = 0.174 \quad (23 \text{ percent less})$$

$$T_{1,\text{new}} = \frac{T_0}{1 + 0.2(0.174)^2} = 497 \text{ K}$$

$$a_{1,\text{new}} \approx 20(497 \text{ K})^{1/2} = 446 \text{ m/s}$$

$$V_{1,\text{new}} = \text{Ma}_1\, a_1 = 0.174(446) = 77.6 \text{ m/s}$$

$$\rho_{1,\text{new}} = \frac{\rho_{01}}{[1 + 0.2(0.174)^2]^{2.5}} = 1.373 \text{ kg/m}^3$$

$$\dot{m}_{\text{new}} = \rho_1 AV_1 = 1.373\left[\frac{\pi}{4}(0.03)^2\right](77.6)$$

$$= 0.0753 \text{ kg/s} \quad (22 \text{ percent less})$$ *Ans. (c)*

Isothermal Flow with Friction   The adiabatic frictional-flow assumption is appropriate to high-speed flow in short ducts. For flow in long ducts, e.g., natural-gas pipelines, the gas state more closely ap-

proximates an isothermal flow. The analysis is the same except that the isoenergetic energy equation (9.60c) is replaced by the simple relation

$$T = \text{const} \qquad dT = 0 \qquad\qquad (9.70)$$

Again it is possible to write all property changes in terms of the Mach number. Integration of the Mach-number–friction relation yields

$$\frac{\bar{f}L_{\text{max}}}{D} = \frac{1 - k\,\text{Ma}^2}{k\,\text{Ma}^2} + \ln\,(k\,\text{Ma}^2) \qquad\qquad (9.71)$$

which is the isothermal analog of Eq. (9.66) for adiabatic flow.

This friction relation has the interesting result that L_{max} becomes zero not at the sonic point but at $\text{Ma}_{\text{crit}} = 1/k^{1/2} = 0.845$ if $k = 1.4$. The inlet flow, whether subsonic or supersonic, tends downstream toward this limiting Mach number $1/k^{1/2}$. If the tube length L is greater than L_{max} from Eq. (9.71), a subsonic flow will choke back to a smaller Ma_1 and mass flow and a supersonic flow will experience a normal-shock adjustment similar to Fig. 9.15.

The exit isothermal choked flow is not sonic, and so the use of the asterisk is inappropriate. Let p', ρ', and V' represent properties at the choking point $L = L_{\text{max}}$. Then the isothermal analysis leads to the following Mach-number relations for the flow properties:

$$\frac{p}{p'} = \frac{1}{\text{Ma}\,k^{1/2}} \qquad \frac{V}{V'} = \frac{\rho'}{\rho} = \text{Ma}\,k^{1/2} \qquad\qquad (9.72)$$

The complete analysis and some examples are given in advanced texts [for example, 8, sec. 6.4].

Mass Flow for a Given Pressure Drop

An interesting by-product of the isothermal analysis is an explicit relation between the pressure drop and duct mass flow. This is a common problem which requires numerical iteration for adiabatic flow, as outlined below. In isothermal flow, we may substitute $dV/V = -dp/p$ and $V^2 = G^2/[p/(RT)]^2$ in Eq. (9.63) to obtain

$$\frac{2p\,dp}{G^2RT} + f\frac{dx}{D} - \frac{2\,dp}{p} = 0$$

Since G^2RT is constant for isothermal flow, this may be integrated in closed form between $(x, p) = (0, p_1)$ and (L, p_2):

$$G^2 = \left(\frac{\dot{m}}{A}\right)^2 = \frac{p_1^2 - p_2^2}{RT[\bar{f}L/D + 2\ln\,(p_1/p_2)]} \qquad\qquad (9.73)$$

Thus mass flow follows directly from the known end pressures, without any use of Mach numbers or tables.

The writer does not know of any direct analogy to Eq. (9.73) for adiabatic flow. However, a useful adiabatic relation, involving velocities instead of pressures, is derived in several textbooks [5, p. 212; 34, p. 418]:

$$V_1^2 = \frac{a_0^2[1 - (V_1/V_2)^2]}{k\bar{f}L/D + (k + 1)\ln\,(V_2/V_1)} \qquad\qquad (9.74)$$

where $a_0 = (kRT_0)^{1/2}$ is the stagnation speed of sound, constant for adiabatic flow. We assign the proof of this as a problem exercise. This may be combined with continuity for constant duct area $V_1/V_2 = \rho_2/\rho_1$, plus the following combination of adiabatic energy and the perfect-gas relation:

$$\frac{V_1}{V_2} = \frac{p_2}{p_1}\frac{T_1}{T_2} = \frac{p_2}{p_1}\left[\frac{2a_0^2 - (k-1)V_1^2}{2a_0^2 - (k-1)V_2^2}\right] \tag{9.75}$$

If we are given the end pressures, neither V_1 nor V_2 will likely be known in advance. Here, if EES is not available, we suggest only the following simple procedure. Begin with $a_0 \approx a_1$ and the bracketed term in Eq. (9.75) approximately equal to 1.0. Solve Eq. (9.75) for a first estimate of V_1/V_2, and use this value in Eq. (9.74) to get a better estimate of V_1. Use V_1 to improve your estimate of a_0, and repeat the procedure. The process should converge in a few iterations.

Equations (9.73) and (9.74) have one flaw: With the Mach number eliminated, the frictional choking phenomenon is not directly evident. Therefore, assuming a subsonic inlet flow, one should check the exit Mach number Ma_2 to ensure that it is not greater than $1/k^{1/2}$ for isothermal flow or greater than 1.0 for adiabatic flow. We illustrate both adiabatic and isothermal flow with the following example.

EXAMPLE 9.13

Air enters a pipe of 1-cm diameter and 1.2-m length at $p_1 = 220$ kPa and $T_1 = 300$ K. If $\bar{f} = 0.025$ and the exit pressure is $p_2 = 140$ kPa, estimate the mass flow for (a) isothermal flow and (b) adiabatic flow.

Solution

Part (a) For isothermal flow Eq. (9.73) applies without iteration:

$$\frac{\bar{f}L}{D} + 2\ln\frac{p_1}{p_2} = \frac{(0.025)(1.2\text{ m})}{0.01\text{ m}} + 2\ln\frac{220}{140} = 3.904$$

$$G^2 = \frac{(220{,}000\text{ Pa})^2 - (140{,}000\text{ Pa})^2}{[287\text{ m}^2/(\text{s}^2 \cdot \text{K})](300\text{ K})(3.904)} = 85{,}700 \quad \text{or} \quad G = 293\text{ kg/(s} \cdot \text{m}^2)$$

Since $A = (\pi/4)(0.01\text{ m})^2 = 7.85$ E-5 m^2, the isothermal mass flow estimate is

$$\dot{m} = GA = (293)(7.85\text{ E-5}) \approx 0.0230\text{ kg/s} \qquad \textit{Ans. (a)}$$

Check that the exit Mach number is not choked:

$$\rho_2 = \frac{p_2}{RT} = \frac{140{,}000}{(287)(300)} = 1.626\text{ kg/m}^3 \qquad V_2 = \frac{G}{\rho_2} = \frac{293}{1.626} = 180\text{ m/s}$$

or

$$Ma_2 = \frac{V_2}{\sqrt{kRT}} = \frac{180}{[1.4(287)(300)]^{1/2}} = \frac{180}{347} \approx 0.52$$

This is well below choking, and the isothermal solution is accurate.

Part (b) For adiabatic flow, we can iterate by hand, in the time-honored fashion, using Eqs. (9.74) and (9.75) plus the definition of stagnation speed of sound. A few years ago the author would have done just that, laboriously. However, EES makes handwork and manipulation of equations un-

EES

necessary, although careful programming and good guesses are required. If we ignore superfluous output such as T_2 and V_2, 13 statements are appropriate. First, spell out the given physical properties (in SI units):

```
k = 1.4
P1 = 220000
P2 = 140000
T1 = 300
```

Next, apply the adiabatic friction relations, Eqs. (9.66) and (9.67), to both points 1 and 2:

```
fLD1 = (1 − Ma1^2)/k/Ma1^2+(k+1)/2/k*LN((k+1)*Ma1^2/(2+(k-1)*Ma1^2))
fLD2 = (1 − Ma2^2)/k/Ma2^2+(k+1)/2/k*LN((k+1)*Ma2^2/(2+(k-1)*Ma2^2))
DeltafLD = 0.025*1.2/0.01
fLD1 = fLD2 + DeltafLD
```

Then apply the pressure-ratio formula (9.68*a*) to both points 1 and 2:

```
P1/Pstar = ((k+1)/(2+(k-1)*Ma1^2))^0.5/Ma1
P2/Pstar = ((k+1)/(2+(k-1)*Ma2^2))^0.5/Ma2
```

These are *adiabatic* relations, so we need not further spell out quantities such as T_0 or a_0 unless we want them as additional output.

   The above 10 statements are a closed algebraic system, and EES will solve them for Ma_1 and Ma_2. However, the problem asks for mass flow, so we complete the system:

```
V1 = Ma1*sqrt(1.4*287*T1)
Rho1 = P1/287/T1
Mdot = Rho1*(pi/4*0.01^2)*V1
```

If we apply no constraints, EES reports "cannot solve", because its default allows all variables to lie between $-\infty$ and $+\infty$. So we enter Variable Information and constrain Ma_1 and Ma_2 to lie between 0 and 1 (subsonic flow). EES still complains that it "cannot solve" but hints that "better guesses are needed". Indeed, the default guesses for EES variables are normally 1.0, too large for the Mach numbers. Guess the Mach numbers equal to 0.8 or even 0.5, and EES still complains, for a subtle reason: Since $f\Delta L/D = 0.025(1.2/0.01) = 3.0$, Ma_1 can be no larger than 0.36 (see Table B.3). Finally, then, we guess Ma_1 and $Ma_2 = 0.3$ or 0.4, and EES happily reports the solution:

$$Ma_1 = 0.3343 \qquad Ma_2 = 0.5175 \qquad \frac{fL}{D_1} = 3.935 \qquad \frac{fL}{D_2} = 0.9348$$

$$p^* = 67,892 \text{ Pa} \qquad \dot{m} = \mathbf{0.0233 \ kg/s} \qquad\qquad \textit{Ans. (b)}$$

Though the programming is complicated, the EES approach is superior to hand iteration and, of course, we can save this program for use again with new data.

9.8 Frictionless Duct Flow with Heat Transfer[5]

Heat addition or removal has an interesting effect on a compressible flow. Advanced texts [for example, 8, chap. 8] consider the combined effect of heat transfer coupled with friction and area change in a duct. Here we confine the analysis to heat transfer with no friction in a constant-area duct.

---

[5] This section may be omitted without loss of continuity.
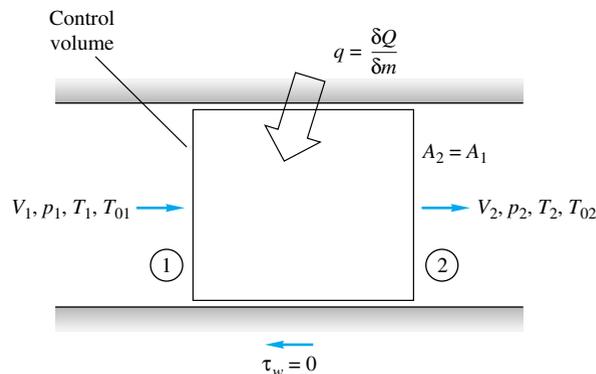
Fig. 9.16 Elemental control volume for frictionless flow in a constant-area duct with heat transfer. The length of the element is indeterminate in this simplified theory.

Consider the elemental duct control volume in Fig. 9.16. Between sections 1 and 2 an amount of heat δQ is added (or removed) to each incremental mass δm passing through. With no friction or area change, the control-volume conservation relations are quite simple:

Continuity:
$$\rho_1 V_1 = \rho_2 V_2 = G = \text{const} \tag{9.76a}$$

x momentum:
$$p_1 - p_2 = G(V_2 - V_1) \tag{9.76b}$$

Energy:
$$\dot{Q} = \dot{m}(h_2 + \tfrac{1}{2}V_2^2 - h_1 - \tfrac{1}{2}V_1^2)$$

or
$$q = \frac{\dot{Q}}{\dot{m}} = \frac{\delta Q}{\delta m} = h_{02} - h_{01} \tag{9.76c}$$

The heat transfer results in a change in stagnation enthalpy of the flow. We shall not specify exactly how the heat is transferred—combustion, nuclear reaction, evaporation, condensation, or wall heat exchange—but simply that it happened in amount q between 1 and 2. We remark, however, that wall heat exchange is not a good candidate for the theory because wall convection is inevitably coupled with wall friction, which we neglected.

To complete the analysis, we use the perfect-gas and Mach-number relations

$$\frac{p_2}{\rho_2 T_2} = \frac{p_1}{\rho_1 T_1} \qquad h_{02} - h_{01} = c_p(T_{02} - T_{01})$$

$$\frac{V_2}{V_1} = \frac{\text{Ma}_2\, a_2}{\text{Ma}_1\, a_1} = \frac{\text{Ma}_2}{\text{Ma}_1}\left(\frac{T_2}{T_1}\right)^{1/2} \tag{9.77}$$

For a given heat transfer $q = \delta Q/\delta m$ or, equivalently, a given change $h_{02} - h_{01}$, Eqs. (9.76) and (9.77) can be solved algebraically for the property ratios p_2/p_1, Ma_2/Ma_1, etc., between inlet and outlet. Note that because the heat transfer allows the entropy to either increase or decrease, the second law imposes no restrictions on these solutions.

Before writing down these property-ratio functions, we illustrate the effect of heat transfer in Fig. 9.17, which shows T_0 and T versus Mach number in the duct. Heating increases T_0, and cooling decreases it. The maximum possible T_0 occurs at $\text{Ma} = 1.0$, and we see that heating, whether the inlet is subsonic or supersonic, drives the duct Mach number toward unity. This is analogous to the effect of friction in the previous section. The temperature of a perfect gas increases from $\text{Ma} = 0$ up to $\text{Ma} = 1/k^{1/2}$ and then decreases. Thus there is a peculiar—or at least unexpected—region where heat-
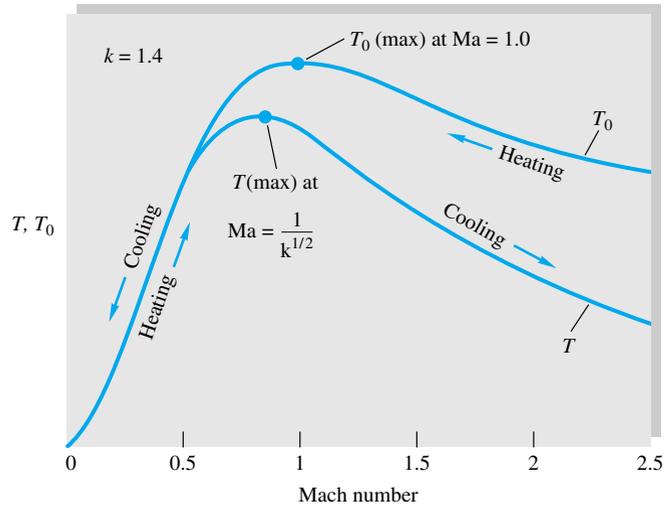
Fig. 9.17 Effect of heat transfer on Mach number.

ing (increasing T_0) actually decreases the gas temperature, the difference being reflected in a large increase of the gas kinetic energy. For $k = 1.4$ this peculiar area lies between $Ma = 0.845$ and $Ma = 1.0$ (interesting but not very useful information).

The complete list of the effects of simple T_0 change on duct-flow properties is as follows:

	Heating		**Cooling**	
	Subsonic	**Supersonic**	**Subsonic**	**Supersonic**
T_0	Increases	Increases	Decreases	Decreases
Ma	Increases	Decreases	Decreases	Increases
p	Decreases	Increases	Increases	Decreases
ρ	Decreases	Increases	Increases	Decreases
V	Increases	Decreases	Decreases	Increases
p_0	Decreases	Decreases	Increases	Increases
s	Increases	Increases	Decreases	Decreases
T	*	Increases	†	Decreases

*Increases up to $Ma = 1/k^{1/2}$ and decreases thereafter.
†Decreases up to $Ma = 1/k^{1/2}$ and increases thereafter.

Probably the most significant item on this list is the stagnation pressure p_0, which always decreases during heating whether the flow is subsonic or supersonic. Thus heating does increase the Mach number of a flow but entails a loss in effective pressure recovery.

Mach-Number Relations

Equations (9.76) and (9.77) can be rearranged in terms of the Mach number and the results tabulated. For convenience, we specify that the outlet section is sonic, $Ma = 1$, with reference properties T_0^*, T^*, p^*, ρ^*, V^*, and p_0^*. The inlet is assumed to be at arbitrary Mach number Ma. Equations (9.76) and (9.77) then take the following form:

$$\frac{T_0}{T_0^*} = \frac{(k + 1) \, Ma^2 \, [2 + (k - 1) \, Ma^2]}{(1 + k \, Ma^2)^2} \tag{9.78a}$$

$$\frac{T}{T^*} = \frac{(k+1)^2\,\mathrm{Ma}^2}{(1+k\,\mathrm{Ma}^2)^2} \tag{9.78b}$$

$$\frac{p}{p^*} = \frac{k+1}{1+k\,\mathrm{Ma}^2} \tag{9.78c}$$

$$\frac{V}{V^*} = \frac{\rho^*}{\rho} = \frac{(k+1)\,\mathrm{Ma}^2}{1+k\,\mathrm{Ma}^2} \tag{9.78d}$$

$$\frac{p_0}{p_0^*} = \frac{k+1}{1+k\,\mathrm{Ma}^2}\left[\frac{2+(k-1)\,\mathrm{Ma}^2}{k+1}\right]^{k/(k-1)} \tag{9.78e}$$

These formulas are all tabulated versus Mach number in Table B.4. The tables are very convenient if inlet properties Ma_1, V_1, etc., are given but are somewhat cumbersome if the given information centers on T_{01} and T_{02}. Let us illustrate with an example.

EXAMPLE 9.14

A fuel-air mixture, approximated as air with $k = 1.4$, enters a duct combustion chamber at $V_1 = 75$ m/s, $p_1 = 150$ kPa, and $T_1 = 300$ K. The heat addition by combustion is 900 kJ/kg of mixture. Compute (a) the exit properties V_2, p_2, and T_2 and (b) the total heat addition which would have caused a sonic exit flow.

Solution

Part (a)
First compute $T_{01} = T_1 + V_1^2/(2c_p) = 300 + (75)^2/[2(1005)] = 303$ K. Then compute the change in stagnation temperature of the gas:

$$q = c_p(T_{02} - T_{01})$$

or $\qquad T_{02} = T_{01} + \dfrac{q}{c_p} = 303\ \mathrm{K} + \dfrac{900{,}000\ \mathrm{J/kg}}{1005\ \mathrm{J/(kg \cdot K)}} = 1199\ \mathrm{K}$

We have enough information to compute the initial Mach number:

$$a_1 = \sqrt{kRT_1} = [1.4(287)(300)]^{1/2} = 347\ \mathrm{m/s} \qquad \mathrm{Ma}_1 = \frac{V_1}{a_1} = \frac{75}{347} = 0.216$$

For this Mach number, use Eq. (9.78a) or Table B.4 to find the sonic value T^*_0:

At $\mathrm{Ma}_1 = 0.216$: $\qquad \dfrac{T_{01}}{T^*_0} \approx 0.1992 \qquad$ or $\qquad T^*_0 = \dfrac{303\ \mathrm{K}}{0.1992} \approx 1521\ \mathrm{K}$

Then the stagnation temperature ratio at section 2 is $T_{02}/T^*_0 = 1199/1521 = 0.788$, which corresponds in Table B.4 to a Mach number $\mathrm{Ma}_2 \approx 0.573$.

Now use Table B.4 at Ma_1 and Ma_2 to tabulate the desired property ratios.

Section	Ma	V/V^*	p/p^*	T/T^*
1	0.216	0.1051	2.2528	0.2368
2	0.573	0.5398	1.6442	0.8876

The exit properties are computed by using these ratios to find state 2 from state 1:

$$V_2 = V_1 \frac{V_2/V^*}{V_1/V^*} = (75 \text{ m/s}) \frac{0.5398}{0.1051} = 385 \text{ m/s} \qquad \text{Ans. (a)}$$

$$p_2 = p_1 \frac{p_2/p^*}{p_1/p^*} = (150 \text{ kPa}) \frac{1.6442}{2.2528} = 109 \text{ kPa} \qquad \text{Ans. (a)}$$

$$T_2 = T_1 \frac{T_2/T^*}{T_1/T^*} = (300 \text{ K}) \frac{0.8876}{0.2368} = 1124 \text{ K} \qquad \text{Ans. (a)}$$

Part (b)   The maximum allowable heat addition would drive the exit Mach number to unity:

$$T_{02} = T_0^* = 1521 \text{ K}$$

$$q_{max} = c_p(T_0^* - T_{01}) = [1005 \text{ J/(kg} \cdot \text{K)}](1521 - 303 \text{ K}) \approx 1.22 \text{ E6 J/kg} \qquad \text{Ans. (b)}$$

Choking Effects due to Simple Heating

Equation (9.78a) and Table B.4 indicate that the maximum possible stagnation temperature in simple heating corresponds to T_0^*, or the sonic exit Mach number. Thus, for given inlet conditions, only a certain maximum amount of heat can be added to the flow, for example, 1.22 MJ/kg in Example 9.14. For a subsonic inlet there is no theoretical limit on heat addition: The flow chokes more and more as we add more heat, with the inlet velocity approaching zero. For supersonic flow, even if Ma_1 is infinite, there is a finite ratio $T_{01}/T_0^* = 0.4898$ for $k = 1.4$. Thus if heat is added without limit to a supersonic flow, a normal-shock-wave adjustment is required to accommodate the required property changes.

In subsonic flow there is no theoretical limit to the amount of cooling allowed: The exit flow just becomes slower and slower, and the temperature approaches zero. In supersonic flow only a finite amount of cooling can be allowed before the exit flow approaches infinite Mach number, with $T_{02}/T_0^* = 0.4898$ and the exit temperature equal to zero. There are very few practical applications for supersonic cooling.

EXAMPLE 9.15

What happens to the inlet flow in Example 9.14 if the heat addition is increased to 1400 kJ/kg and the inlet pressure and stagnation temperature are fixed? What will be the subsequent decrease in mass flow?

Solution

For $q = 1400$ kJ/kg, the exit will be choked at the stagnation temperature

$$T_0^* = T_{01} + \frac{q}{c_p} = 303 + \frac{1.4 \text{ E6 J/kg}}{1005 \text{ J/(kg} \cdot \text{K)}} \approx 1696 \text{ K}$$

This is higher than the value $T_0^* = 1521$ K in Example 9.14, so we know that condition 1 will have to choke down to a lower Mach number. The proper value is found from the ratio $T_{01}/T_0^* = 303/1696 = 0.1787$. From Table B.4 or Eq. (9.78a) for this condition, we read the

new, lowered entrance Mach number: $Ma_{1,new} \approx 0.203$. With T_{01} and p_1 known, the other inlet properties follow from this Mach number:

$$T_1 = \frac{T_{01}}{1 + 0.2 \, Ma_1^2} = \frac{303}{1 + 0.2(0.203)^2} = 301 \text{ K}$$

$$a_1 = \sqrt{kRT_1} = [1.4(287)(301)]^{1/2} = 348 \text{ m/s}$$

$$V_1 = Ma_1 \, a_1 = (0.202)(348 \text{ m/s}) = 70 \text{ m/s}$$

$$\rho_1 = \frac{p_1}{RT_1} = \frac{150,000}{(287)(301)} = 1.74 \text{ kg/m}^3$$

Finally, the new lowered mass flow per unit area is

$$\frac{\dot{m}_{new}}{A} = \rho_1 V_1 = (1.74 \text{ kg/m}^3)(70 \text{ m/s}) = 122 \text{ kg/(s} \cdot \text{m}^2)$$

This is 7 percent less than in Example 9.14, due to choking by excess heat addition.

Relationship to the Normal-Shock Wave

The normal-shock-wave relations of Sec. 9.5 actually lurk within the simple heating relations as a special case. From Table B.4 or Fig. 9.17 we see that for a given stagnation temperature less than T_0^* there are two flow states which satisfy the simple heating relations, one subsonic and the other supersonic. These two states have (1) the same value of T_0, (2) the same mass flow per unit area, and (3) the same value of $p + \rho V^2$. Therefore these two states are exactly equivalent to the conditions on each side of a normal-shock wave. The second law would again require that the upstream flow Ma_1 be supersonic.

To illustrate this point, take $Ma_1 = 3.0$ and from Table B.4 read $T_{01}/T_0^* = 0.6540$ and $p_1/p^* = 0.1765$. Now, for the same value $T_{02}/T_0^* = 0.6540$, use Table B.4 or Eq. (9.78a) to compute $Ma_2 = 0.4752$ and $p_2/p^* = 1.8235$. The value of Ma_2 is exactly what we read in the shock table, Table B.2, as the downstream Mach number when $Ma_1 = 3.0$. The pressure ratio for these two states is $p_2/p_1 = (p_2/p^*)/(p_1/p^*) = 1.8235/0.1765 = 10.33$, which again is just what we read in Table B.2 for $Ma_1 = 3.0$. This illustration is meant only to show the physical background of the simple heating relations; it would be silly to make a practice of computing normal-shock waves in this manner.

9.9 Two-Dimensional Supersonic Flow

Up to this point we have considered only one-dimensional compressible-flow theories. This illustrated many important effects, but a one-dimensional world completely loses sight of the wave motions which are so characteristic of supersonic flow. The only "wave motion" we could muster in a one-dimensional theory was the normal-shock wave, which amounted only to a flow discontinuity in the duct.

Mach Waves

When we add a second dimension to the flow, wave motions immediately become apparent if the flow is supersonic. Figure 9.18 shows a celebrated graphical construction which appears in every fluid-mechanics textbook and was first presented by Ernst Mach in 1887. The figure shows the pattern of pressure disturbances (sound waves) sent out by a small particle moving at speed U through a still fluid whose sound velocity is a.
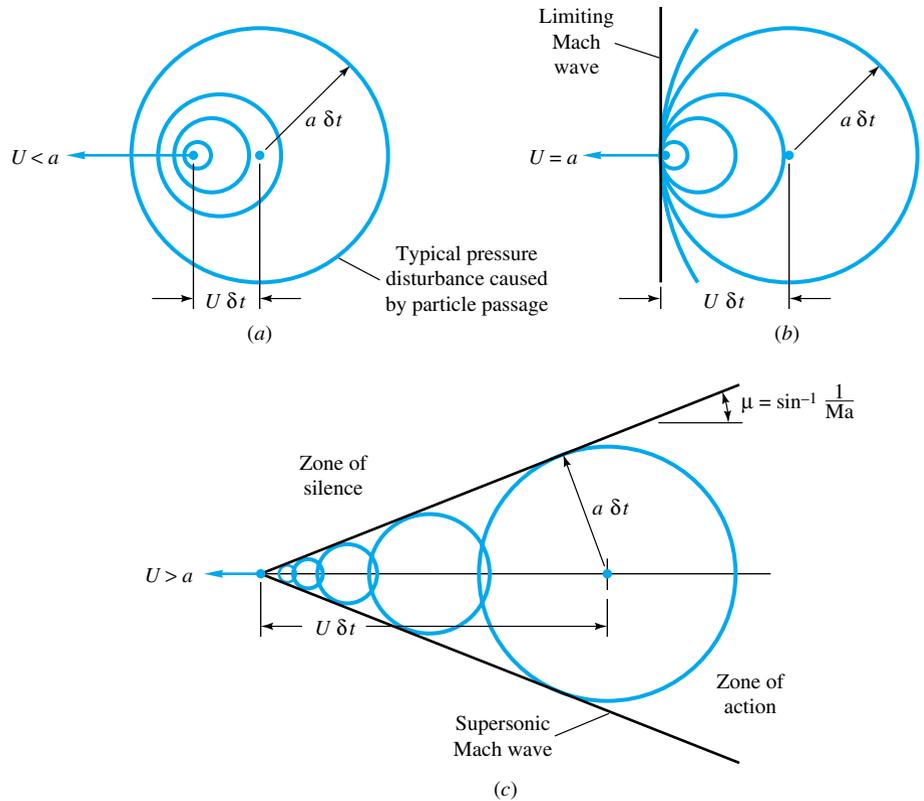
Fig. 9.18 Wave patterns set up by a particle moving at speed U into still fluid of sound velocity a: (a) subsonic, (b) sonic, and (c) supersonic motion.

As the particle moves, it continually crashes against fluid particles and sends out spherical sound waves emanating from every point along its path. A few of these spherical disturbance fronts are shown in Fig. 9.18. The behavior of these fronts is quite different according to whether the particle speed is subsonic or supersonic.

In Fig. 9.18a, the particle moves subsonically, $U < a$, $Ma = U/a < 1$. The spherical disturbances move out in all directions and do not catch up with one another. They move well out in front of the particle also, because they travel a distance $a\ \delta t$ during the time interval δt in which the particle has moved only $U\ \delta t$. Therefore a subsonic body motion makes its presence felt everywhere in the flow field: You can "hear" or "feel" the pressure rise of an oncoming body before it reaches you. This is apparently why that pigeon in the road, without turning around to look at you, takes to the air and avoids being hit by your car.

At sonic speed, $U = a$, Fig. 9.18b, the pressure disturbances move at exactly the speed of the particle and thus pile up on the left at the position of the particle into a sort of "front locus," which is now called a *Mach wave*, after Ernst Mach. No disturbance reaches beyond the particle. If you are stationed to the left of the particle, you cannot "hear" the oncoming motion. If the particle blew its horn, you couldn't hear that either: A sonic car can sneak up on a pigeon.

In supersonic motion, $U > a$, the lack of advance warning is even more pronounced. The disturbance spheres cannot catch up with the fast-moving particle which created them. They all trail behind the particle and are tangent to a conical locus called the *Mach cone*. From the geometry of Fig. 9.18c the angle of the Mach cone is seen to be
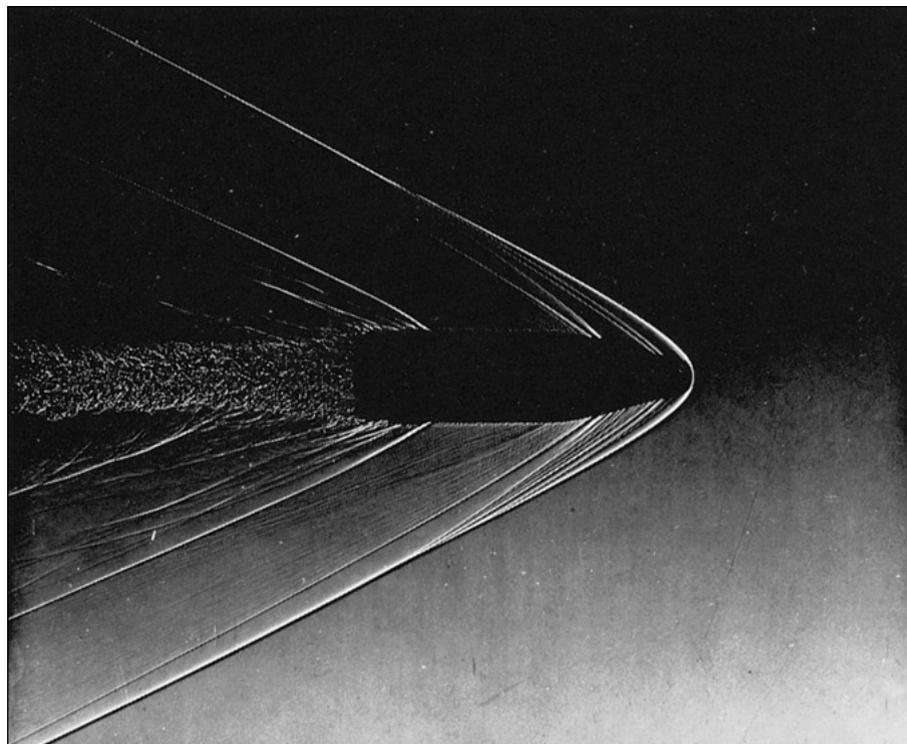
Fig. 9.19 Supersonic wave pattern emanating from a projectile moving at Ma ≈ 2.0. The heavy lines are oblique-shock waves and the light lines Mach waves (*Courtesy of U.S. Army Ballistic Research Laboratory, Aberdeen Proving Ground.*)

$$\mu = \sin^{-1}\frac{a}{U}\frac{\delta t}{\delta t} = \sin^{-1}\frac{a}{U} = \sin^{-1}\frac{1}{\text{Ma}} \tag{9.79}$$

The higher the particle Mach number, the more slender the Mach cone; for example, μ is 30° at Ma = 2.0 and 11.5° at Ma = 5.0. For the limiting case of sonic flow, Ma = 1, μ = 90°; the Mach cone becomes a plane front moving with the particle, in agreement with Fig. 9.18*b*.

You cannot "hear" the disturbance caused by the supersonic particle in Fig. 9.18*c* until you are in the *zone of action* inside the Mach cone. No warning can reach your ears if you are in the *zone of silence* outside the cone. Thus an observer on the ground beneath a supersonic airplane does not hear the *sonic boom* of the passing cone until the plane is well past.

The Mach wave need not be a cone: Similar waves are formed by a small disturbance of any shape moving supersonically with respect to the ambient fluid. For example, the "particle" in Fig. 9.18*c* could be the leading edge of a sharp flat plate, which would form a Mach wedge of exactly the same angle μ. Mach waves are formed by small roughnesses or boundary-layer irregularities in a supersonic wind tunnel or at the surface of a supersonic body. Look again at Fig. 9.10: Mach waves are clearly visible along the body surface downstream of the recompression shock, especially at the rear corner. Their angle is about 30°, indicating a Mach number of about 2.0 along this surface. A more complicated system of Mach waves emanates from the supersonic projectile in Fig. 9.19. The Mach angles change, indicating a variable supersonic Mach

number along the body surface. There are also several stronger oblique-shock waves formed along the surface.

EXAMPLE 9.16

An observer on the ground does not hear the sonic boom caused by an airplane moving at 5-km altitude until it is 9 km past her. What is the approximate Mach number of the plane? Assume a small disturbance and neglect the variation of sound speed with altitude.

Solution

A finite disturbance like an airplane will create a finite-strength oblique-shock wave whose angle will be somewhat larger than the Mach-wave angle μ and will curve downward due to the variation in atmospheric sound speed. If we neglect these effects, the altitude and distance are a measure of μ, as seen in Fig. E9.16. Thus
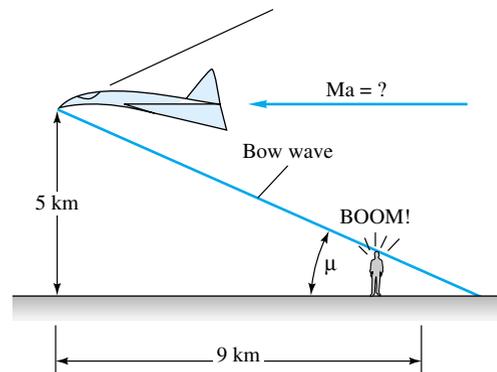
E9.16

$$\tan \mu = \frac{5 \text{ km}}{9 \text{ km}} = 0.5556 \qquad \text{or} \qquad \mu = 29.05°$$

Hence, from Eq. (9.79),

$$\text{Ma} = \csc \mu = 2.06 \qquad\qquad\qquad Ans.$$

The Oblique-Shock Wave

Figures 9.10 and 9.19 and our earlier discussion all indicate that a shock wave can form at an oblique angle to the oncoming supersonic stream. Such a wave will deflect the stream through an angle θ, unlike the normal-shock wave, for which the downstream flow is in the same direction. In essence, an oblique shock is caused by the necessity for a supersonic stream to turn through such an angle. Examples could be a finite wedge at the leading edge of a body and a ramp in the wall of a supersonic wind tunnel.

The flow geometry of an oblique shock is shown in Fig. 9.20. As for the normal shock of Fig. 9.8, state 1 denotes the upstream conditions and state 2 is downstream. The shock angle has an arbitrary value β, and the downstream flow V_2 turns at an angle θ which is a function of β and state 1 conditions. The upstream flow is always supersonic, but the downstream Mach number $\text{Ma}_2 = V_2/a_2$ may be subsonic, sonic, or supersonic, depending upon the conditions.

It is convenient to analyze the flow by breaking it up into normal and tangential components with respect to the wave, as shown in Fig. 9.20. For a thin control volume
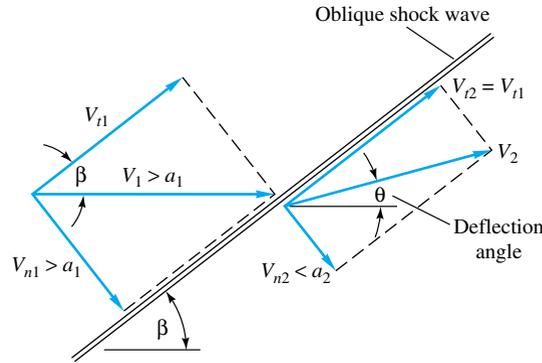
Fig. 9.20 Geometry of flow through an oblique-shock wave.

just encompassing the wave, we can then derive the following integral relations, canceling out $A_1 = A_2$ on each side of the wave:

Continuity: $$\rho_1 V_{n1} = \rho_2 V_{n2} \tag{9.80a}$$

Normal momentum: $$p_1 - p_2 = \rho_2 V_{n2}^2 - \rho_1 V_{n1}^2 \tag{9.80b}$$

Tangential momentum: $$0 = \rho_1 V_{n1}(V_{t2} - V_{t1}) \tag{9.80c}$$

Energy: $$h_1 + \tfrac{1}{2}V_{n1}^2 + \tfrac{1}{2}V_{t1}^2 = h_2 + \tfrac{1}{2}V_{n2}^2 + \tfrac{1}{2}V_{t2}^2 = h_0 \tag{9.80d}$$

We see from Eq. (9.80c) that there is no change in tangential velocity across an oblique shock

$$V_{t2} = V_{t1} = V_t = \text{const} \tag{9.81}$$

Thus tangential velocity has as its only effect the addition of a constant kinetic energy $\tfrac{1}{2}V_t^2$ to each side of the energy equation (9.80d). We conclude that Eqs. (9.80) are identical to the normal-shock relations (9.49), with V_1 and V_2 replaced by the normal components V_{n1} and V_{n2}. All the various relations from Sec. 9.5 can be used to compute properties of an oblique-shock wave. The trick is to use the "normal" Mach numbers in place of Ma_1 and Ma_2:

$$Ma_{n1} = \frac{V_{n1}}{a_1} = Ma_1 \sin \beta$$

$$Ma_{n2} = \frac{V_{n2}}{a_2} = Ma_2 \sin (\beta - \theta) \tag{9.82}$$

Then, for a perfect gas with constant specific heats, the property ratios across the oblique shock are the analogs of Eqs. (9.55) to (9.58) with Ma_1 replaced by Ma_{n1}:

$$\frac{p_2}{p_1} = \frac{1}{k + 1} [2k \, Ma_1^2 \sin^2 \beta - (k - 1)] \tag{9.83a}$$

$$\frac{\rho_2}{\rho_1} = \frac{\tan \beta}{\tan (\beta - \theta)} = \frac{(k + 1) \, Ma_1^2 \sin^2 \beta}{(k - 1) \, Ma_1^2 \sin^2 \beta + 2} = \frac{V_{n1}}{V_{n2}} \tag{9.83b}$$

$$\frac{T_2}{T_1} = [2 + (k - 1) \, Ma_1^2 \sin^2 \beta] \frac{2k \, Ma_1^2 \sin^2 \beta - (k - 1)}{(k + 1)^2 \, Ma_1^2 \sin^2 \beta} \tag{9.83c}$$

$$T_{02} = T_{01} \tag{9.83d}$$

$$\frac{p_{02}}{p_{01}} = \left[\frac{(k+1)\,\mathrm{Ma}_1^2\,\sin^2\beta}{2+(k-1)\,\mathrm{Ma}_1^2\,\sin^2\beta}\right]^{k/(k-1)}\left[\frac{k+1}{2k\,\mathrm{Ma}_1^2\,\sin^2\beta-(k-1)}\right]^{1/(k-1)} \tag{9.83e}$$

$$\mathrm{Ma}_{n2}^2 = \frac{(k-1)\,\mathrm{Ma}_{n1}^2+2}{2k\,\mathrm{Ma}_{n1}^2-(k-1)} \tag{9.83f}$$

All these are tabulated in the normal-shock Table B.2. If you wondered why that table listed the Mach numbers as Ma_{n1} and Ma_{n2}, it should be clear now that the table is also valid for the oblique-shock wave.

Thinking all this over, we realize by hindsight that an oblique-shock wave is the flow pattern one would observe by running along a normal-shock wave (Fig. 9.8) at a constant tangential speed V_t. Thus the normal and oblique shocks are related by a galilean, or inertial, velocity transformation and therefore satisfy the same basic equations.

If we continue with this run-along-the-shock analogy, we find that the deflection angle θ increases with speed V_t up to a maximum and then decreases. From the geometry of Fig. 9.20 the deflection angle is given by

$$\theta = \tan^{-1}\frac{V_t}{V_{n2}} - \tan^{-1}\frac{V_t}{V_{n1}} \tag{9.84}$$

If we differentiate θ with respect to V_t and set the result equal to zero, we find that the maximum deflection occurs when $V_t/V_{n1} = (V_{n2}/V_{n1})^{1/2}$. We can substitute this back into Eq. (9.84) to compute

$$\theta_{\max} = \tan^{-1} r^{1/2} - \tan^{-1} r^{-1/2} \qquad r = \frac{V_{n1}}{V_{n2}} \tag{9.85}$$

For example, if $\mathrm{Ma}_{n1} = 3.0$, from Table B.2 we find that $V_{n1}/V_{n2} = 3.8571$, the square root of which is 1.9640. Then Eq. (9.85) predicts a maximum deflection of $\tan^{-1} 1.9640 - \tan^{-1}(1/1.9640) = 36.03°$. The deflection is quite limited even for infinite Ma_{n1}: From Table B.2 for this case $V_{n1}/V_{n2} = 6.0$, and we compute from Eq. (9.85) that $\theta_{\max} = 45.58°$.

This limited-deflection idea and other facts become more evident if we plot some of the solutions of Eqs. (9.83). For given values of V_1 and a_1, assuming as usual that $k = 1.4$, we can plot all possible solutions for V_2 downstream of the shock. Figure 9.21 does this in velocity-component coordinates V_x and V_y, with x parallel to V_1. Such a plot is called a *hodograph*. The heavy dark line which looks like a fat airfoil is the locus, or *shock polar*, of all physically possible solutions for the given Ma_1. The two dashed-line fishtails are solutions which increase V_2; they are physically impossible because they violate the second law.

Examining the shock polar in Fig. 9.21, we see that a given deflection line of small angle θ crosses the polar at two possible solutions: the *strong* shock, which greatly decelerates the flow, and the *weak* shock, which causes a much milder deceleration. The flow downstream of the strong shock is always subsonic, while that of the weak shock is usually supersonic but occasionally subsonic if the deflection is large. Both types of shock occur in practice. The weak shock is more prevalent, but the strong shock will occur if there is a blockage or high-pressure condition downstream.

Since the shock polar is only of finite size, there is a maximum deflection $\theta_{\max}$, shown in Fig. 9.21, which just grazes the upper edge of the polar curve. This verifies the kinematic discussion which led to Eq. (9.85). What happens if a supersonic flow is forced to deflect through an angle greater than $\theta_{\max}$? The answer is illustrated in Fig. 9.22 for flow past a wedge-shaped body.
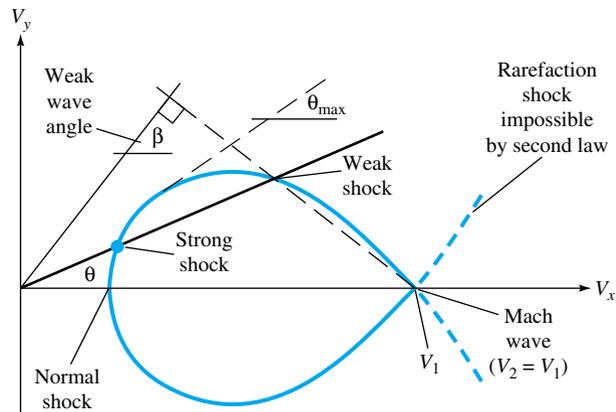
Fig. 9.21 The oblique-shock polar hodograph, showing double solutions (strong and weak) for small deflection angle and no solutions at all for large deflection.

In Fig. 9.22a the wedge half-angle θ is less than θ_{max}, and thus an oblique shock forms at the nose of wave angle β just sufficient to cause the oncoming supersonic stream to deflect through the wedge angle θ. Except for the usually small effect of boundary-layer growth (see, e.g., Ref. 19, sec. 7–5.2), the Mach number Ma_2 is constant along the wedge surface and is given by the solution of Eqs. (9.83). The pressure, density, and temperature along the surface are also nearly constant, as predicted by Eqs. (9.83). When the flow reaches the corner of the wedge, it expands to higher Mach number and forms a wake (not shown) similar to that in Fig. 9.10.

(a)

(b)
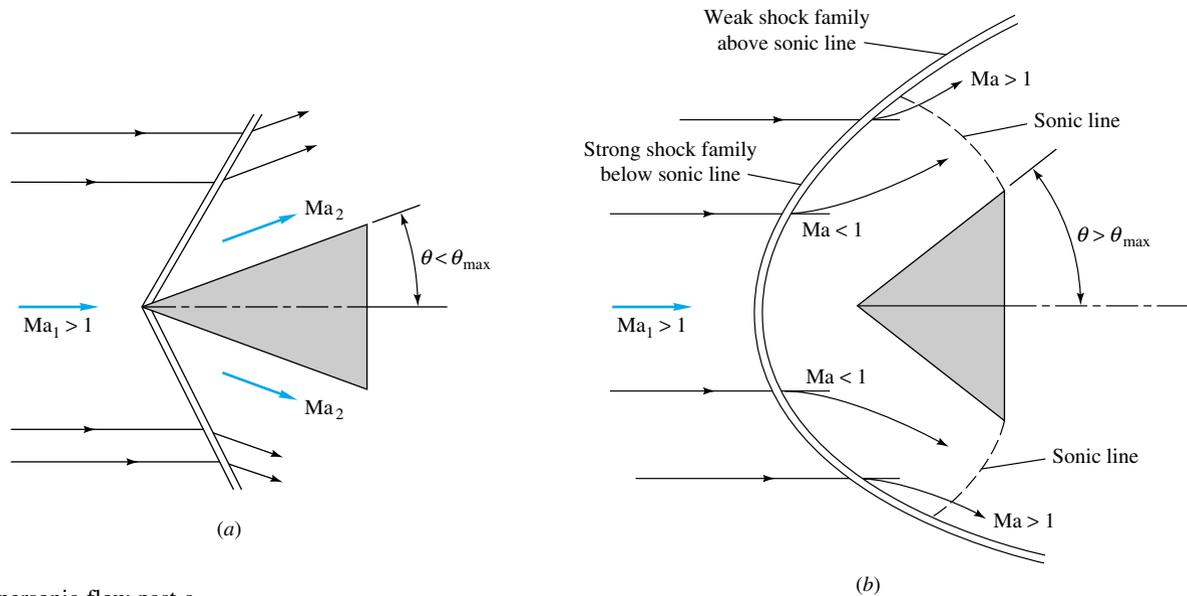
Fig. 9.22 Supersonic flow past a wedge: (a) small wedge angle, attached oblique shock forms; (b) large wedge angle, attached shock not possible, broad curved detached shock forms.

In Fig. 9.22b the wedge half-angle is greater than θ_{max}, and an attached oblique shock is impossible. The flow cannot deflect at once through the entire angle θ_{max}, yet somehow the flow must get around the wedge. A detached curve shock wave forms in front of the body, discontinuously deflecting the flow through angles smaller than θ_{max}.
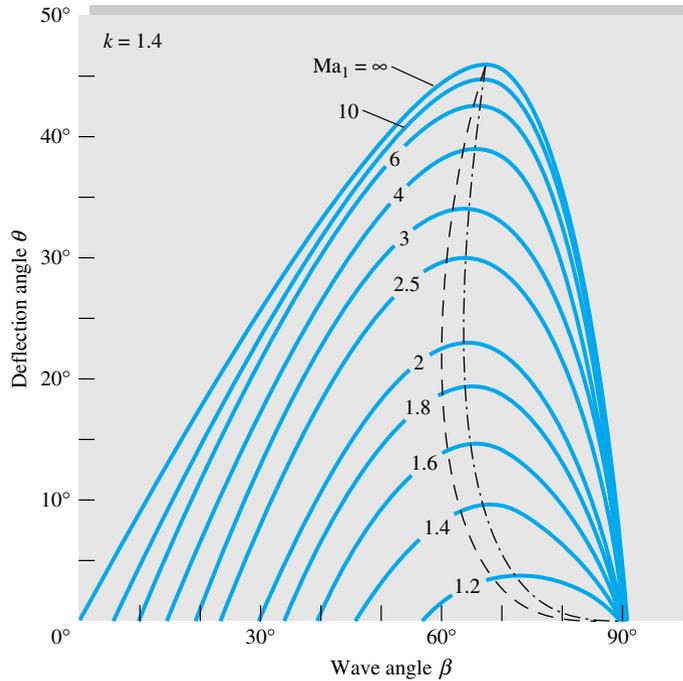
Fig. 9.23 Oblique-shock deflection versus wave angle for various upstream Mach numbers, $k = 1.4$: dash-dot curve, locus of θ_{max}, divides strong (right) from weak (left) shocks; dashed curve, locus of sonic points, divides subsonic Ma_2 (right) from supersonic Ma_2 (left).

The flow then curves, expands, and deflects subsonically around the wedge, becoming sonic and then supersonic as it passes the corner region. The flow just inside each point on the curved shock exactly satisfies the oblique-shock relations (9.83) for that particular value of β and the given Ma_1. Every condition along the curved shock is a point on the shock polar of Fig. 9.21. Points near the front of the wedge are in the strong-shock family, and points aft of the sonic line are in the weak-shock family. The analysis of detached shock waves is extremely complex, and experimentation is usually needed, e.g., the shadowgraph optical technique of Fig. 9.10.

The complete family of oblique-shock solutions can be plotted or computed from Eqs. (9.83). For a given k, the wave angle β varies with Ma_1 and θ, from Eq. (9.83b). By using a trigonometric identity for $\tan(\beta - \theta)$ this can be rewritten in the more convenient form

$$\tan \theta = \frac{2 \cot \beta \, (Ma_1^2 \sin^2 \beta - 1)}{Ma_1^2 \, (k + \cos 2\beta) + 2} \tag{9.86}$$

All possible solutions of Eq. (9.86) for $k = 1.4$ are shown in Fig. 9.23. For deflections $\theta < \theta_{max}$ there are two solutions: a weak shock (small β) and a strong shock (large β), as expected. All points along the dash-dot line for θ_{max} satisfy Eq. (9.85). A dashed line has been added to show where Ma_2 is exactly sonic. We see that there is a narrow region near maximum deflection where the weak-shock downstream flow is subsonic.

For zero deflections ($\theta = 0$) the weak-shock family satisfies the wave-angle relation

$$\beta = \mu = \sin^{-1} \frac{1}{Ma_1} \tag{9.87}$$

Thus weak shocks of vanishing deflection are equivalent to Mach waves. Meanwhile the strong shocks all converge at zero deflection to the normal-shock condition $\beta = 90°$.

Two additional oblique-shock charts are given in App. B, where Fig. B.1 gives the downstream Mach number Ma_2 and Fig. B.2 the pressure ratio p_2/p_1, each plotted as a function of Ma_1 and θ. Additional graphs, tables, and computer programs are given in Refs. 24 and 25.

Very Weak Shock Waves

For any finite θ the wave angle β for a weak shock is greater than the Mach angle μ. For small θ Eq. (9.86) can be expanded in a power series in tan θ with the following linearized result for the wave angle:

$$\sin \beta = \sin \mu + \frac{k + 1}{4 \cos \mu} \tan \theta + \cdots + \mathbb{O}(\tan^2 \theta) + \cdots \tag{9.88}$$

For Ma_1 between 1.4 and 20.0 and deflections less than 6° this relation predicts β to within 1° for a weak shock. For larger deflections it can be used as a useful initial guess for iterative solution of Eq. (9.86).

Other property changes across the oblique shock can also be expanded in a power series for small deflection angles. Of particular interest is the pressure change from Eq. (9.83a), for which the linearized result for a weak shock is

$$\frac{p_2 - p_1}{p_1} = \frac{k \, Ma_1^2}{(Ma_1^2 - 1)^{1/2}} \tan \theta + \cdots + \mathbb{O}(\tan^2 \theta) + \cdots \tag{9.89}$$
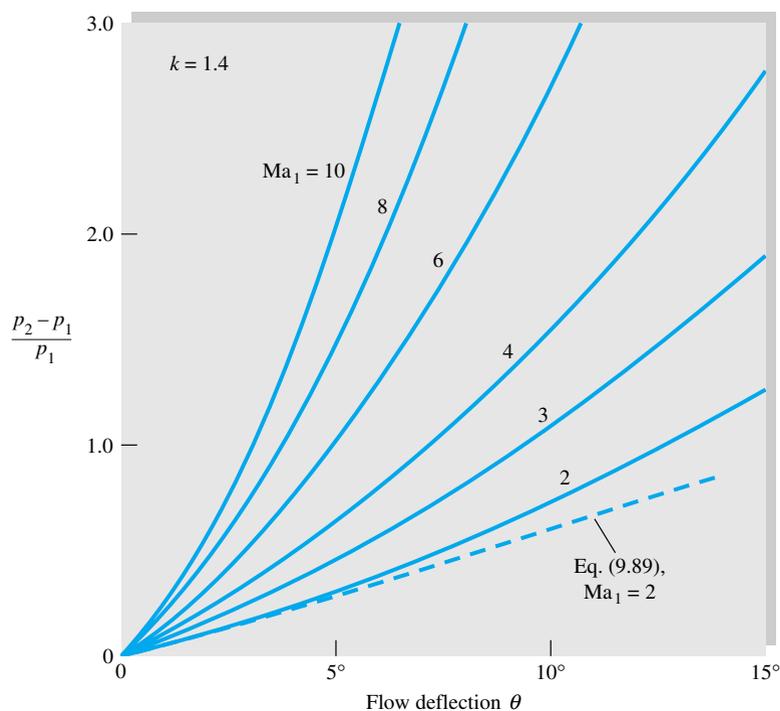
Fig. 9.24 Pressure jump across a weak oblique-shock wave from Eq. (9.83a) for $k = 1.4$. For very small deflections Eq. (9.89) applies.

The differential form of this relation is used in the next section to develop a theory for supersonic expansion turns. Figure 9.24 shows the exact weak-shock pressure jump computed from Eq. (9.83a). At very small deflections the curves are linear with slopes given by Eq. (9.89).

Finally, it is educational to examine the entropy change across a very weak shock. Using the same power-series expansion technique, we can obtain the following result for small flow deflections:

$$\frac{s_2 - s_1}{c_p} = \frac{(k^2 - 1)Ma_1^6}{12(Ma_1^2 - 1)^{3/2}} \tan^3 \theta + \cdots + \mathbb{O}(\tan^4 \theta) + \cdots \qquad (9.90)$$

The entropy change is cubic in the deflection angle θ. Thus weak shock waves are very nearly isentropic, a fact which is also used in the next section.

EXAMPLE 9.17

Ma$_2$

Ma$_1$ = 2.0

p_1 = 10 lbf/in^2

β

10°

E9.17

EES
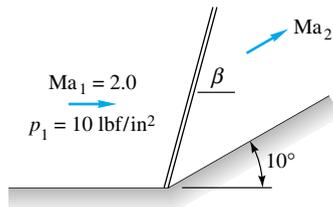
Air at Ma = 2.0 and $p = 10$ lbf/in^2 absolute is forced to turn through 10° by a ramp at the body surface. A weak oblique shock forms as in Fig. E9.17. For $k = 1.4$ compute from exact oblique-shock theory (a) the wave angle β, (b) Ma$_2$, and (c) p_2. Also use the linearized theory to estimate (d) β and (e) p_2.

Solution

With Ma$_1$ = 2.0 and θ = 10° known, we can estimate $\beta \approx 40° \pm 2°$ from Fig. 9.23. For more (hand calculated) accuracy, we have to solve Eq. (9.86) by iteration. Or we can program Eq. (9.86) in EES with six statements (in SI units, with angles in degrees):

```
Ma = 2.0
k = 1.4
Theta = 10
Num = 2*(Ma^2*SIN(Beta)^2 − 1)/TAN(Beta)
Denom = Ma^2*(k + COS(2*Beta)) + 2
Theta = ARCTAN(Num/Denom)
```

Specify that Beta > 0 and EES promptly reports an accurate result:

$$\beta = 39.32° \qquad \qquad Ans. (a)$$

The normal Mach number upstream is thus

$$Ma_{n1} = Ma_1 \sin \beta = 2.0 \sin 39.32° = 1.267$$

With Ma$_{n1}$ we can use the normal-shock relations (Table B.2) or Fig. 9.9 or Eqs. (9.56) to (9.58) to compute

$$Ma_{n2} = 0.8031 \qquad \frac{p_2}{p_1} = 1.707$$

Thus the downstream Mach number and pressure are

$$Ma_2 = \frac{Ma_{n2}}{\sin (\beta - \theta)} = \frac{0.8031}{\sin (39.32° - 10°)} = 1.64 \qquad Ans. (b)$$

$$p_2 = (10 \text{ lbf/in}^2 \text{ absolute})(1.707) = 17.07 \text{ lbf/in}^2 \text{ absolute} \qquad Ans. (c)$$

Notice that the computed pressure ratio agrees with Figs. 9.24 and B.2.

For the linearized theory the Mach angle is $\mu = \sin^{-1}(1/2.0) = 30°$. Equation (9.88) then estimates that

$$\sin \beta \approx \sin 30° + \frac{2.4 \tan 10°}{4 \cos 30°} = 0.622$$

or
$$\beta \approx 38.5°$$ *Ans. (d)*

Equation (9.89) estimates that

$$\frac{p_2}{p_1} \approx 1 + \frac{1.4(2)^2 \tan 10°}{(2^2 - 1)^{1/2}} = 1.57$$

or
$$p_2 \approx 1.57(10 \text{ lbf/in}^2 \text{ absolute}) \approx 15.7 \text{ lbf/in}^2 \text{ absolute}$$ *Ans. (e)*

These are reasonable estimates in spite of the fact that 10° is really not a "small" flow deflection.

9.10 Prandtl-Meyer Expansion Waves

The oblique-shock solution of Sec. 9.9 is for a finite compressive deflection θ which obstructs a supersonic flow and thus decreases its Mach number and velocity. The present section treats gradual changes in flow angle which are primarily *expansive*; i.e., they widen the flow area and increase the Mach number and velocity. The property changes accumulate in infinitesimal increments, and the linearized relations (9.88) and (9.89) are used. The local flow deflections are infinitesimal, so that the flow is nearly isentropic according to Eq. (9.90).

Figure 9.25 shows four examples, one of which (Fig. 9.25c) fails the test for gradual changes. The gradual compression of Fig. 9.25a is essentially isentropic, with a
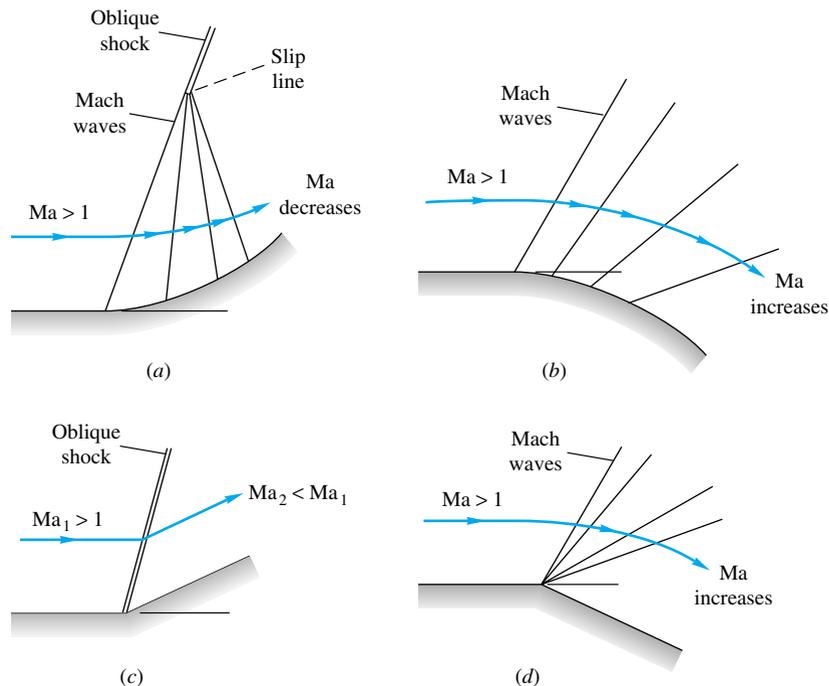
9.25 Some examples of supersonic expansion and compression: (a) gradual isentropic compression on a concave surface, Mach waves coalesce farther out to form oblique shock; (b) gradual isentropic expansion on convex surface, Mach waves diverge; (c) sudden compression, nonisentropic shock forms; (d) sudden expansion, centered isentropic fan of Mach waves forms.

smooth increase in pressure along the surface, but the Mach angle decreases along the surface and the waves tend to coalesce farther out into an oblique-shock wave. The gradual expansion of Fig. 9.25b causes a smooth isentropic increase of Mach number and velocity along the surface, with diverging Mach waves formed.

The sudden compression of Fig. 9.25c cannot be accomplished by Mach waves: An oblique shock forms, and the flow is nonisentropic. This could be what you would see if you looked at Fig. 9.25a from far away. Finally, the sudden expansion of Fig. 9.25d is isentropic and forms a fan of centered Mach waves emanating from the corner. Note that the flow on any streamline passing through the fan changes smoothly to higher Mach number and velocity. In the limit as we near the corner the flow expands almost discontinuously at the surface. The cases in Fig. 9.25a, b, and d can all be handled by the Prandtl-Meyer supersonic-wave theory of this section, first formulated by Ludwig Prandtl and his student Theodor Meyer in 1907 to 1908.

Note that none of this discussion makes sense if the upstream Mach number is subsonic, since Mach wave and shock wave patterns cannot exist in subsonic flow.

The Prandtl-Meyer Perfect-Gas Function

Consider a small, nearly infinitesimal flow deflection $d\theta$ such as occurs between the first two Mach waves in Fig. 9.25a. From Eqs. (9.88) and (9.89) we have, in the limit,

$$\beta \approx \mu = \sin^{-1} \frac{1}{\text{Ma}} \tag{9.91a}$$

$$\frac{dp}{p} \approx \frac{k\,\text{Ma}^2}{(\text{Ma}^2 - 1)^{1/2}}\, d\theta \tag{9.91b}$$

Since the flow is nearly isentropic, we have the frictionless differential momentum equation for a perfect gas

$$dp = -\rho V\, dV = -kp\,\text{Ma}^2\, \frac{dV}{V} \tag{9.92}$$

Combining Eqs. (9.91a) and (9.92) to eliminate dp, we obtain a relation between turning angle and velocity change

$$d\theta = -(\text{Ma}^2 - 1)^{1/2}\, \frac{dV}{V} \tag{9.93}$$

This can be integrated into a functional relation for finite turning angles if we can relate V to Ma. We do this from the definition of Mach number

$$V = \text{Ma}\, a$$

or

$$\frac{dV}{V} = \frac{d\,\text{Ma}}{\text{Ma}} + \frac{da}{a} \tag{9.94}$$

Finally, we can eliminate da/a because the flow is isentropic and hence a_0 is constant for a perfect gas

$$a = a_0[1 + \tfrac{1}{2}(k - 1)\,\text{Ma}^2]^{-1/2}$$

or

$$\frac{da}{a} = \frac{-\tfrac{1}{2}(k - 1)\,\text{Ma}\, d\,\text{Ma}}{1 + \tfrac{1}{2}(k - 1)\,\text{Ma}^2} \tag{9.95}$$

Eliminating dV/V and da/a from Eqs. (9.93) to (9.95), we obtain a relation solely between turning angle and Mach number

$$d\theta = -\frac{(Ma^2 - 1)^{1/2}}{1 + \frac{1}{2}(k - 1)\, Ma^2}\, \frac{d\, Ma}{Ma} \tag{9.96}$$

Before integrating this expression, we note that the primary application is to expansions, i.e., increasing Ma and decreasing θ. Therefore, for convenience, we define the Prandtl-Meyer angle $\omega(Ma)$ which increases when θ decreases and is zero at the sonic point

$$d\omega = -d\theta \qquad \omega = 0 \quad \text{at} \quad Ma = 1 \tag{9.97}$$

Thus we integrate Eq. (9.96) from the sonic point to any value of Ma

$$\int_0^\omega d\omega = \int_1^{Ma} \frac{(Ma^2 - 1)^{1/2}}{1 + \frac{1}{2}(k - 1)\, Ma^2}\, \frac{d\, Ma}{Ma} \tag{9.98}$$

The integrals are evaluated in closed form, with the result, in radians,

$$\omega(Ma) = K^{1/2} \tan^{-1}\left(\frac{Ma^2 - 1}{K}\right)^{1/2} - \tan^{-1}(Ma^2 - 1)^{1/2} \tag{9.99}$$

where

$$K = \frac{k + 1}{k - 1}$$

This is the *Prandtl-Meyer supersonic expansion function*, which is plotted in Fig. 9.26
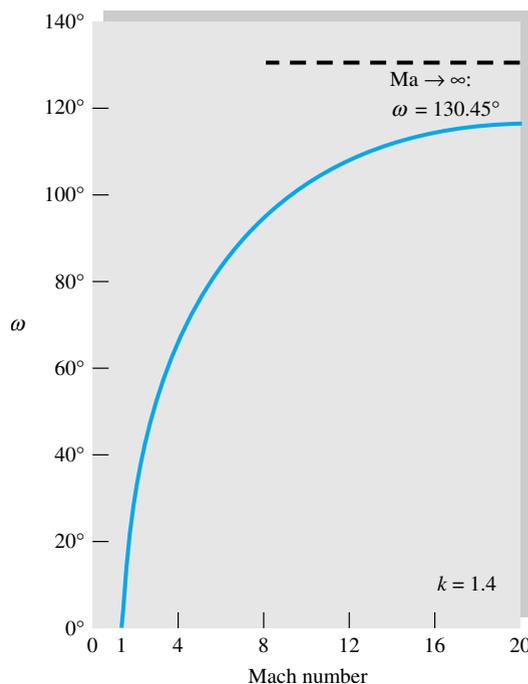
Fig,. 9.26 The Prandtl-Meyer supersonic expansion from Eq. (9.99) for $k = 1.4$.

and tabulated in Table B.5 for $k = 1.4$, $K = 6$. The angle ω changes rapidly at first and then levels off at high Mach number to a limiting value as $Ma \to \infty$:

$$\omega_{max} = \frac{\pi}{2}(K^{1/2} - 1) = 130.45° \qquad \text{if} \qquad k = 1.4 \qquad (9.100)$$

Thus a supersonic flow can expand only through a finite turning angle before it reaches infinite Mach number, maximum velocity, and zero temperature.

Gradual expansion or compression between finite Mach numbers Ma_1 and Ma_2, neither of which is unity, is computed by relating the turning angle $\Delta\omega$ to the difference in Prandtl-Meyer angles for the two conditions

$$\Delta\omega_{1\to2} = \omega(Ma_2) - \omega(Ma_1) \qquad (9.101)$$

The change $\Delta\omega$ may be either positive (expansion) or negative (compression) as long as the end conditions lie in the supersonic range. Let us illustrate with an example.

EES

EXAMPLE 9.18

Air ($k = 1.4$) flows at $Ma_1 = 3.0$ and $p_1 = 200$ kPa. Compute the final downstream Mach number and pressure for (*a*) an expansion turn of 20° and (*b*) a gradual compression turn of 20°.

Solution

Part (a)   The isentropic stagnation pressure is

$$p_0 = p_1[1 + 0.2(3.0)^2]^{3.5} = 7347 \text{ kPa}$$

and this will be the same at the downstream point. For $Ma_1 = 3.0$ we find from Table B.5 or Eq. (9.99) that $\omega_1 = 49.757°$. The flow expands to a new condition such that

$$\omega_2 = \omega_1 + \Delta\omega = 49.757° + 20° = 69.757°$$

EES

Linear interpolation in Table B.5 is quite accurate, yielding $Ma_2 \approx 4.32$. Inversion of Eq. (9.99), to find Ma when ω is given, is impossible without iteration. Once again, our friend EES easily handles Eq. (9.99) with four statements (angles specified in degrees):

```
k = 1.4
C = ((k+1)/(k − 1))^0.5
Omega = 69.757
Omega = C*ARCTAN((Ma^2−1)^0.5/C) − ARCTAN((Ma^2−1)^0.5)
```

Specify that Ma > 1, and EES readily reports an accurate result:[6]

$$Ma_2 = 4.32 \qquad\qquad \textit{Ans. (a)}$$

The isentropic pressure at this new condition is

$$p_2 = \frac{p_0}{[1 + 0.2(4.32)^2]^{3.5}} = \frac{7347}{230.1} = 31.9 \text{ kPa} \qquad\qquad \textit{Ans. (a)}$$

---

[6]The author saves these little programs for further use, giving them names such as *Prandtl-Meyer.*

Part (b) The flow compresses to a lower Prandtl-Meyer angle

$$\omega_2 = 49.757° - 20° = 29.757°$$

Again from Eq. (9.99), Table B.5, or EES we compute that

$$Ma_2 = 2.125 \qquad \qquad \textit{Ans. (b)}$$

$$p_2 = \frac{p_0}{[1 + 0.2(2.125)^2]^{3.5}} = \frac{7347}{9.51} = 773 \text{ kPa} \qquad \textit{Ans. (b)}$$

Similarly, density and temperature changes are computed by noticing that T_0 and ρ_0 are constant for isentropic flow.

Application to Supersonic Airfoils

The oblique-shock and Prandtl-Meyer expansion theories can be used to patch together a number of interesting and practical supersonic flow fields. This marriage, called *shock expansion theory*, is limited by two conditions: (1) Except in rare instances the flow must be supersonic throughout, and (2) the wave pattern must not suffer interference from waves formed in other parts of the flow field.

A very successful application of shock expansion theory is to supersonic airfoils. Figure 9.27 shows two examples, a flat plate and a diamond-shaped foil. In contrast to subsonic-flow designs (Fig. 8.21), these airfoils must have sharp leading edges, which form attached oblique shocks or expansion fans. Rounded supersonic leading edges would cause detached bow shocks, as in Fig. 9.19 or 9.22b, greatly increasing the drag and lowering the lift.

In applying shock expansion theory, one examines each surface turning angle to see whether it is an expansion ("opening up") or compression (obstruction) to the surface flow. Figure 9.27a shows a flat-plate foil at an angle of attack. There is a leading-edge shock on the lower edge with flow deflection $\theta = \alpha$, while the upper edge has an expansion fan with increasing Prandtl-Meyer angle $\Delta\omega = \alpha$. We compute p_3 with expansion theory and p_2 with oblique-shock theory. The force on the plate is thus $F = (p_2 - p_3)Cb$, where C is the chord length and b the span width (assuming no wingtip effects). This force is normal to the plate, and thus the lift force normal to the stream is $L = F \cos \alpha$, and the drag parallel to the stream is $D = F \sin \alpha$. The dimensionless coefficients C_L and C_D have the same definitions as in low-speed flow, Eq. (7.66), except that the perfect-gas-law identity $\frac{1}{2}\rho V^2 \equiv \frac{1}{2}kp \text{ Ma}^2$ is very useful here

$$C_L = \frac{L}{\frac{1}{2}kp_\infty \text{ Ma}_\infty^2 \, bC} \qquad C_D = \frac{D}{\frac{1}{2}kp_\infty \text{ Ma}_\infty^2 \, bC} \qquad (9.102)$$

The typical supersonic lift coefficient is much smaller than the subsonic value $C_L \approx 2\pi\alpha$, but the lift can be very large because of the large value of $\frac{1}{2}\rho V^2$ at supersonic speeds.

At the trailing edge in Fig. 9.27a, a shock and fan appear in reversed positions and bend the two flows back so that they are parallel in the wake and have the same pressure. They do not have quite the same velocity because of the unequal shock strengths on the upper and lower surfaces; hence a vortex sheet trails behind the wing. This is very interesting, but in the theory you ignore the trailing-edge pattern entirely, since it

α

Expansion
fan

Ma_∞

p_∞

$p_{0\infty}$

Oblique
shock

$\mathrm{Ma}_3 > \mathrm{Ma}_\infty$

$p_3 < p_\infty$

$p_{03} = p_{0\infty}$

Oblique
shock

$\mathrm{Ma}_2 < \mathrm{Ma}_\infty$

$p_2 > p_\infty$

$p_{02} < p_{0\infty}$

Vortex
sheet

Expansion
fan

(a)

α

Ma_∞

p_∞

$p_3 > p_\infty$

$p_2 > p_3$

$p_5 < p_3$

$p_4 > p_5$

$p_4 < p_2$

(b)
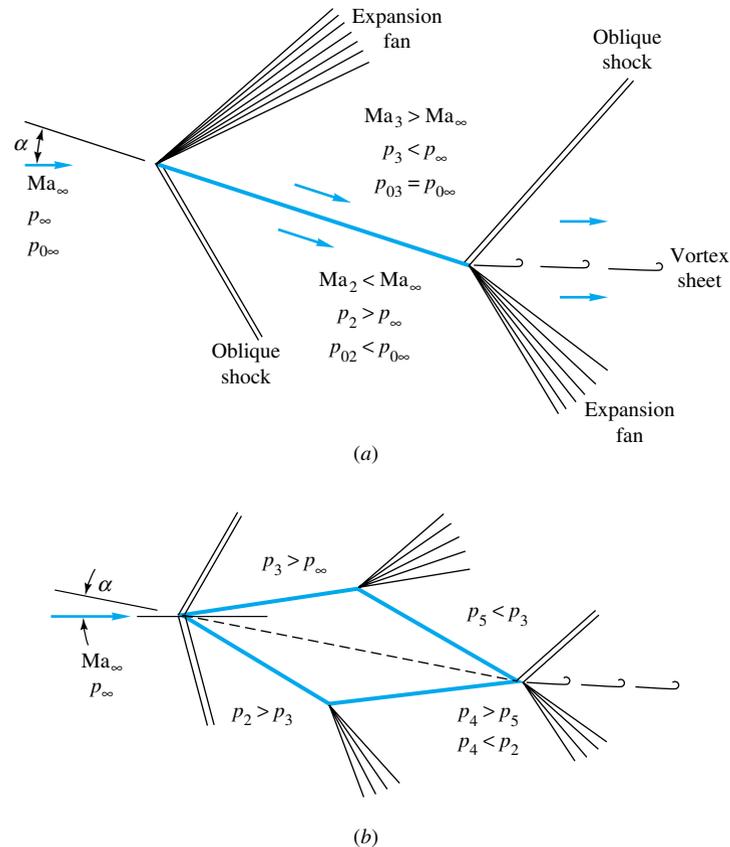
Fig. 9.27 Supersonic airfoils:
(a) flat plate, higher pressure on
lower surface, drag due to small
downstream component of net pres-
sure force; (b) diamond foil, higher
pressures on both lower surfaces,
additional drag due to body thick-
ness.

does not affect the surface pressures: The supersonic surface flow cannot "hear" the
wake disturbances.

The diamond foil in Fig. 9.27b adds two more wave patterns to the flow. At this
particular α less than the diamond half-angle, there are leading-edge shocks on both
surfaces, the upper shock being much weaker. Then there are expansion fans on each
shoulder of the diamond: The Prandtl-Meyer angle change $\Delta\omega$ equals the sum of the
leading-edge and trailing-edge diamond half-angles. Finally, the trailing-edge pattern
is similar to that of the flat plate (9.27a) and can be ignored in the calculation. Both
lower-surface pressures p_2 and p_4 are greater than their upper counterparts, and the lift
is nearly that of the flat plate. There is an additional drag due to thickness, because p_4
and p_5 on the trailing surfaces are lower than their counterparts p_2 and p_3. The dia-
mond drag is greater than the flat-plate drag, but this must be endured in practice to
achieve a wing structure strong enough to hold these forces.

The theory sketched in Fig. 9.27 is in good agreement with measured supersonic
lift and drag as long as the Reynolds number is not too small (thick boundary layers)
and the Mach number not too large (hypersonic flow). It turns out that for large Re_C
and moderate supersonic Ma_∞ the boundary layers are thin and separation seldom oc-
curs, so that the shock expansion theory, although frictionless, is quite successful. Let
us look now at an example.

EXAMPLE 9.19

A flat-plate airfoil with $C = 2$ m is immersed at $\alpha = 8°$ in a stream with $\mathrm{Ma}_\infty = 2.5$ and $p_\infty = 100$ kPa. Compute (a) C_L and (b) C_D, and compare with low-speed airfoils. Compute (c) lift and (d) drag in newtons per unit span width.

Solution

Instead of using a lot of space outlining the detailed oblique-shock and Prandtl-Meyer expansion computations, we list all pertinent results in Fig. E9.19 on the upper and lower surfaces. Using the theories of Secs. 9.9 and 9.10, you should verify every single one of the calculations in Fig. E9.19 to make sure that all details of shock expansion theory are well understood.

E9.19
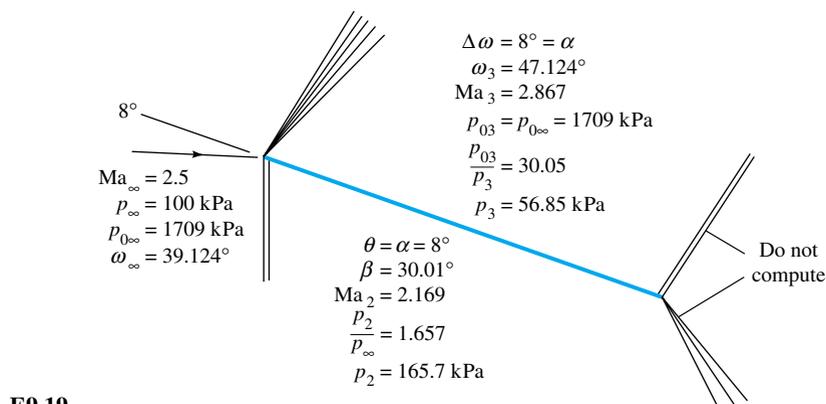
The important final results are p_2 and p_3, from which the total force per unit width on the plate is

$$F = (p_2 - p_3)bC = (165.7 - 56.85)(\text{kPa})(1\ \text{m})(2\ \text{m}) = 218\ \text{kN}$$

The lift and drag per meter width are thus

$$L = F \cos 8° = 216\ \text{kN} \qquad\qquad\qquad \textit{Ans. (c)}$$

$$D = F \sin 8° = 30\ \text{kN} \qquad\qquad\qquad \textit{Ans. (d)}$$

These are very large forces for only 2 m^2 of wing area.

From Eq. (9.102) the lift coefficient is

$$C_L = \frac{216\ \text{kN}}{\frac{1}{2}(1.4)(100\ \text{kPa})(2.5)^2(2\ \text{m}^2)} = 0.246 \qquad\qquad \textit{Ans. (a)}$$

The comparable low-speed coefficient from Eq. (8.64) is $C_L = 2\pi \sin 8° = 0.874$, which is 3.5 times larger.

From Eq. (9.102) the drag coefficient is

$$C_D = \frac{30\ \text{kN}}{\frac{1}{2}(1.4)(100\ \text{kPa})(2.5)^2(2\ \text{m}^2)} = 0.035 \qquad\qquad \textit{Ans. (b)}$$

From Fig. 7.25 for the NACA 0009 airfoil C_D at $\alpha = 8°$ is about 0.009, or about 4 times smaller.

Notice that this supersonic theory predicts a finite drag in spite of assuming frictionless flow with infinite wing aspect ratio. This is called *wave drag*, and we see that the d'Alembert paradox of zero body drag does not occur in supersonic flow.

Thin-Airfoil Theory

In spite of the simplicity of the flat-plate geometry, the calculations in Example 9.19 were laborious. In 1925 Ackeret [21] developed simple yet effective expressions for the lift, drag, and center of pressure of supersonic airfoils, assuming small thickness and angle of attack.

The theory is based on the linearized expression (9.89), where $\tan \theta \approx$ surface deflection relative to the free stream and condition 1 is the free stream, $\text{Ma}_1 = \text{Ma}_\infty$. For the flat-plate airfoil, the total force F is based on

$$\frac{p_2 - p_3}{p_\infty} = \frac{p_2 - p_\infty}{p_\infty} - \frac{p_3 - p_\infty}{p_\infty}$$

$$= \frac{k\,\text{Ma}_\infty^2}{(\text{Ma}_\infty^2 - 1)^{1/2}} [\alpha - (-\alpha)] \tag{9.103}$$

Substitution into Eq. (9.102) gives the linearized lift coefficient for a supersonic flat-plate airfoil

$$C_L \approx \frac{(p_2 - p_3)bC}{\frac{1}{2}kp_\infty\,\text{Ma}_\infty^2\,bC} \approx \frac{4\alpha}{(\text{Ma}_\infty^2 - 1)^{1/2}} \tag{9.104}$$

Computations for diamond and other finite-thickness airfoils show no first-order effect of thickness on lift. Therefore Eq. (9.104) is valid for any sharp-edged supersonic thin airfoil at a small angle of attack.

The flat-plate drag coefficient is

$$C_D = C_L \tan \alpha \approx C_L \alpha \approx \frac{4\alpha^2}{(\text{Ma}_\infty^2 - 1)^{1/2}} \tag{9.105}$$

However, the thicker airfoils have additional thickness drag. Let the chord line of the airfoil be the *x*-axis, and let the upper-surface shape be denoted by $y_u(x)$ and the lower profile by $y_l(x)$. Then the complete Ackeret drag theory (see, e.g., Ref. 8, sec. 14.6, for details) shows that the additional drag depends on the mean square of the slopes of the upper and lower surfaces, defined by

$$\overline{y'^2} = \frac{1}{C} \int_0^C \left(\frac{dy}{dx}\right)^2 dx \tag{9.106}$$

The final expression for drag [8, p. 442] is

$$C_D \approx \frac{4}{(\text{Ma}_\infty^2 - 1)^{1/2}} \left[\alpha^2 + \frac{1}{2}\,(\overline{y_u'^2} + \overline{y_l'^2})\right] \tag{9.107}$$

These are all in reasonable agreement with more exact computations, and their extreme simplicity makes them attractive alternatives to the laborious but accurate shock expansion theory. Consider the following example.

EXAMPLE 9.20

Repeat parts (a) and (b) of Example 9.19, using the linearized Ackeret theory.

Solution

From Eqs. (9.104) and (9.105) we have, for $Ma_\infty = 2.5$ and $\alpha = 8° = 0.1396$ rad,

$$C_L \approx \frac{4(0.1396)}{(2.5^2 - 1)^{1/2}} = 0.244 \qquad C_D = \frac{4(0.1396)^2}{(2.5^2 - 1)^{1/2}} = 0.034 \qquad\qquad Ans.$$

These are less than 3 percent lower than the more exact computations of Example 9.19.

A further result of the Ackeret linearized theory is an expression for the position x_{CP} of the center of pressure (CP) of the force distribution on the wing:

$$\frac{x_{CP}}{C} = 0.5 + \frac{S_u - S_l}{2\alpha C^2} \tag{9.108}$$

where S_u is the cross-sectional area between the upper surface and the chord and S_l is the area between the chord and the lower surface. For a symmetric airfoil ($S_l = S_u$) we obtain x_{CP} at the half-chord point, in contrast with the low-speed airfoil result of Eq. (8.66), where x_{CP} is at the quarter-chord.

The difference in difficulty between the simple Ackeret theory and shock expansion theory is even greater for a thick airfoil, as the following example shows.

EXAMPLE 9.21

By analogy with Example 9.19 analyze a diamond, or double-wedge, airfoil of 2° half-angle and $C = 2$ m at $\alpha = 8°$ and $Ma_\infty = 2.5$. Compute C_L and C_D by (a) shock expansion theory and (b) Ackeret theory. Pinpoint the difference from Example 9.19.

Solution

Part (a)

Again we omit the details of shock expansion theory and simply list the properties computed on each of the four airfoil surfaces in Fig. E9.21. Assume $p_\infty = 100$ kPa. There are both a force F normal to the chord line and a force P parallel to the chord. For the normal force the pressure difference on the front half is $p_2 - p_3 = 186.4 - 65.9 = 120.5$ kPa, and on the rear half it is $p_4 - p_5 = 146.9 - 48.1 = 98.1$ kPa. The average pressure difference is $\frac{1}{2}(120.5 + 98.1) = 109.3$ kPa, so that the normal force is

$$F = (109.3 \text{ kPa})(2 \text{ m}^2) = 218.6 \text{ kN}$$

For the chordwise force P the pressure difference on the top half is $p_3 - p_5 = 65.9 - 48.8 = 17.1$ kPa, and on the bottom half it is $p_2 - p_4 = 186.4 - 146.9 = 39.5$ kPa. The average difference is $\frac{1}{2}(17.1 + 39.5) = 28.3$ kPa, which when multiplied by the frontal area (maximum thickness times 1-m width) gives

$$P = (28.3 \text{ kPa})(0.07 \text{ m})(1 \text{ m}) = 2.0 \text{ kN}$$

Chord length = 2 m

8°

$\Delta\omega = 6°$
$\omega_3 = 45.124°$
$\text{Ma}_3 = 2.770$
$p_3 = 65.9$ kPa

$\Delta\omega = 4°$
$\omega_5 = 49.124°$
$\text{Ma}_5 = 2.967$
$p_5 = 48.8$ kPa

$\text{Ma}_\infty = 2.5$
$p_\infty = 100$ kPa
$p_{0\infty} = 1709$ kPa
$\omega_\infty = 39.124°$

4°

0.07 m

$\theta = 10°$
$\beta = 31.85°$
$\text{Ma}_2 = 2.086$
$\omega_2 = 28.721°$
$p_{02} = 1668$ kPa
$p_2 = 186.4$ kPa

$\Delta\omega = 4°$
$\omega_4 = 32.721°$
$\text{Ma}_4 = 2.238$
$p_4 = 146.9$ kPa
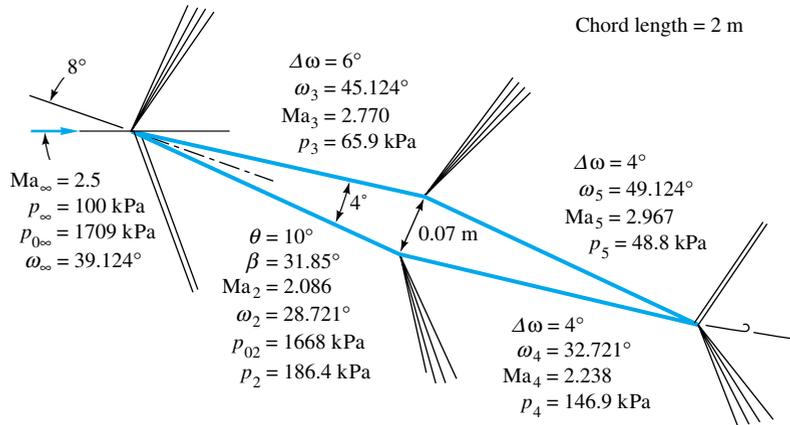
E9.21

Both F and P have components in the lift and drag directions. The lift force normal to the free stream is

$$L = F \cos 8° - P \sin 8° = 216.2 \text{ kN}$$

and

$$D = F \sin 8° + P \cos 8° = 32.4 \text{ kN}$$

For computing the coefficients, the denominator of Eq. (9.102) is the same as in Example 9.19: $\frac{1}{2}kp_\infty \text{ Ma}_\infty^2 bC = \frac{1}{2}(1.4)(100 \text{ kPa})(2.5)^2(2 \text{ m}^2) = 875 \text{ kN}$. Thus, finally, shock expansion theory predicts

$$C_L = \frac{216.2 \text{ kN}}{875 \text{ kN}} = 0.247 \qquad C_D = \frac{32.4 \text{ kN}}{875 \text{ kN}} = 0.0370 \qquad \textit{Ans. (a)}$$

Part (b) Meanwhile, by Ackeret theory, C_L is the same as in Example 9.20:

$$C_L = \frac{4(0.1396)}{(2.5^2 - 1)^{1/2}} = 0.244 \qquad \textit{Ans. (b)}$$

This is 1 percent less than the shock expansion result above. For the drag we need the mean-square slopes from Eq. (9.106)

$$\overline{y_u'^2} = \overline{y_l'^2} = \tan^2 2° = 0.00122$$

Then Eq. (9.107) predicts the linearized result

$$C_D = \frac{4}{(2.5^2 - 1)^{1/2}} [(0.1396)^2 + \tfrac{1}{2}(0.00122 + 0.00122)] = 0.0362 \qquad \textit{Ans. (b)}$$

This is 2 percent lower than shock expansion theory predicts. We could judge Ackeret theory to be "satisfactory." Ackeret theory predicts $p_2 = 167$ kPa (-11 percent), $p_3 = 60$ kPa (-9 percent), $p_4 = 140$ kPa (-5 percent), and $p_5 = 33$ kPa (-6 percent).

Three-Dimensional Supersonic Flow

We have gone about as far as we can go in an introductory treatment of compressible flow. Of course, there is much more, and you are invited to study further in the references at the end of the chapter.
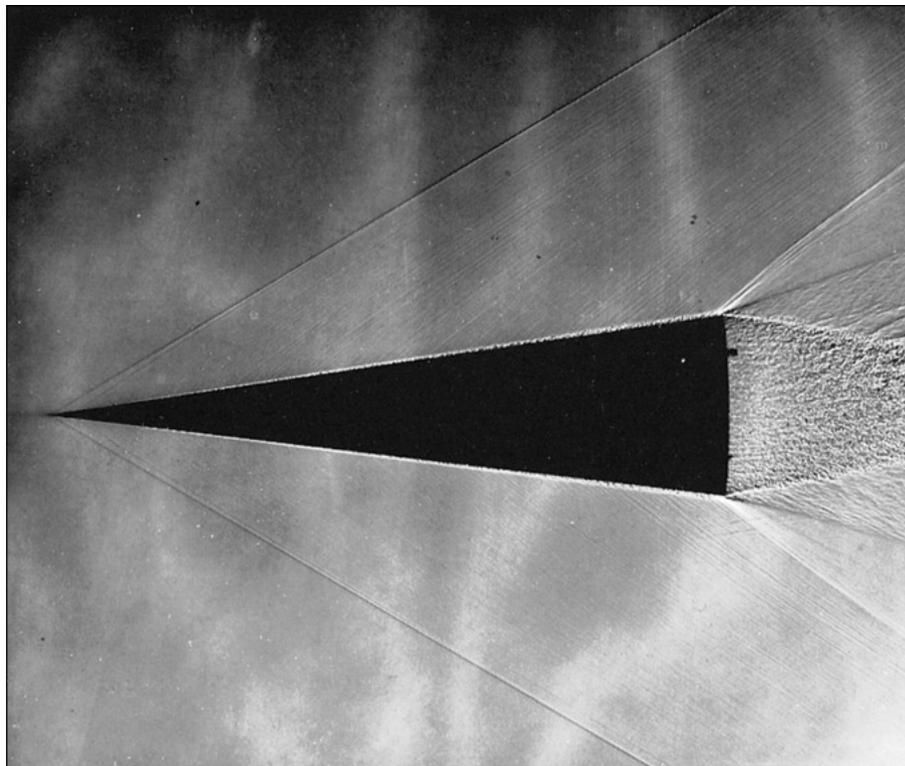
Fig. 9.28 Shadowgraph of flow past an 8° half-angle cone at $Ma_\infty = 2.0$. The turbulent boundary layer is clearly visible. The Mach lines curve slightly, and the Mach number varies from 1.98 just inside the shock to 1.90 at the surface. *(Courtesy of U.S. Army Ballistic Research Center, Aberdeen Proving Ground.)*

Three-dimensional supersonic flows are highly complex, especially if they concern blunt bodies, which therefore contain embedded regions of subsonic and transonic flow, e.g., Fig. 9.10. Some flows, however, yield to accurate theoretical treatment such as flow past a cone at zero incidence, as shown in Fig. 9.28. The exact theory of cone flow is discussed in advanced texts [for example, 8, chap. 17], and extensive tables of such solutions have been published [22, 23]. There are similarities between cone flow and the wedge flows illustrated in Fig. 9.22: an attached oblique shock, a thin turbulent boundary layer, and an expansion fan at the rear corner. However, the conical shock deflects the flow through an angle less than the cone half-angle, unlike the wedge shock. As in the wedge flow, there is a maximum cone angle above which the shock must detach, as in Fig. 9.22b. For $k = 1.4$ and $Ma_\infty = \infty$, the maximum cone half-angle for an attached shock is about 57°, compared with the maximum wedge angle of 45.6° (see Ref. 23).

For more complicated body shapes one usually resorts to experimentation in a supersonic wind tunnel. Figure 9.29 shows a wind-tunnel study of supersonic flow past a model of an interceptor aircraft. The many junctions and wingtips and shape changes make theoretical analysis very difficult. Here the surface-flow patterns, which indicate boundary-layer development and regions of flow separation, have been visualized by the smearing of oil drops placed on the model surface before the test.
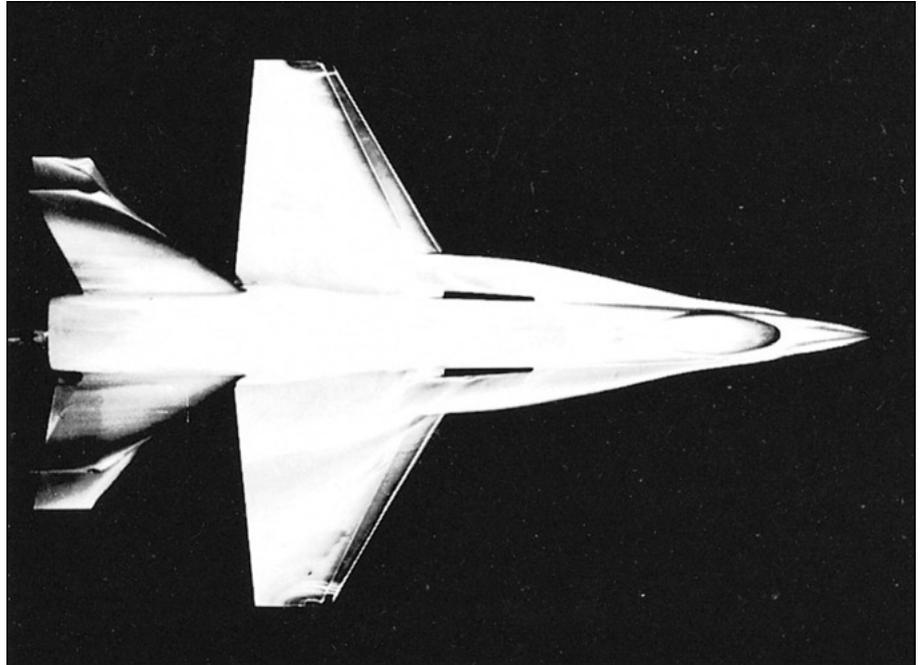
Fig. 9.29 Wind-tunnel test of the Cobra P-530 supersonic interceptor. The surface flow patterns are visualized by the smearing of oil droplets. *(Courtesy of Northrop Corp.)*

As we shall see in the next chapter, there is an interesting analogy between gas-dynamic shock waves and the surface water waves which form in an open-channel flow. Chapter 11 of Ref. 14 explains how a water channel can be used in an inexpensive simulation of supersonic-flow experiments.

Reusable Hypersonic Launch Vehicles

Having achieved reliable supersonic flight with both military and commercial aircraft, the next step is probably to develop a hypersonic vehicle that can achieve orbit, yet be retrieved. Presently the United States employs the Space Shuttle, where only the manned vehicle is retrieved, the very expensive giant rocket boosters being lost. In 1996, NASA selected Lockheed-Martin to develop the X-33, the first smaller-scale step toward a retrievable single-stage-to-orbit (SSTO) vehicle, to be called the VentureStar [36].

The X-33, shown in an artist's rendering in Fig. 9.30, will be 20 m long, about half the size of the VentureStar, and it will be *suborbital*. It will take off vertically, rise to a height of 73 km, and coast back to earth at a steep (stressful) angle. Such a flight will test many new plans for the VentureStar [37], such as metallic tiles, titanium components, graphite composite fuel tanks, high-voltage control actuators, and Rocketdyne's novel "aerospike" rocket nozzles. If successful, the VentureStar is planned as a standard reusable, low-cost orbital vehicle. VentureStar will be 39 m long and weigh 9.7 MN, of which 88 percent (965 tons!) will be propellant
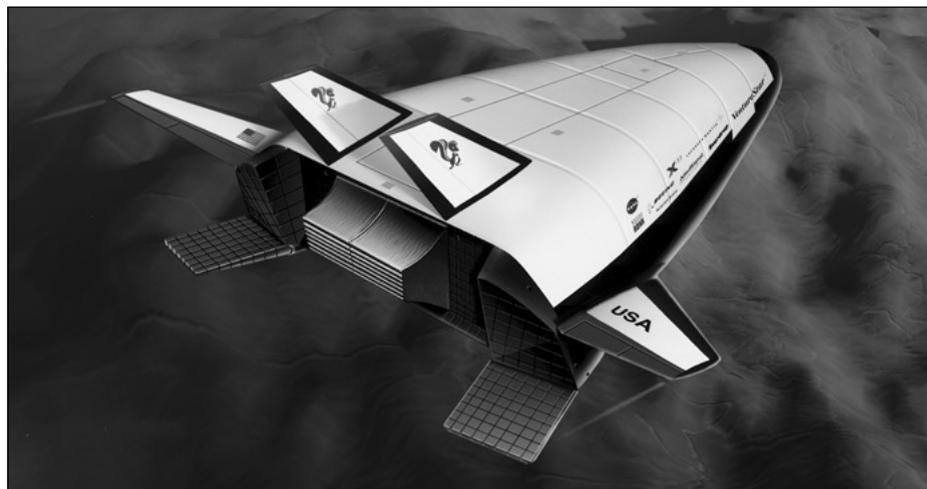
Fig. 9.30 The X-33 is a half-size suborbital test version of the VentureStar, which is planned as an orbital, low-cost retrievable space vehicle. It takes off vertically but then uses its lifting shape to glide back to earth and land horizontally [36, 37]. *(Courtesy of Lockheed Martin Corp.)*

and only 2.7 percent (260 kN) will be payload. The dream is that the X-33 and VentureStar and their progeny will lead to an era of routine, low-cost space travel appropriate to the new millennium.

Summary

This chapter is a brief introduction to a very broad subject, compressible flow, sometimes called *gas dynamics*. The primary parameter is the Mach number $Ma = V/a$, which is large and causes the fluid density to vary significantly. This means that the continuity and momentum equations must be coupled to the energy relation and the equation of state to solve for the four unknowns (p, ρ, T, $\mathbf{V}$).

The chapter reviews the thermodynamic properties of an ideal gas and derives a formula for the speed of sound of a fluid. The analysis is then simplified to one-dimensional steady adiabatic flow without shaft work, for which the stagnation enthalpy of the gas is constant. A further simplification to isentropic flow enables formulas to be derived for high-speed gas flow in a variable-area duct. This reveals the phenomenon of sonic-flow *choking* (maximum mass flow) in the throat of a nozzle. At supersonic velocities there is the possibility of a normal-shock wave, where the gas discontinuously reverts to subsonic conditions. The normal shock explains the effect of back pressure on the performance of converging-diverging nozzles.

To illustrate nonisentropic flow conditions, there is a brief study of constant-area duct flow with friction and with heat transfer, both of which lead to choking of the exit flow.

The chapter ends with a discussion of two-dimensional supersonic flow, where oblique-shock waves and Prandtl-Meyer (isentropic) expansion waves appear. With a proper combination of shocks and expansions one can analyze supersonic airfoils.

Problems

Most of the problems herein are fairly straightforward. More difficult or open-ended assignments are labeled with an asterisk. Problems labeled with an EES icon will benefit from the use of the Engineering Equations Solver (EES), while problems labeled with a computer icon may require the use of a computer. The standard end-of-chapter problems 9.1 to 9.157 (categorized in the problem list below) are followed by word problems W9.1 to W9.8, fundamentals of engineering exam problems FE9.1 to FE9.10, comprehensive problems C9.1 to C9.3, and design projects D9.1 and D9.2.

Problem distribution

Section	Topic	Problems
9.1	Introduction	9.1–9.9
9.2	The speed of sound	9.10–9.18
9.3	Adiabatic and isentropic flow	9.19–9.33
9.4	Isentropic flow with area changes	9.34–9.53
9.5	The normal-shock wave	9.54–9.62
9.6	Converging and diverging nozzles	9.63–9.85
9.7	Duct flow with friction	9.86–9.107
9.8	Frictionless duct flow with heat transfer	9.108–9.115
9.9	Mach waves	9.116–9.121
9.9	The oblique-shock wave	9.122–9.139
9.10	Prandtl-Meyer expansion waves	9.140–9.147
9.10	Supersonic airfoils	9.148–9.157

P9.1 An ideal gas flows adiabatically through a duct. At section 1, $p_1 = 140$ kPa, $T_1 = 260°C$, and $V_1 = 75$ m/s. Farther downstream, $p_2 = 30$ kPa and $T_2 = 207°C$. Calculate V_2 in m/s and $s_2 - s_1$ in J/(kg · K) if the gas is (a) air, $k = 1.4$, and (b) argon, $k = 1.67$.

P9.2 Solve Prob. 9.1 if the gas is steam. Use two approaches: (a) an ideal gas from Table A.4 and (b) real gas data from the steam tables [15].

P9.3 If 8 kg of oxygen in a closed tank at 200°C and 300 kPa is heated until the pressure rises to 400 kPa, calculate (a) the new temperature, (b) the total heat transfer, and (c) the change in entropy.

P9.4 Compressibility effects become important when the Mach number exceeds approximately 0.3. How fast can a two-dimensional cylinder travel in sea-level standard air before compressibility becomes important *somewhere* in its vicinity?

P9.5 Steam enters a nozzle at 377°C, 1.6 MPa, and a steady speed of 200 m/s and accelerates isentropically until it exits at saturation conditions. Estimate the exit velocity and temperature.

P9.6 Is it possible for the steam in Prob. 9.5 to continue accelerating until it exits with a moisture content of 12 percent? If so, estimate the new exit velocity and temperature.

P9.7 Carbon dioxide ($k = 1.28$) enters a constant-area duct at 400°F, 100 lbf/in² absolute, and 500 ft/s. Farther downstream the properties are $V_2 = 1000$ ft/s and $T_2 = 900°F$. Compute (a) p_2, (b) the heat added between sections, (c) the entropy change between sections, and (d) the mass flow per unit area. *Hint:* This problem requires the continuity equation.

P9.8 Atmospheric air at 20°C enters and fills an insulated tank which is initially evacuated. Using a control-volume analysis from Eq. (3.63), compute the tank air temperature when it is full.

P9.9 Liquid hydrogen and oxygen are burned in a combustion chamber and fed through a rocket nozzle which exhausts at $V_{exit} = 1600$ m/s to an ambient pressure of 54 kPa. The nozzle exit diameter is 45 cm, and the jet exit density is 0.15 kg/m³. If the exhaust gas has a molecular weight of 18, estimate (a) the exit gas temperature, (b) the mass flow, and (c) the thrust developed by the rocket.

P9.10 A certain aircraft flies at the same Mach number regardless of its altitude. Compared to its speed at 12,000-m standard altitude, it flies 127 km/h faster at sea level. Determine its Mach number.

P9.11 At 300°C and 1 atm, estimate the speed of sound of (a) nitrogen, (b) hydrogen, (c) helium, (d) steam, and (e) $^{238}UF_6$ ($k \approx 1.06$).

P9.12 Assume that water follows Eq. (1.19) with $n \approx 7$ and $B \approx 3000$. Compute the bulk modulus (in kPa) and the speed of sound (in m/s) at (a) 1 atm and (b) 1100 atm (the deepest part of the ocean). (c) Compute the speed of sound at 20°C and 9000 atm and compare with the measured value of 2650 m/s (A. H. Smith and A. W. Lawson, *J. Chem. Phys.,* vol. 22, 1954, p. 351).

P9.13 From Prob. 1.33, mercury data fit Eq. (1.19) with $n \approx 6$ and $B \approx 41,000$. Estimate (a) the bulk modulus and (b) the speed of sound of mercury at 2500 atm and compare with Table 9.1.

P9.14 Assume steady adiabatic flow of a perfect gas. Show that the energy equation (9.21), when plotted as speed of sound versus velocity, forms an ellipse. Sketch this ellipse; label the intercepts and the regions of subsonic, sonic, and supersonic flow; and determine the ratio of the major and minor axes.

P9.15 A weak pressure wave (sound wave) with a pressure change $\Delta p = 40$ Pa propagates through air at 20°C and 1 atm. Estimate (a) the density change, (b) the temperature change, and (c) the velocity change across the wave.

P9.16 A weak pressure pulse Δp propagates through still air. Discuss the type of reflected pulse which occurs and the boundary conditions which must be satisfied when the

wave strikes normal to, and is reflected from, (a) a solid wall and (b) a free liquid surface.

P9.17 A submarine at a depth of 800 m sends a sonar signal and receives the reflected wave back from a similar submerged object in 15 s. Using Prob. 9.12 as a guide, estimate the distance to the other object.

*P9.18 The properties of a dense gas (high pressure and low temperature) are often approximated by van der Waals' equation of state [17, 18]:

$$p = \frac{\rho RT}{1 - b_1 \rho} - a_1 \rho^2$$

where constants a_1 and b_1 can be found from the critical temperature and pressure

$$a_1 = \frac{27 R^2 T_c^2}{64 p_c} = 9.0 \times 10^5 \text{ lbf} \cdot \text{ft}^4/\text{slug}^2$$

for air, and

$$b_1 = \frac{R T_c}{8 p_c} = 0.65 \text{ ft}^3/\text{slug}$$

for air. Find an analytic expression for the speed of sound of a van der Waals gas. Assuming $k = 1.4$, compute the speed of sound of air in ft/s at $-100°F$ and 20 atm for (a) a perfect gas and (b) a van der Waals gas. What percentage higher density does the van der Waals relation predict?

P9.19 The Concorde aircraft flies at Ma ≈ 2.3 at 11-km standard altitude. Estimate the temperature in °C at the front stagnation point. At what Mach number would it have a front stagnation-point temperature of 450°C?

P9.20 A gas flows at $V = 200$ m/s, $p = 125$ kPa, and $T = 200°C$. For (a) air and (b) helium, compute the maximum pressure and the maximum velocity attainable by expansion or compression.

P9.21 Air expands isentropically through a duct from $p_1 = 125$ kPa and $T_1 = 100°C$ to $p_2 = 80$ kPa and $V_2 = 325$ m/s. Compute (a) T_2, (b) Ma$_2$, (c) T_0, (d) p_0, (e) V_1, and (f) Ma$_1$.

P9.22 Given the pitot stagnation temperature and pressure and the static-pressure measurements in Fig. P9.22, estimate the air velocity V, assuming (a) incompressible flow and (b) compressible flow.
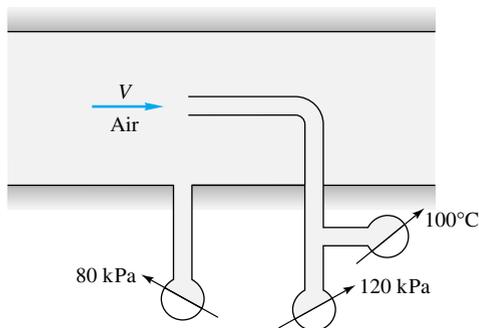
P9.23 A large rocket engine delivers hydrogen at 1500°C and 3 MPa, $k = 1.41$, $R = 4124$ J/(kg·K), to a nozzle which exits with gas pressure equal to the ambient pressure of 54 kPa. Assuming isentropic flow, if the rocket thrust is 2 MN, what is (a) the exit velocity and (b) the mass flow of hydrogen?

P9.24 For low-speed (nearly incompressible) gas flow, the stagnation pressure can be computed from Bernoulli's equation

$$p_0 = p + \frac{1}{2} \rho V^2$$

(a) For higher subsonic speeds, show that the isentropic relation (9.28a) can be expanded in a power series as follows:

$$p_0 \approx p + \frac{1}{2} \rho V^2 \left(1 + \frac{1}{4} \text{Ma}^2 + \frac{2 - k}{24} \text{Ma}^4 + \cdots \right)$$

(b) Suppose that a pitot-static tube in air measures the pressure difference $p_0 - p$ and uses the Bernoulli relation, with stagnation density, to estimate the gas velocity. At what Mach number will the error be 4 percent?

P9.25 If it is known that the air velocity in the duct is 750 ft/s, use the mercury-manometer measurement in Fig. P9.25 to estimate the static pressure in the duct in lbf/in^2 absolute.
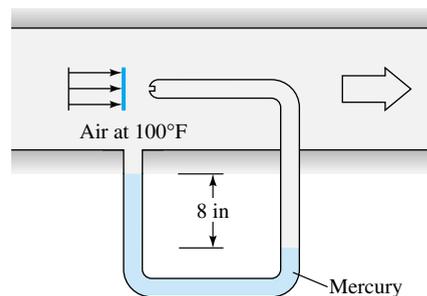
P9.25

P9.26 Show that for isentropic flow of a perfect gas if a pitot-static probe measures p_0, p, and T_0, the gas velocity can be calculated from

$$V^2 = 2 c_p T_0 \left[1 - \left(\frac{p}{p_0} \right)^{(k-1)/k} \right]$$

What would be a source of error if a shock wave were formed in front of the probe?

P9.27 In many problems the sonic (*) properties are more useful reference values than the stagnation properties. For isentropic flow of a perfect gas, derive relations for p/p^*,

P9.22

T/T^*, and ρ/ρ^* as functions of the Mach number. Let us help by giving the density-ratio formula:

$$\frac{\rho}{\rho^*} = \left[\frac{k+1}{2+(k-1)\,\text{Ma}^2}\right]^{1/(k-1)}$$

P9.28 A large vacuum tank, held at 60 kPa absolute, sucks sea-level standard air through a converging nozzle whose throat diameter is 3 cm. Estimate (a) the mass-flow rate through the nozzle and (b) the Mach number at the throat.

P9.29 Steam from a large tank, where $T = 400°C$ and $p = 1$ MPa, expands isentropically through a nozzle until, at a section of 2-cm diameter, the pressure is 500 kPa. Using the steam tables [15], estimate (a) the temperature, (b) the velocity, and (c) the mass flow at this section. Is the flow subsonic?

P9.30 Air flows in a duct of diameter 5 cm. At one section, $T_0 = 300°C$, $p = 120$ kPa, and $\dot{m} = 0.4$ kg/s. Estimate, at this section, (a) V, (b) Ma, and (c) ρ_0.

P9.31 Air flows adiabatically through a duct. At one section $V_1 = 400$ ft/s, $T_1 = 200°F$, and $p_1 = 35$ lbf/in^2 absolute, while farther downstream $V_2 = 1100$ ft/s and $p_2 = 18$ lbf/in^2 absolute. Compute (a) Ma_2, (b) U_{max}, and (c) p_{02}/p_{01}.

P9.32 The large compressed-air tank in Fig. P9.32 exhausts from a nozzle at an exit velocity of 235 m/s. The mercury manometer reads $h = 30$ cm. Assuming isentropic flow, compute the pressure (a) in the tank and (b) in the atmosphere. (c) What is the exit Mach number?
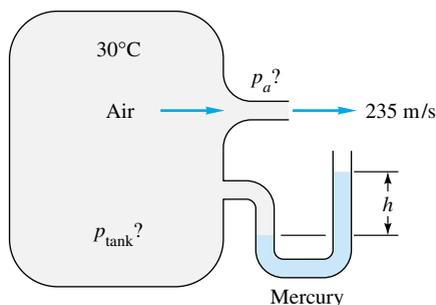
P9.32

P9.33 Air flows isentropically from a reservoir, where $p = 300$ kPa and $T = 500$ K, to section 1 in a duct, where $A_1 = 0.2$ m^2 and $V_1 = 550$ m/s. Compute (a) Ma_1, (b) T_1, (c) p_1, (d) $\dot{m}$, and (e) A^*. Is the flow choked?

P9.34 Steam in a tank at 450°F and 100 lbf/in^2 absolute exhausts through a converging nozzle of 0.1-in^2 throat area to a 1-atm environment. Compute the initial mass flow (a) for an ideal gas and (b) from the steam tables [15].

P9.35 Helium, at $T_0 = 400$ K, enters a nozzle isentropically. At section 1, where $A_1 = 0.1$ m^2, a pitot-static arrangement (see Fig. P9.25) measures stagnation pressure of 150 kPa and static pressure of 123 kPa. Estimate (a) Ma_1, (b) mass flow $\dot{m}$, (c) T_1, and (d) A^*.

P9.36 An air tank of volume 1.5 m^3 is initially at 800 kPa and 20°C. At $t = 0$, it begins exhausting through a converging nozzle to sea-level conditions. The throat area is 0.75 cm^2. Estimate (a) the initial mass flow in kg/s, (b) the time required to blow down to 500 kPa, and (c) the time at which the nozzle ceases being choked.

P9.37 Make an exact control-volume analysis of the blowdown process in Fig. P9.37, assuming an insulated tank with negligible kinetic and potential energy within. Assume critical flow at the exit, and show that both p_0 and T_0 decrease during blowdown. Set up first-order differential equations for $p_0(t)$ and $T_0(t)$, and reduce and solve as far as you can.
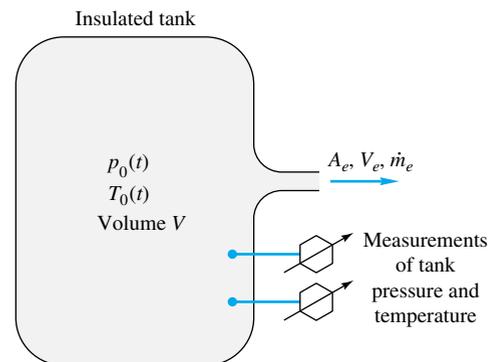
P9.37

P9.38 Prob. 9.37 makes an ideal senior project or combined laboratory and computer problem, as described in Ref. 30, sec. 8.6. In Bober and Kenyon's lab experiment, the tank had a volume of 0.0352 ft^3 and was initially filled with air at 50 lb/in^2 gage and 72°F. Atmospheric pressure was 14.5 lb/in^2 absolute, and the nozzle exit diameter was 0.05 in. After 2 s of blowdown, the measured tank pressure was 20 lb/in^2 gage and the tank temperature was −5°F. Compare these values with the theoretical analysis of Prob. 9.37.

P9.39 Consider isentropic flow in a channel of varying area, from section 1 to section 2. We know that $\text{Ma}_1 = 2.0$ and desire that the velocity ratio V_2/V_1 be 1.2. Estimate (a) Ma_2 and (b) A_2/A_1. (c) Sketch what this channel looks like. For example, does it converge or diverge? Is there a throat?

P9.40 Air, with stagnation conditions of 800 kPa and 100°C, expands isentropically to a section of a duct where $A_1 = 20$ cm^2 and $p_1 = 47$ kPa. Compute (a) Ma_1, (b) the throat area, and (c) $\dot{m}$. At section 2 between the throat and section 1, the area is 9 cm^2. (d) Estimate the Mach number at section 2.

P9.41 Air, with a stagnation pressure of 100 kPa, flows through the nozzle in Fig. P9.41, which is 2 m long and has an area variation approximated by
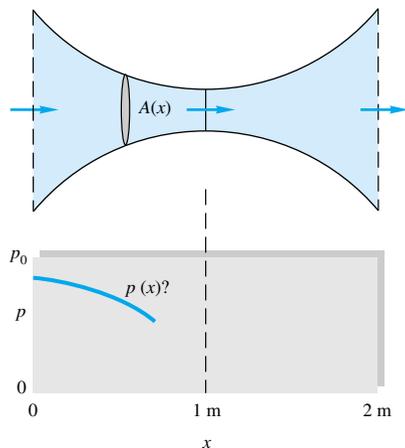
P9.41

$$A \approx 20 - 20x + 10x^2$$

with A in cm^2 and x in m. It is desired to plot the complete family of isentropic pressures $p(x)$ in this nozzle, for the range of inlet pressures $1 < p(0) < 100$ kPa. Indicate those inlet pressures which are not physically possible and discuss briefly. If your computer has an online graphics routine, plot at least 15 pressure profiles; otherwise just hit the highlights and explain.

P9.42 A bicycle tire is filled with air at an absolute pressure of 169.12 kPa, and the temperature inside is 30.0°C. Suppose the valve breaks, and air starts to exhaust out of the tire into the atmosphere ($p_a = 100$ kPa absolute and $T_a = 20.0$°C). The valve exit is 2.00 mm in diameter and is the smallest cross-sectional area of the entire system. Frictional losses can be ignored here, i.e., one-dimensional isentropic flow is a reasonable assumption. (a) Find the Mach number, velocity, and temperature at the exit plane of the valve (initially). (b) Find the initial mass-flow rate out of the tire. (c) Estimate the velocity at the exit plane using the incompressible Bernoulli equation. How well does this estimate agree with the "exact" answer of part (a)? Explain.

P9.43 Air flows isentropically through a duct with $T_0 = 300$°C. At two sections with identical areas of 25 cm^2, the pressures are $p_1 = 120$ kPa and $p_2 = 60$ kPa. Determine (a) the mass flow, (b) the throat area, and (c) Ma$_2$.

P9.44 In Prob. 3.34 we knew nothing about compressible flow at the time, so we merely assumed exit conditions p_2 and T_2 and computed V_2 as an application of the continuity equation. Suppose that the throat diameter is 3 in. For the given stagnation conditions in the rocket chamber in Fig. P3.34 and assuming $k = 1.4$ and a molecular weight of 26,

compute the actual exit velocity, pressure, and temperature according to one-dimensional theory. If $p_a = 14.7$ lbf/in^2 absolute, compute the thrust from the analysis of Prob. 3.68. This thrust is entirely independent of the stagnation temperature (check this by changing T_0 to 2000°R if you like). Why?

P9.45 At a point upstream of the throat of a converging-diverging nozzle the properties are $V_1 = 200$ m/s, $T_1 = 300$ K, and $p_1 = 125$ kPa. If the exit flow is supersonic, compute, from isentropic theory, (a) $\dot{m}$ and (b) A_1. The throat area is 35 cm^2.

P9.46 If the author did not falter, the results of Prob. 9.43 are (a) 0.671 kg/s, (b) 23.3 cm^2, and (c) 1.32. Do not tell your friends who are still working on Prob. 9.43. Consider a control volume which encloses the nozzle between these two 25-cm^2 sections. If the pressure outside the duct is 1 atm, determine the total force acting on this section of nozzle.

P9.47 In wind-tunnel testing near Mach 1, a small area decrease caused by model blockage can be important. Suppose the test section area is 1 m^2, with unblocked test conditions Ma $= 1.10$ and $T = 20$°C. What model area will first cause the test section to choke? If the model cross section is 0.004 m^2 (0.4 percent blockage), what percentage change in test-section velocity results?

P9.48 A force $F = 1100$ N pushes a piston of diameter 12 cm through an insulated cylinder containing air at 20°C, as in Fig. P9.48. The exit diameter is 3 mm, and $p_a = 1$ atm. Estimate (a) V_e, (b) V_p, and (c) $\dot{m}_e$.
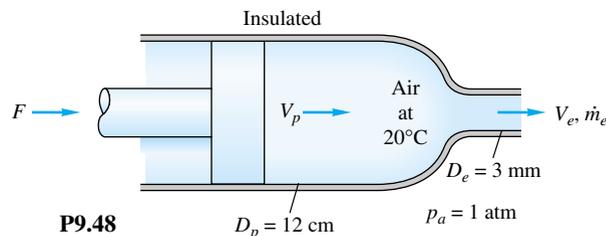
P9.48

P9.49 Air expands through a nozzle and exits supersonically. The throat area is 10 cm^2, and the throat pressure is 100 kPa. Find the pressure on either side of the throat where the duct area is 24 cm^2.

P9.50 Argon expands isentropically in a converging nozzle whose entrance conditions are $D_1 = 10$ cm, $p_1 = 150$ kPa, $T_1 = 100$°C, and $\dot{m} = 1$ kg/s. The flow discharges smoothly to an ambient pressure of 101 kPa. (a) What is the exit diameter of the nozzle? (b) How much further can the ambient pressure be reduced before it affects the inlet mass flow?

P9.51 Air, at stagnation conditions of 500 K and 200 kPa, flows through a nozzle. At section 1, where the area is 12 cm^2,

the density is 0.32 kg/m³. Assuming isentropic flow, (a) find the mass flow. (b) Is the flow choked? If so, estimate A^*. Also estimate (c) p_1 and (d) Ma_1.

P9.52 A converging-diverging nozzle exits smoothly to sea-level standard atmosphere. It is supplied by a 40-m³ tank initially at 800 kPa and 100°C. Assuming isentropic flow in the nozzle, estimate (a) the throat area and (b) the tank pressure after 10 s of operation. The exit area is 10 cm².

P9.53 Air flows steadily from a reservoir at 20°C through a nozzle of exit area 20 cm² and strikes a vertical plate as in Fig. P9.53. The flow is subsonic throughout. A force of 135 N is required to hold the plate stationary. Compute (a) V_e, (b) Ma_e, and (c) p_0 if p_a = 101 kPa.
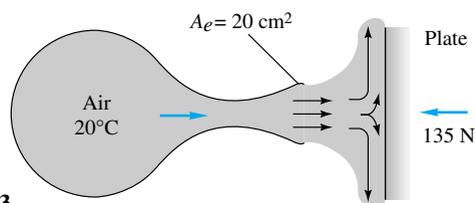
P9.53

P9.54 For flow of air through a normal shock the upstream conditions are V_1 = 600 m/s, T_{01} = 500 K, and p_{01} = 700 kPa. Compute the downstream conditions Ma_2, V_2, T_2, p_2, and p_{02}.

P9.55 Air, supplied by a reservoir at 450 kPa, flows through a converging-diverging nozzle whose throat area is 12 cm². A normal shock stands where A_1 = 20 cm². (a) Compute the pressure just downstream of this shock. Still farther downstream, at A_3 = 30 cm², estimate (b) p_3, (c) A_3^*, and (d) Ma_3.

P9.56 Air from a reservoir at 20°C and 500 kPa flows through a duct and forms a normal shock downstream of a throat of area 10 cm². By an odd coincidence it is found that the stagnation pressure downstream of this shock exactly equals the throat pressure. What is the area where the shock wave stands?

P9.57 Air flows from a tank through a nozzle into the standard atmosphere, as in Fig. P9.57. A normal shock stands in the exit of the nozzle, as shown. Estimate (a) the pressure in the tank and (b) the mass flow.
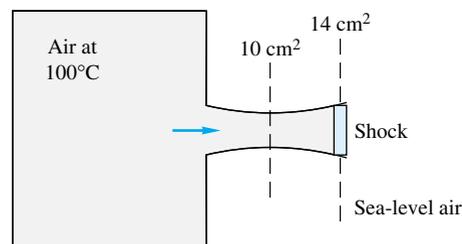
P9.57

P9.58 Argon (Table A.4) approaches a normal shock with V_1 = 700 m/s, p_1 = 125 kPa, and T_1 = 350 K. Estimate (a) V_2 and (b) p_2. (c) What pressure p_2 would result if the same velocity change V_1 to V_2 were accomplished isentropically?

P9.59 Air, at stagnation conditions of 450 K and 250 kPa, flows through a nozzle. At section 1, where the area is 15 cm², there is a normal shock wave. If the mass flow is 0.4 kg/s, estimate (a) the Mach number and (b) the stagnation pressure just downstream of the shock.

P9.60 When a pitot tube such as in Fig. 6.30 is placed in a supersonic flow, a normal shock will stand in front of the probe. Suppose the probe reads p_0 = 190 kPa and p = 150 kPa. If the stagnation temperature is 400 K, estimate the (supersonic) Mach number and velocity upstream of the shock.

P9.61 Repeat Prob. 9.56 except this time let the odd coincidence be that the *static* pressure downstream of the shock exactly equals the throat pressure. What is the area where the shock stands?

P9.62 An atomic explosion propagates into still air at 14.7 lbf/in² absolute and 520°R. The pressure just inside the shock is 5000 lbf/in² absolute. Assuming k = 1.4, what are the speed C of the shock and the velocity V just inside the shock?

P9.63 Sea-level standard air is sucked into a vacuum tank through a nozzle, as in Fig. P9.63. A normal shock stands where the nozzle area is 2 cm², as shown. Estimate (a) the pressure in the tank and (b) the mass flow.
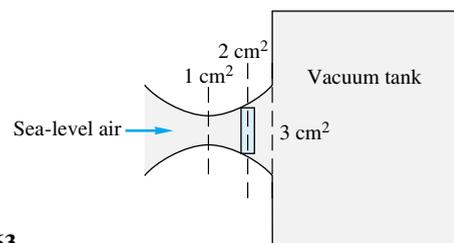
P9.63

P9.64 Air in a large tank at 100°C and 150 kPa exhausts to the atmosphere through a converging nozzle with a 5-cm² throat area. Compute the exit mass flow if the atmospheric pressure is (a) 100 kPa, (b) 60 kPa, and (c) 30 kPa.

P9.65 Air flows through a converging-diverging nozzle between two large reservoirs, as shown in Fig. P9.65. A mercury manometer between the throat and the downstream reservoir reads h = 15 cm. Estimate the downstream reservoir pressure. Is there a normal shock in the flow? If so, does it stand in the exit plane or farther upstream?

P9.66 In Prob. 9.65 what would be the mercury-manometer reading h if the nozzle were operating exactly at supersonic design conditions?
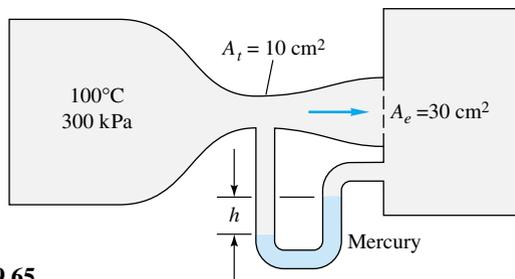
P9.65

P9.67 In Prob. 9.65 estimate the complete range of manometer readings h for which the flow through the nozzle is entirely isentropic, except possibly in the exit plane.

P9.68 Air in a tank at 120 kPa and 300 K exhausts to the atmosphere through a 5-cm^2-throat converging nozzle at a rate of 0.12 kg/s. What is the atmospheric pressure? What is the maximum mass flow possible at low atmospheric pressure?

P9.69 With reference to Prob. 3.68, show that the thrust of a rocket engine exhausting into a vacuum is given by

$$F = \frac{p_0 A_e (1 + k \, \text{Ma}_e^2)}{\left(1 + \dfrac{k-1}{2} \, \text{Ma}_e^2\right)^{k/(k-1)}}$$

where A_e = exit area
Ma_e = exit Mach number
p_0 = stagnation pressure in combustion chamber

Note that stagnation temperature does not enter into the thrust.

P9.70 Air, at stagnation temperature 100°C, expands isentropically through a nozzle of 6-cm^2 throat area and 18-cm^2 exit area. The mass flow is at its maximum value of 0.5 kg/s. Estimate the exit pressure for (a) subsonic and (b) supersonic exit flow.

P9.71 For the nozzle of Prob. 9.70, allowing for nonisentropic flow, what is the range of exit tank pressures p_b for which (a) the diverging nozzle flow is fully supersonic, (b) the exit flow is subsonic, (c) the mass flow is independent of p_b, (d) the exit plane pressure p_e is independent of p_b, and (e) $p_e < p_b$?

P9.72 Suppose the nozzle flow of Prob. 9.70 is not isentropic but instead has a normal shock at the position where area is 15 cm^2. Compute the resulting mass flow, exit pressure, and exit Mach number.

P9.73 Air flows isentropically in a converging-diverging nozzle with a throat area of 3 cm^2. At section 1, the pressure is 101 kPa, the temperature is 300 K, and the velocity is 868 m/s. (a) Is the nozzle choked? Determine (b) A_1 and (c) the mass flow. Suppose, without changing stagnation conditions or A_1, the (flexible) throat is reduced to 2 cm^2. As-

suming shock-free flow, will there be any change in the gas properties at section 1? If so, compute new p_1, V_1, and T_1 and explain.

P9.74 The perfect-gas assumption leads smoothly to Mach-number relations which are very convenient (and tabulated). This is not so for a real gas such as steam. To illustrate, let steam at $T_0 = 500$°C and $p_0 = 2$ MPa expand isentropically through a converging nozzle whose exit area is 10 cm^2. Using the steam tables, find (a) the exit pressure and (b) the mass flow when the flow is sonic, or choked. What complicates the analysis?

*P9.75 A double-tank system in Fig. P9.75 has two identical converging nozzles of 1-in^2 throat area. Tank 1 is very large, and tank 2 is small enough to be in steady-flow equilibrium with the jet from tank 1. Nozzle flow is isentropic, but entropy changes between 1 and 3 due to jet dissipation in tank 2. Compute the mass flow. (If you give up, Ref. 14, pp. 288–290, has a good discussion.)
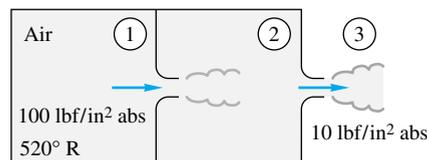
P9.75

P9.76 A large reservoir at 20°C and 800 kPa is used to fill a small insulated tank through a converging-diverging nozzle with 1-cm^2 throat area and 1.66-cm^2 exit area. The small tank has a volume of 1 m^3 and is initially at 20°C and 100 kPa. Estimate the elapsed time when (a) shock waves begin to appear inside the nozzle and (b) the mass flow begins to drop below its maximum value.

P9.77 A perfect gas (not air) expands isentropically through a supersonic nozzle with an exit area 5 times its throat area. The exit Mach number is 3.8. What is the specific-heat ratio of the gas? What might this gas be? If $p_0 = 300$ kPa, what is the exit pressure of the gas?

P9.78 The orientation of a hole can make a difference. Consider holes A and B in Fig. P9.78, which are identical but reversed. For the given air properties on either side, compute the mass flow through each hole and explain why they are different.
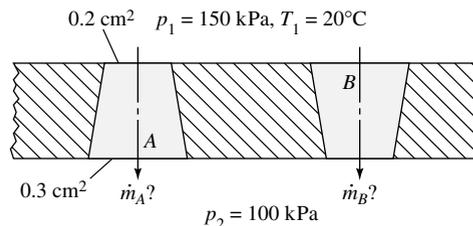
P9.78

P9.79 Air with $p_0 = 300$ kPa and $T_0 = 500$ K flows through a converging-diverging nozzle with throat area of 1 cm^2 and exit area of 3 cm^2 into a receiver tank. The mass flow is 195.2 kg/h. For what range of receiver pressure is this mass flow possible?

P9.80 A sea-level automobile tire is initially at 32 lbf/in^2 gage pressure and 75°F. When it is punctured with a hole which resembles a converging nozzle, its pressure drops to 15 lbf/in^2 gage in 12 min. Estimate the size of the hole, in thousandths of an inch. The tire volume is 2.5 ft^2.

P9.81 Helium, in a large tank at 100°C and 400 kPa, discharges to a receiver through a converging-diverging nozzle designed to exit at Ma = 2.5 with exit area 1.2 cm^2. Compute (a) the receiver pressure and (b) the mass flow at design conditions. (c) Also estimate the range of receiver pressures for which mass flow will be a maximum.

P9.82 Air at 500 K flows through a converging-diverging nozzle with throat area of 1 cm^2 and exit area of 2.7 cm^2. When the mass flow is 182.2 kg/h, a pitot-static probe placed in the exit plane reads $p_0 = 250.6$ kPa and $p = 240.1$ kPa. Estimate the exit velocity. Is there a normal shock wave in the duct? If so, compute the Mach number just downstream of this shock.

P9.83 When operating at design conditions (smooth exit to sea-level pressure), a rocket engine has a thrust of 1 million lbf. The chamber pressure and temperature are 600 lbf/in^2 absolute and 4000°R, respectively. The exhaust gases approximate $k = 1.38$ with a molecular weight of 26. Estimate (a) the exit Mach number and (b) the throat diameter.

P9.84 Air flows through a duct as in Fig. P9.84, where $A_1 = 24$ cm^2, $A_2 = 18$ cm^2, and $A_3 = 32$ cm^2. A normal shock stands at section 2. Compute (a) the mass flow, (b) the Mach number, and (c) the stagnation pressure at section 3.

Ma$_1$ = 2.5
p_1 = 40 kPa
T_1 = 30°C
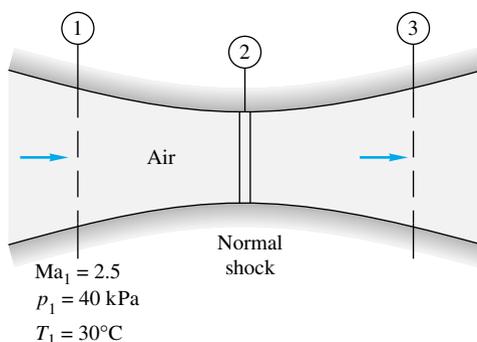
P9.84

P9.85 A large tank delivers air through a nozzle of 1-cm^2 throat area and 2.7-cm^2 exit area. When the receiver pressure is 125 kPa, a normal shock stands in the exit plane. Estimate

(a) the throat pressure and (b) the stagnation pressure in the upstream supply tank.

P9.86 Air enters a 3-cm-diameter pipe 15 m long at $V_1 = 73$ m/s, $p_1 = 550$ kPa, and $T_1 = 60$°C. The friction factor is 0.018. Compute V_2, p_2, T_2, and p_{02} at the end of the pipe. How much additional pipe length would cause the exit flow to be sonic?

P9.87 Air enters a duct of $L/D = 40$ at $V_1 = 170$ m/s and $T_1 = 300$ K. The flow at the exit is choked. What is the average friction factor in the duct for adiabatic flow?

P9.88 Air enters a 5- by 5-cm square duct at $V_1 = 900$ m/s and $T_1 = 300$ K. The friction factor is 0.02. For what length duct will the flow exactly decelerate to Ma = 1.0? If the duct length is 2 m, will there be a normal shock in the duct? If so, at what Mach number will it occur?

P9.89 Air flows adiabatically in a 5-cm-diameter tube with $f \approx$ 0.025. At section 1, $V_1 = 75$ m/s, $T_1 = 350$ K, and $p_1 = 300$ kPa. How much further down the tube will (a) the pressure be 156 kPa, (b) the temperature be 343 K, and (c) the flow reach the choking point?

P9.90 Air, supplied at $p_0 = 700$ kPa and $T_0 = 330$ K, flows through a converging nozzle into a pipe of 2.5-cm diameter which exits to a near vacuum. If $\bar{f} = 0.022$, what will be the mass flow through the pipe if its length is (a) 0 m, (b) 1 m, and (c) 10 m?

P9.91 Air flows steadily from a tank through the pipe in Fig. P9.91. There is a converging nozzle on the end. If the mass flow is 3 kg/s and the nozzle is choked, estimate (a) the Mach number at section 1 and (b) the pressure inside the tank.
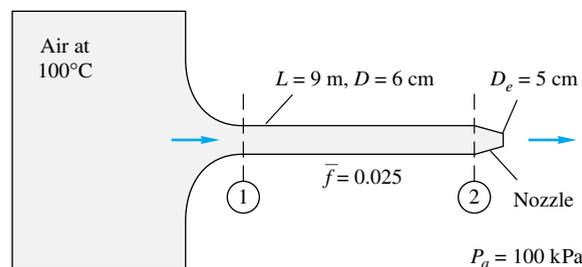
P9.91

P9.92 Modify Prob. 9.91 as follows. Let the pressure in the tank be 700 kPa, and let the nozzle be choked. Determine (a) Ma$_2$ and (b) the mass flow.

P9.93 Air flows adiabatically in a 3-cm-diameter duct. The average friction factor is 0.015. If, at the entrance, $V = 950$ m/s and $T = 250$ K, how far down the tube will (a) the Mach number be 1.8 or (b) the flow be choked?

P9.94 Compressible pipe flow with friction, Sec. 9.7, assumes constant stagnation enthalpy and mass flow but variable

momentum. Such a flow is often called *Fanno flow*, and a line representing all possible property changes on a temperature-entropy chart is called a *Fanno line*. Assuming a perfect gas with $k = 1.4$ and the data of Prob. 9.86, draw a Fanno curve of the flow for a range of velocities from very low (Ma $\ll$ 1) to very high (Ma $\gg$ 1). Comment on the meaning of the maximum-entropy point on this curve.

P9.95 Helium (Table A.4) enters a 5-cm-diameter pipe at $p_1 = 550$ kPa, $V_1 = 312$ m/s, and $T_1 = 40°C$. The friction factor is 0.025. If the flow is choked, determine (a) the length of the duct and (b) the exit pressure.

P9.96 Derive and verify the adiabatic-pipe-flow velocity relation of Eq. (9.74), which is usually written in the form

$$\frac{\bar{f}L}{D} + \frac{k+1}{k} \ln \frac{V_2}{V_1} = \frac{a_0^2}{k}\left(\frac{1}{V_1^2} - \frac{1}{V_2^2}\right)$$

P9.97 By making a few algebraic substitutions, show that Eq. (9.74), or the relation in Prob. 9.96, may be written in the density form

$$\rho_1^2 = \rho_2^2 + \rho^{*2}\left(\frac{2k}{k+1}\frac{\bar{f}L}{D} + 2 \ln \frac{\rho_1}{\rho_2}\right)$$

Why is this formula awkward if one is trying to solve for the mass flow when the pressures are given at sections 1 and 2?

P9.98 Compressible *laminar* flow, $f \approx 64/\text{Re}$, may occur in capillary tubes. Consider air, at stagnation conditions of 100°C and 200 kPa, entering a tube 3 cm long and 0.1 mm in diameter. If the receiver pressure is near vacuum, estimate (a) the average Reynolds number, (b) the Mach number at the entrance, and (c) the mass flow in kg/h.

P9.99 A compressor forces air through a smooth pipe 20 m long and 4 cm in diameter, as in Fig. P9.99. The air leaves at 101 kPa and 200°C. The compressor data for pressure rise versus mass flow are shown in the figure. Using the Moody chart to estimate $\bar{f}$, compute the resulting mass flow.
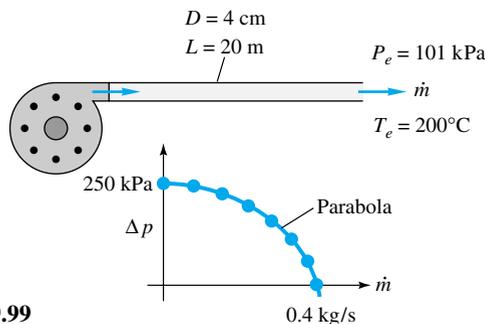
P9.99

P9.100 Modify Prob. 9.99 as follows. Find the length of 4-cm-diameter pipe for which the pump pressure rise will be exactly 200 kPa.

P9.101 How do the compressible-pipe-flow formulas behave for small pressure drops? Let air at 20°C enter a tube of diameter 1 cm and length 3 m. If $\bar{f} = 0.028$ with $p_1 = 102$ kPa and $p_2 = 100$ kPa, estimate the mass flow in kg/h for (a) isothermal flow, (b) adiabatic flow, and (c) incompressible flow (Chap. 6) at the entrance density.

P9.102 Air at 550 kPa and 100°C enters a smooth 1-m-long pipe and then passes through a second smooth pipe to a 30-kPa reservoir, as in Fig. P9.102. Using the Moody chart to compute $\bar{f}$, estimate the mass flow through this system. Is the flow choked?
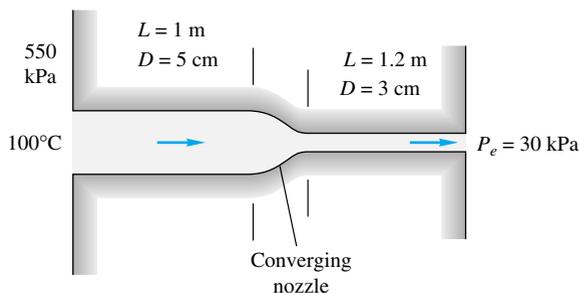
P9.102

P9.103 Natural gas, with $k \approx 1.3$ and a molecular weight of 16, is to be pumped through 100 km of 81-cm-diameter pipeline. The downstream pressure is 150 kPa. If the gas enters at 60°C, the mass flow is 20 kg/s, and $\bar{f} = 0.024$, estimate the required entrance pressure for (a) isothermal flow and (b) adiabatic flow.

P9.104 A tank of oxygen (Table A.4) at 20°C is to supply an astronaut through an umbilical tube 12 m long and 2 cm in diameter. The exit pressure in the tube is 40 kPa. If the desired mass flow is 90 kg/h and $\bar{f} = 0.025$, what should be the pressure in the tank?

P9.105 Air enters a 5-cm-diameter pipe at $p_1 = 200$ kPa and $T_1 = 350$ K. The downstream receiver pressure is 74 kPa. The friction factor is 0.02. If the exit is choked, what is (a) the length of the pipe and (b) the mass flow? (c) If p_1, T_1, and p_{receiver} stay the same, what pipe length will cause the mass flow to increase by 50 percent over (b)? *Hint*: In part (c) the exit pressure does not equal the receiver pressure.

P9.106 Air at 300 K flows through a duct 50 m long with $\bar{f} = 0.019$. What is the minimum duct diameter which can carry the flow without choking if the entrance velocity is (a) 50 m/s, (b) 150 m/s, and (c) 420 m/s?

P9.107 A fuel-air mixture, assumed equivalent to air, enters a duct combustion chamber at $V_1 = 104$ m/s and $T_1 = 300$ K. What amount of heat addition in kJ/kg will cause the exit flow to be choked? What will be the exit Mach number and temperature if 504 kJ/kg is added during combustion?

P9.108 What happens to the inlet flow of Prob. 9.107 if the combustion yields 1500 kJ/kg heat addition and p_{01} and T_{01} remain the same? How much is the mass flow reduced?

P9.109 A jet engine at 7000-m altitude takes in 45 kg/s of air and adds 550 kJ/kg in the combustion chamber. The chamber cross section is 0.5 m^2, and the air enters the chamber at 80 kPa and 5°C. After combustion the air expands through an isentropic converging nozzle to exit at atmospheric pressure. Estimate (*a*) the nozzle throat diameter, (*b*) the nozzle exit velocity, and (*c*) the thrust produced by the engine.

P9.110 Compressible pipe flow with heat addition, Sec. 9.8, assumes constant momentum ($p + \rho V^2$) and constant mass flow but variable stagnation enthalpy. Such a flow is often called *Rayleigh flow*, and a line representing all possible property changes on a temperature-entropy chart is called a *Rayleigh line*. Assuming air passing through the flow state $p_1 = 548$ kPa, $T_1 = 588$ K, $V_1 = 266$ m/s, and $A = 1$ m^2, draw a Rayleigh curve of the flow for a range of velocities from very low (Ma $\ll$ 1) to very high (Ma $\gg$ 1). Comment on the meaning of the maximum-entropy point on this curve.

P9.111 Add to your Rayleigh line of Prob. 9.110 a Fanno line (see Prob. 9.94) for stagnation enthalpy equal to the value associated with state 1 in Prob. 9.110. The two curves will intersect at state 1, which is subsonic, and at a certain state 2, which is supersonic. Interpret these two states vis-à-vis Table B.2.

P9.112 Air enters a duct subsonically at section 1 at 1.2 kg/s. When 650 kW of heat is added, the flow chokes at the exit at $p_2 = 95$ kPa and $T_2 = 700$ K. Assuming frictionless heat addition, estimate (*a*) the velocity and (*b*) the stagnation pressure at section 1.

P9.113 Air enters a constant-area duct at $p_1 = 90$ kPa, $V_1 = 520$ m/s, and $T_1 = 558$°C. It is then cooled with negligible friction until it exits at $p_2 = 160$ kPa. Estimate (*a*) V_2, (*b*) T_2, and (*c*) the total amount of cooling in kJ/kg.

P9.114 We have simplified things here by separating friction (Sec. 9.7) from heat addition (Sec. 9.8). Actually, they often occur together, and their effects must be evaluated simultaneously. Show that, for flow with friction *and* heat transfer in a constant-diameter pipe, the continuity, momentum, and energy equations may be combined into the following differential equation for Mach-number changes:

$$\frac{d\,\mathrm{Ma}^2}{\mathrm{Ma}^2} = \frac{1 + k\,\mathrm{Ma}^2}{1 - \mathrm{Ma}^2}\frac{dQ}{c_p T}$$
$$+ \frac{k\,\mathrm{Ma}^2\,[2 + (k-1)\,\mathrm{Ma}^2]}{2(1 - \mathrm{Ma}^2)}\frac{f\,dx}{D}$$

where dQ is the heat added. A complete derivation, including many additional combined effects such as area change and mass addition, is given in chap. 8 of Ref. 8.

P9.115 Air flows subsonically in a duct with negligible friction. When heat is added in the amount of 948 kJ/kg, the pressure drops from $p_1 = 200$ to $p_2 = 106$ kPa. Estimate (*a*) Ma_1, (*b*) T_1, and (*c*) V_1, assuming $T_{01} = 305$ K.

P9.116 An observer at sea level does not hear an aircraft flying at 12,000-ft standard altitude until it is 5 (statute) mi past her. Estimate the aircraft speed in ft/s.

P9.117 An observer at sea level does not hear an aircraft flying at 6000-m standard altitude until 15 s after it has passed overhead. Estimate the aircraft speed in m/s.

P9.118 A particle moving at uniform velocity in sea-level standard air creates the two disturbance spheres shown in Fig. P9.118. Compute the particle velocity and Mach number.
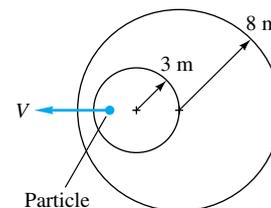
P9.118   Particle

P9.119 The particle in Fig. P9.119 is moving supersonically in sea-level standard air. From the two given disturbance spheres, compute the particle Mach number, velocity, and Mach angle.

P9.119
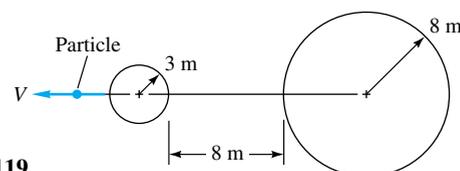
P9.120 The particle in Fig. P9.120 is moving in sea-level standard air. From the two disturbance spheres shown, estimate (*a*) the position of the particle at this instant and (*b*) the temperature in °C at the front stagnation point of the particle.

P9.120
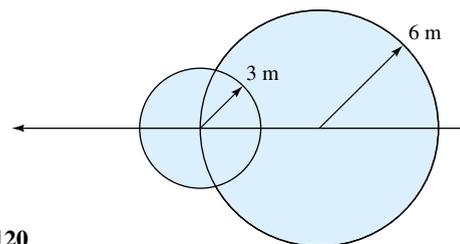
P9.121 A thermistor probe, in the shape of a needle parallel to the flow, reads a static temperature of -25°C when inserted into a supersonic airstream. A conical disturbance cone of half-angle 17° is created. Estimate (*a*) the Mach number,

(b) the velocity, and (c) the stagnation temperature of the stream.

P9.122 Supersonic air takes a 5° compression turn, as in Fig. P9.122. Compute the downstream pressure and Mach number and the wave angle, and compare with small-disturbance theory.
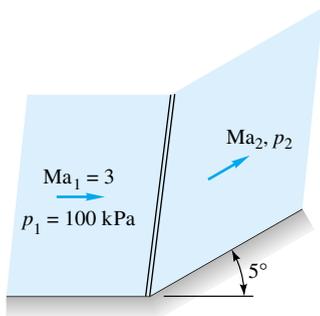
P9.122

P9.123 Modify Prob. 9.122 as follows. Let the 5° total turn be in the form of five separate compression turns of 1° each. Compute the final Mach number and pressure, and compare the pressure with an isentropic expansion to the same final Mach number.

P9.124 Determine the validity of the following alternate relation for the pressure ratio across an oblique shock wave:

$$\frac{p_2}{p_1} = \frac{\cot \theta \sin 2\beta - \cos 2\beta + k}{\cot \theta \sin 2\beta - \cos 2\beta - k}$$

If necessary, your proof (or disproof) may be somewhat tentative and heuristic.

P9.125 Show that, as the upstream Mach number approaches infinity, the Mach number downstream of an attached oblique-shock wave will have the value

$$\text{Ma}_2 \approx \sqrt{\frac{k-1}{2k \sin^2 (\beta - \theta)}}$$

P9.126 Consider airflow at $\text{Ma}_1 = 2.2$. Calculate, to two decimal places, (a) the deflection angle for which the downstream flow is sonic and (b) the maximum deflection angle.

P9.127 Do the Mach waves upstream of an oblique-shock wave intersect with the shock? Assuming supersonic downstream flow, do the downstream Mach waves intersect the shock? Show that for small deflections the shock-wave angle β lies halfway between μ_1 and $\mu_2 + \theta$ for any Mach number.

P9.128 Air flows past a two-dimensional wedge-nosed body as in Fig. P9.128. Determine the wedge half-angle δ for which the horizontal component of the total pressure force on the nose is 35 kN/m of depth into the paper.
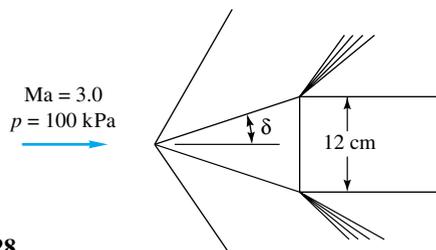
P9.128

P9.129 Air flows at supersonic speed toward a compression ramp, as in Fig. P9.129. A scratch on the wall at point a creates a wave of 30° angle, while the oblique shock created has a 50° angle. What is (a) the ramp angle θ and (b) the wave angle ϕ caused by a scratch at b?
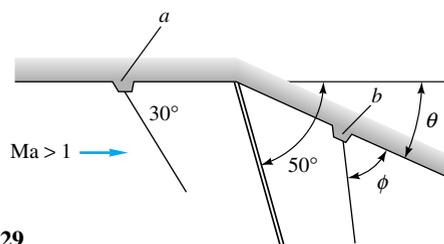
P9.129

P9.130 Modify Prob. 9.129 as follows. If the wave angle ϕ is 42°, determine (a) the shock-wave angle and (b) the deflection angle.

P9.131 In Fig. P9.128, assume that the approach stream temperature is 20°C. For what wedge half-angle δ will the stream temperature along the wedge surface be 200°C?

P9.132 Air flows at $\text{Ma} = 3$ and $p = 10$ lbf/in² absolute toward a wedge of 16° angle at zero incidence in Fig. P9.132. If the pointed edge is forward, what will be the pressure at point A? If the blunt edge is forward, what will be the pressure at point B?
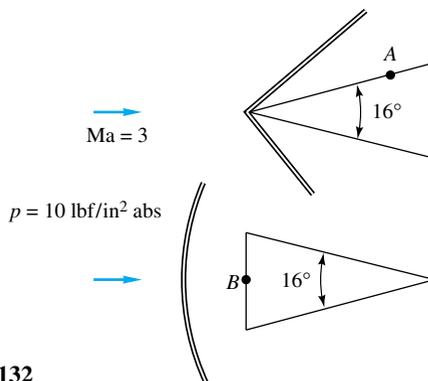
P9.132

P9.133 Air flows supersonically toward the double-wedge system in Fig. P9.133. The (x, y) coordinates of the tips are given.
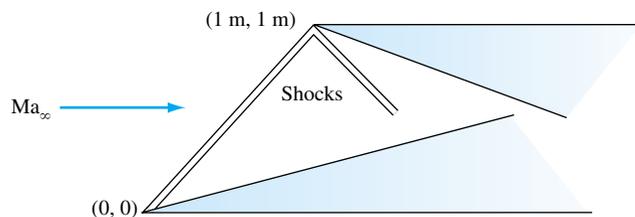
P9.133

The shock wave of the forward wedge strikes the tip of the aft wedge. Both wedges have 15° deflection angles. What is the free-stream Mach number?

P9.134 When an oblique shock strikes a solid wall, it reflects as a shock of sufficient strength to cause the exit flow Ma_3 to be parallel to the wall, as in Fig. P9.134. For airflow with $Ma_1 = 2.5$ and $p_1 = 100$ kPa, compute Ma_3, p_3, and the angle ϕ.
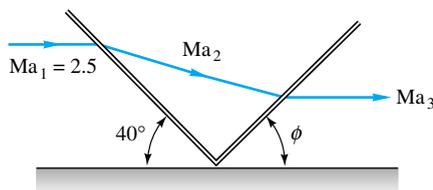
P9.134

P9.135 A bend in the bottom of a supersonic duct flow induces a shock wave which reflects from the upper wall, as in Fig. P9.135. Compute the Mach number and pressure in region 3.
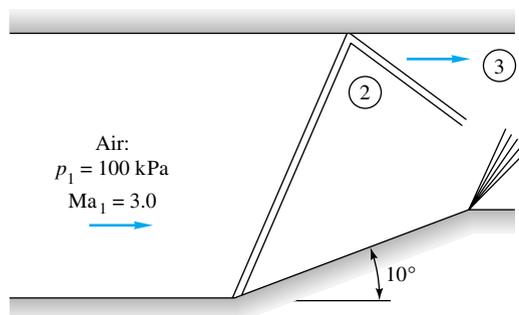
P9.135

P9.136 Figure P9.136 is a special application of Prob. 9.135. With careful design, one can orient the bend on the lower wall so that the reflected wave is exactly canceled by the return bend, as shown. This is a method of reducing the Mach number in a channel (a supersonic diffuser). If the bend angle is $\phi = 10°$, find (a) the downstream width h and (b) the downstream Mach number. Assume a weak shock wave.
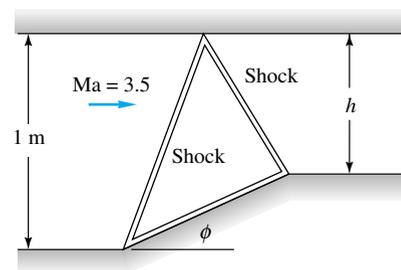
P9.136

P9.137 Generalize Prob. 9.136 into a computer study as follows. Assuming weak shocks, find and plot all combinations of ϕ and h in Fig. P9.136 for which the canceled or "swallowed" reflected shock is possible.

P9.138 The supersonic nozzle of Fig. P9.138 is overexpanded (case G of Fig. 9.12) with $A_e/A_t = 3.0$ and a stagnation pressure of 350 kPa. If the jet edge makes a 4° angle with the nozzle centerline, what is the back pressure p_r in kPa?
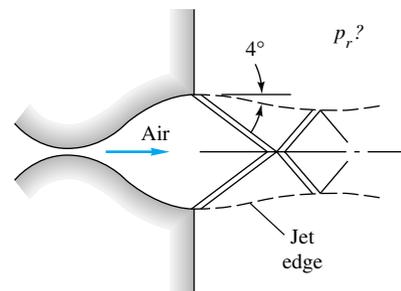
P9.138

P9.139 Airflow at $Ma = 2.2$ takes a compression turn of 12° and then another turn of angle θ in Fig. P9.139. What is the maximum value of θ for the second shock to be attached? Will the two shocks intersect for any θ less than θ_{max}?
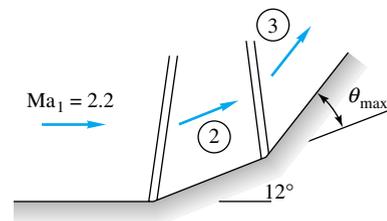
P9.139

P9.140 The solution to Prob. 9.122 is $Ma_2 = 2.750$, and $p_2 = 145.5$ kPa. Compare these results with an isentropic compression turn of 5°, using Prandtl-Meyer theory.

P9.141 Supersonic airflow takes a 5° expansion turn, as in Fig. P9.141. Compute the downstream Mach number and pressure, and compare with small-disturbance theory.
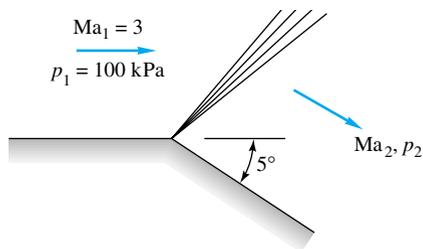
P9.141

P9.142 A supersonic airflow at $Ma_1 = 3.2$ and $p_1 = 50$ kPa undergoes a compression shock followed by an isentropic expansion turn. The flow deflection is $30°$ for each turn. Compute Ma_2 and p_2 if (a) the shock is followed by the expansion and (b) the expansion is followed by the shock.

P9.143 Airflow at $Ma_1 = 3.2$ passes through a $25°$ oblique-shock deflection. What isentropic expansion turn is required to bring the flow back to (a) Ma_1 and (b) p_1?

P9.144 Consider a smooth isentropic compression turn of $20°$, as shown in Fig. P9.144. The Mach waves thus generated will form a converging fan. Sketch this fan as accurately as possible, using at least five equally spaced waves, and demonstrate how the fan indicates the probable formation of an oblique-shock wave.
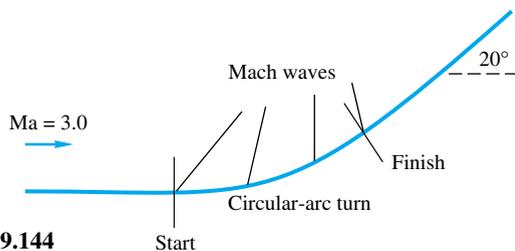
P9.144

P9.145 Air at $Ma_1 = 2.0$ and $p_1 = 100$ kPa undergoes an isentropic expansion to a downstream pressure of 50 kPa. What is the desired turn angle in degrees?

P9.146 Helium, at $20°C$ and $V_1 = 2010$ m/s, undergoes a Prandtl-Meyer expansion until the temperature is $-50°C$. Estimate the turn angle in degrees.

P9.147 A converging-diverging nozzle with a 4:1 exit-area ratio and $p_0 = 500$ kPa operates in an underexpanded condition (case I of Fig. 9.12b) as in Fig. P9.147. The receiver pressure is $p_a = 10$ kPa, which is less than the exit pressure, so that expansion waves form outside the exit. For the given conditions, what will the Mach number Ma_2 and the angle ϕ of the edge of the jet be? Assume $k = 1.4$ as usual.

P9.148 Repeat Example 9.19 for an angle of attack of $6°$. Is the lift coefficient linear with angle α in this range of $0° \leq \alpha \leq 8°$? Is the drag coefficient parabolic with α in this range?

P9.149 Repeat Example 9.21 for an angle of attack of $2°$. Is the lift coefficient linear with angle α in this range of $0° \leq \alpha$
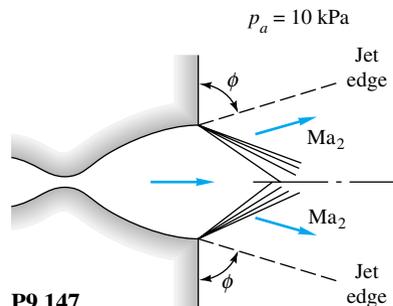
P9.147

$\leq 8°$? Why does the drag coefficient not have the simple parabolic form $C_D \approx K\alpha^2$ in this range?

P9.150 A flat-plate airfoil with $C = 1.2$ m is to have a lift of 30 kN/m when flying at 5000-m standard altitude with $U_\infty = 641$ m/s. Using Ackeret theory, estimate (a) the angle of attack and (b) the drag force in N/m.

P9.151 Air flows at $Ma = 2.5$ past a half-wedge airfoil whose angles are $4°$, as in Fig. P9.151. Compute the lift and drag coefficient at α equal to (a) $0°$ and (b) $6°$.
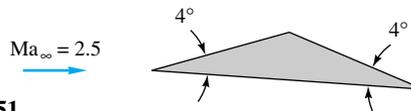
P9.151

P9.152 A supersonic airfoil has a parabolic symmetric shape for upper and lower surfaces

$$y_{u,l} = \pm 2t \left(\frac{x}{C} - \frac{x^2}{C^2} \right)$$

such that the maximum thickness is t at $x = \frac{1}{2}C$. Compute the drag coefficient at zero incidence by Ackeret theory, and compare with a symmetric double wedge of the same thickness.

P9.153 A supersonic transport has a mass of 65 Mg and cruises at 11-km standard altitude at a Mach number of 2.25. If the angle of attack is $2°$ and its wings can be approximated by flat plates, estimate (a) the required wing area in m^2 and (b) the thrust required in N.

P9.154 A symmetric supersonic airfoil has its upper and lower surfaces defined by a sine-wave shape:

$$y = \frac{t}{2} \sin \frac{\pi x}{C}$$

where t is the maximum thickness, which occurs at $x = C/2$. Use Ackeret theory to derive an expression for the drag coefficient at zero angle of attack. Compare your result with Ackeret theory for a symmetric double-wedge airfoil of the same thickness.

P9.155 For the sine-wave airfoil shape of Prob. 9.154, with $Ma_\infty = 2.5$, $k = 1.4$, $t/C = 0.1$, and $\alpha = 0°$, plot (without com-

puting the overall forces) the pressure distribution $p(x)/p_\infty$ along the upper surface for (a) Ackeret theory and (b) an oblique shock plus a continuous Prandtl-Meyer expansion.

P9.156 A thin circular-arc airfoil is shown in Fig. P9.156. The leading edge is parallel to the free stream. Using linearized (small-turning-angle) supersonic-flow theory, derive a formula for the lift and drag coefficient for this orientation, and compare with Ackeret-theory results for an angle of attack $\alpha = \tan^{-1}(h/L)$.
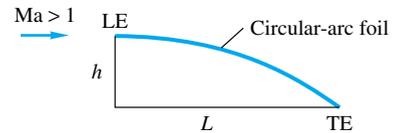
P9.156

P9.157 Prove from Ackeret theory that for a given supersonic airfoil shape with sharp leading and trailing edges and a given thickness, the minimum-thickness drag occurs for a symmetric double-wedge shape.

Word Problems

W9.1 Notice from Table 9.1 that (a) water and mercury and (b) aluminum and steel have nearly the same speeds of sound, yet the second of the two materials is much denser. Can you account for this oddity? Can molecular theory explain it?

W9.2 When an object approaches you at Ma = 0.8, you can hear it, according to Fig. 9.18a. But would there be a Doppler shift? For example, would a musical tone seem to you to have a higher or a lower pitch?

W9.3 The subject of this chapter is commonly called *gas dynamics*. But can liquids not perform in this manner? Using water as an example, make a rule-of-thumb estimate of the pressure level needed to drive a water flow at velocities comparable to the sound speed.

W9.4 Suppose a gas is driven at compressible subsonic speeds by a large pressure drop, p_1 to p_2. Describe its behavior on an appropriately labeled Mollier chart for (a) frictionless flow in a converging nozzle and (b) flow with friction in a long duct.

W9.5 Describe physically what the "speed of sound" represents. What kind of pressure changes occur in air sound waves during ordinary conversation?

W9.6 Give a physical description of the phenomenon of choking in a converging-nozzle gas flow. Could choking happen even if wall friction were not negligible?

W9.7 Shock waves are treated as discontinuities here, but they actually have a very small finite thickness. After giving it some thought, sketch your idea of the distribution of gas velocity, pressure, temperature, and entropy through the inside of a shock wave.

W9.8 Describe how an observer, running along a normal-shock wave at finite speed V, will see what appears to be an oblique-shock wave. Is there any limit to the running speed?

Fundamentals of Engineering Exam Problems

One-dimensional compressible-flow problems have become quite popular on the FE Exam, especially in the afternoon sessions. In the following problems, assume one-dimensional flow of ideal air, $R = 287$ J/(kg·K) and $k = 1.4$.

FE9.1 For steady isentropic flow, if the absolute temperature increases 50 percent, by what ratio does the static pressure increase?
(a) 1.12, (b) 1.22, (c) 2.25, (d) 2.76, (e) 4.13

FE9.2 For steady isentropic flow, if the density doubles, by what ratio does the static pressure increase?
(a) 1.22, (b) 1.32, (c) 1.44, (d) 2.64, (e) 5.66

FE9.3 A large tank, at 500 K and 200 kPa, supplies isentropic airflow to a nozzle. At section 1, the pressure is only 120 kPa. What is the Mach number at this section?
(a) 0.63, (b) 0.78, (c) 0.89, (d) 1.00, (e) 1.83

FE9.4 In Prob. FE9.3 what is the temperature at section 1?
(a) 300 K, (b) 408 K, (c) 417 K, (d) 432 K, (e) 500 K

FE9.5 In Prob. FE9.3, if the area at section 1 is 0.15 m², what is the mass flow?
(a) 38.1 kg/s, (b) 53.6 kg/s, (c) 57.8 kg/s, (d) 67.8 kg/s, (e) 77.2 kg/s

FE9.6 For steady isentropic flow, what is the maximum possible mass flow through the duct in Fig. FE9.6?
(a) 9.5 kg/s, (b) 15.1 kg/s, (c) 26.2 kg/s, (d) 30.3 kg/s, (e) 52.4 kg/s
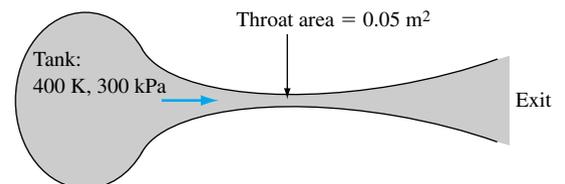
FE9.6

FE9.7 If the exit Mach number in Fig. FE9.6 is 2.2, what is the exit area?
(a) 0.10 m², (b) 0.12 m², (c) 0.15 m² , (d) 0.18 m²,
(e) 0.22 m²

FE9.8 If there are no shock waves and the pressure at one duct section in Fig. FE9.6 is 55.5 kPa, what is the velocity at that section?
(a) 166 m/s, (b) 232 m/s, (c) 554 m/s, (d) 706 m/s,
(e) 774 m/s

FE9.9 If, in Fig. FE9.6, there is a normal shock wave at a section where the area is 0.07 m², what is the air density just upstream of that shock?
(a) 0.48 kg/m³, (b) 0.78 kg/m³, (c) 1.35 kg/m³,
(d) 1.61 kg/m³, (e) 2.61 kg/m³

FE9.10 In Prob. FE9.9, what is the Mach number just downstream of the shock wave?
(a) 0.42, (b) 0.55, (c) 0.63, (d) 1.00, (e) 1.76

Comprehensive Problems

C9.1 The converging-diverging nozzle sketched in Fig. C9.1 is designed to have a Mach number of 2.00 at the exit plane (assuming the flow remains nearly isentropic). The flow travels from tank a to tank b, where tank a is much larger than tank b. (a) Find the area at the exit A_e and the back pressure p_b which will allow the system to operate at design conditions. (b) As time goes on, the back pressure will grow, since the second tank slowly fills up with more air. Since tank a is huge, the flow in the nozzle will remain the same, however, until a normal shock wave appears at the exit plane. At what back pressure will this occur? (c) If tank b is held at constant temperature, $T = 20°C$, estimate how long it will take for the flow to go from design conditions
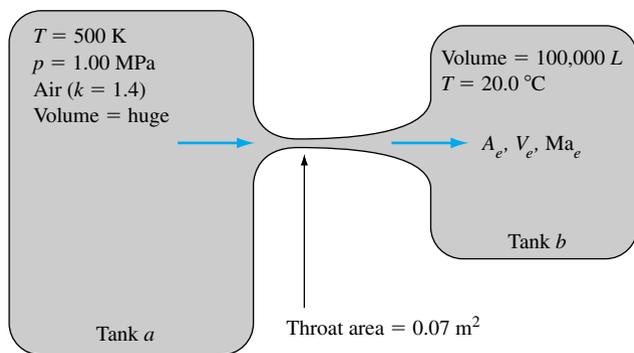
to the condition of part (b), i.e., with a shock wave at the exit plane.

C9.2 Two large air tanks, one at 400 K and 300 kPa and the other at 300 K and 100 kPa, are connected by a straight tube 6 m long and 5 cm in diameter. The average friction factor is 0.0225. Assuming adiabatic flow, estimate the mass flow through the tube.

*C9.3 Figure C9.3 shows the exit of a converging-diverging nozzle, where an oblique-shock pattern is formed. In the exit plane, which has an area of 15 cm², the air pressure is 16 kPa and the temperature is 250 K. Just outside the exit shock, which makes an angle of 50° with the exit plane, the temperature is 430 K. Estimate (a) the mass flow, (b) the throat area, (c) the turning angle of the exit flow, and, in the tank supplying the air, (d) the pressure and (e) the temperature.

$T = 500$ K
$p = 1.00$ MPa
Air ($k = 1.4$)
Volume = huge

Volume = 100,000 L
$T = 20.0 °C$

A_e, V_e, Ma$_e$

Tank b

Tank a

Throat area = 0.07 m²

C9.1

430 K

50°

Shock waves
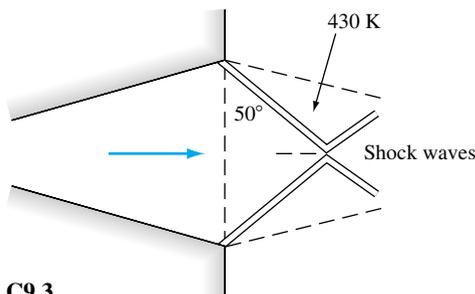
C9.3

Design Projects

D9.1 It is desired to select a rectangular wing for a fighter aircraft. The plane must be able (a) to take off and land on a 4500-ft-long sea-level runway and (b) to cruise supersonically at Ma = 2.3 at 28,000-ft altitude. For simplicity, assume a wing with zero sweepback. Let the aircraft maximum weight equal $(30 + n)(1000)$ lbf, where n is the number of letters in your surname. Let the available sea-level maximum thrust be one-third of the maximum weight, decreasing at altitude proportional to ambient density. Mak-

ing suitable assumptions about the effect of finite aspect ratio on wing lift and drag for both subsonic and supersonic flight, select a wing of minimum area sufficient to perform these takeoff/landing and cruise requirements. Some thought should be given to analyzing the wingtips and wing roots in supersonic flight, where Mach cones form and the flow is not two-dimensional. If no satisfactory solution is possible, gradually increase the available thrust to converge to an acceptable design.
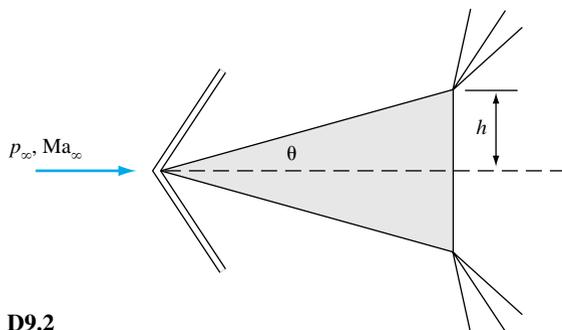
D9.2

D9.2 Consider supersonic flow of air at sea-level conditions past a wedge of half-angle θ, as shown in Fig. D9.2. Assume that the pressure on the back of the wedge equals the fluid pressure as it exits the Prandtl-Meyer fan. (*a*) Suppose $Ma_\infty = 3.0$. For what angle θ will the supersonic wave-drag coefficient C_D, based on frontal area, be exactly 0.5? (*b*) Suppose that $\theta = 20°$. Is there a free-stream Mach number for which the wave-drag coefficient C_D, based on frontal area, will be exactly 0.5? (*c*) Investigate the percent increase in C_D from (*a*) and (*b*) due to including boundary-layer friction drag in the calculation.

References

1. A. Y. Pope, *Aerodynamics of Supersonic Flight*, 2d ed., Pitman, New York, 1958.
2. A. B. Cambel and B. H. Jennings, *Gas Dynamics*, McGraw-Hill, New York, 1958.
3. F. Cheers, *Elements of Compressible Flow*, Wiley, New York, 1963.
4. J. E. John, *Gas Dynamics*, 2d ed., Allyn & Bacon, Boston, 1984.
5. A. J. Chapman and W. F. Walker, *Introductory Gas Dynamics*, Holt, New York, 1971.
6. B. W. Imrie, *Compressible Fluid Flow*, Halstead, New York, 1974.
7. R. Courant and K. O. Friedrichs, *Supersonic Flow and Shock Waves*, Interscience, New York, 1948; reprinted by Springer-Verlag, New York, 1977.
8. A. H. Shapiro, *The Dynamics and Thermodynamics of Compressible Fluid Flow*, Ronald, New York, 1953.
9. H. W. Liepmann and A. Roshko, *Elements of Gas Dynamics*, Wiley, New York, 1957.
10. R. von Mises, *Mathematical Theory of Compressible Fluid Flow*, Academic, New York, 1958.
11. J. A. Owczarek, *Gas Dynamics*, International Textbook, Scranton, PA, 1964.
12. W. G. Vincenti and C. Kruger, *Introduction to Physical Gas Dynamics*, Wiley, New York, 1965.
13. J. D. Anderson, *Hypersonic and High-Temperature Gas Dynamics*, McGraw-Hill, New York, 1989.
14. P. A. Thompson, *Compressible Fluid Dynamics*, McGraw-Hill, New York, 1972.
15. J. H. Keenan et al., *Steam Tables: SI Version*, 2 vols., Wiley, New York, 1985.
16. J. H. Keenan et al., *Gas Tables*, 2d ed., Wiley-Interscience, New York, 1983.
17. Y. A. Cengel and M. A. Boles, *Thermodynamics: An Engineering Approach*, 3d ed., McGraw-Hill, New York, 1998.
18. K. Wark, *Thermodynamics*, 6th ed., McGraw-Hill, New York, 1999.
19. F. M. White, *Viscous Fluid Flow*, 2d ed., McGraw-Hill, New York, 1991.
20. J. H. Keenan and E. P. Neumann, "Measurements of Friction in a Pipe for Subsonic and Supersonic Flow of Air," *J. Appl. Mech.,* vol. 13, no. 2, 1946, p. A-91.
21. J. Ackeret, "Air Forces on Airfoils Moving Faster than Sound Velocity," *NACA Tech. Mem.* 317, 1925.
22. Z. Kopal, "Tables of Supersonic Flow around Cones," *M.I.T. Center Anal. Tech. Rep.* 1, 1947 (see also *Tech. Rep.* 3 and 5, 1947).
23. J. L. Sims, *Tables for Supersonic Flow around Right Circular Cones at Zero Angle of Attack*, NASA SP-3004, 1964 (see also NASA SP-3007).
24. J. Palmer et al., *Compressible Flow Tables for Engineers: With Appropriate Computer Programs*, Scholium Intl., Port Washington, NY, 1989.
25. S. M. Yahya (ed.), *Gas Tables for Compressible Flow Calculations*, Wiley Eastern, New Delhi, India, 1985.
26. S. M. Yahya, *Fundamentals of Compressible Flow*, Wiley Eastern, New Delhi, India, 1982.
27. S. Schreier, *Compressible Flow*, Wiley, New York, 1982.
28. M. A. Saad, *Compressible Fluid Flow*, 2d ed., Prentice-Hall, Englewood Cliffs, NJ, 1992.
29. A. Y. Pope and K. L. Goin, *High Speed Wind Tunnel Testing*, Wiley, New York, 1965.
30. W. Bober and R. A. Kenyon, *Fluid Mechanics*, Wiley, New York, 1980.
31. J. D. Anderson, *Modern Compressible Flow: With Historical Perspective*, 2d ed., McGraw-Hill, New York, 1990.

32. M. J. Zucrow and J. D. Hoffman, *Gas Dynamics*, Wiley, New York, 1976.

33. Z. Husain, *Gas Dynamics through Problems*, Halsted Press, New York, 1989.

34. J. E. Plapp, *Engineering Fluid Mechanics*, Prentice-Hall, Englewood Cliffs, NJ, 1968.

35. P. H. Oosthuizen and W. E. Carscallen, *Compressible Fluid Flow*, McGraw-Hill, New York, 1997.

36. M. H. Kaplan, "The Reusable Launch Vehicle: Is the Stage Set*?" Launchspace Magazine*, March 1997, pp. 26–30.

37. T. K. Mattingly, "A Simpler Ride into Space," *Scientific American*, October 1997, pp. 120–125.